DETERMINATION OF PERCHLORATE AND THIOCYANATE IONS BY ION-SELECTIVE MEMBRANE AND BULK OPTODE TECHNIQUES USING EXPERIMENTAL DESIGN APPROACH

Miss Supacha Wirojsaengthong

A Dissertation Submitted in Partial Fulfillment of the Requirements
for the Degree of Doctor of Philosophy in Chemistry
Department of Chemistry
FACULTY OF SCIENCE
Chulalongkorn University
Academic Year 2019

การตรวจวัดไอออนเปอร์คลอเรตและไทโอไซยาเนตด้วยเทคนิคเมมเบรนชนิดเลือกจำเพาะต่อไอออนและเทคนิคบัลค์ออปโทดโดยวิธีการออกแบบการทดลอง

น.ส.ศุภชา วิโรจน์แสงทอง

วิทยานิพนธ์นี้เป็นส่วนหนึ่งของการศึกษาตามหลักสูตรปริญญาวิทยาศาสตรดุษฎีบัณฑิต
สาขาวิชาเคมี ภาควิชาเคมี
คณะวิทยาศาสตร์ จุฬาลงกรณ์มหาวิทยาลัย
ปีการศึกษา 2562

Thesis Title	DETERMINATION OF PERCHLORATE AND THIOCYANATE IONS BY ION-SELECTIVE MEMBRANE AND BULK OPTODE TECHNIQUES USING EXPERIMENTAL DESIGN APPROACH
By	Miss Supacha Wirojsaengthong
Field of Study	Chemistry
Thesis Advisor	Associate Professor Dr. WANLAPA AEUNGMAITREPIROM

Accepted by the FACULTY OF SCIENCE, Chulalongkorn University in Partial Fulfillment of the Requirement for the Doctor of Philosophy

..... Dean of the FACULTY OF SCIENCE
(Professor Dr. POLKIT SANGVANICH)

DISSERTATION COMMITTEE

..... Chairman
(Associate Professor Dr. VUDHICHAI PARASUK)
..... Thesis Advisor
(Associate Professor Dr. WANLAPA AEUNGMAITREPIROM)
..... Examiner
(Assistant Professor Dr. PASSAPOL NGAMUKOT)
..... Examiner
(Professor Dr. THAWATCHAI TUNTULANI)
..... External Examiner
(Assistant Professor Dr. Wanwisa Janrungroatsakul)

ศุภชา วิโรจน์แสงทอง : การตรวจวัดไอออนเปอร์คลอเรตและไทโอไซยาเนตด้วยเทคนิคเมมเบรนชนิดเลือกจำเพาะต่อไอออนและเทคนิคบัลค์ออปโทดโดยวิธีการออกแบบการทดลอง. (DETERMINATION OF PERCHLORATE AND THIOCYANATE IONS BY ION-SELECTIVE MEMBRANE AND BULK OPTODE TECHNIQUES USING EXPERIMENTAL DESIGN APPROACH) อ.ที่ปรึกษาหลัก : รศ. ดร.วัลภา เอื้องไมตรีภิรมย์

งานวิจัยนี้ได้พัฒนาวิธีการตรวจวัดสำหรับเปอร์คลอเรตและไทโอไซยาเนตในสารละลายด้วยเทคนิคโพเทนชิออเมตรีและการวัดค่าสี ภาวะที่เหมาะสมออกแบบโดย central composite design (CCD) กับ response surface methodology (RSM) ศึกษาการตอบสนองเชิงโพเทนชิออเมตรีของอิเล็กโทรดชนิดเลือกจำเพาะต่อเปอร์คลอเรตซึ่งประกอบด้วยพีวีซีเมมเบรนที่มีสารประกอบเชิงซ้อนไดไตรโพดอล เอมีน คาลิกซ์[4]เอรีน คอปเปอร์(II) (L1-Cu) พบว่าพีเอชที่เหมาะสมเท่ากับ 8.0 ความเข้มข้นของไอออนเอกซ์เชนจ์เจอร์และไอโอโนฟอร์ที่เหมาะสมเท่ากับ 3.25 มิลลิโมลต่อกิโลกรัม และ 13.25 มิลลิโมลต่อกิโลกรัมตามลำดับ ซึ่งให้ค่าความชันของเนินสต์เป็น –58.02 มิลลิโวลต์ต่อดีเคด R^2 เท่ากับ 0.9994 ที่ช่วงความเข้มข้นทำงาน $1.00\times10^{-6} – 1.00\times10^{-2}$ โมลาร์ และขีดจำกัดการตรวจวัดเป็น 3.00×10^{-5} โมลาร์ เมมเบรนนี้แสดงการเลือกจำเพาะต่อเปอร์คลอเรตสูงที่สุดเมื่อเทียบกับแอนไอออนชนิดอื่น นอกจากนี้ได้พัฒนาอุปกรณ์รับรู้ออปโทดกระดาษเพื่อตรวจวัดไทโอไซยาเนตในสารละลายด้วยการวัดค่าสีสำเร็จโดยใช้เมทัลโลพอร์ไฟรินไอโอโนฟอร์ได้แก่ สารประกอบเชิงซ้อน 5,10,15,20–เทททระคิส(4–เมทอกซีเฟนิล)พอร์ไฟริน โคบอลต์(II) (L2) และสารประกอบเชิงซ้อน 5,10,15,20–เทททระคิส(4–ออกทิลออกซีเฟนิล)พอร์ไฟริน โคบอลต์(II) (L3) ร่วมกับไอออนเอกซ์เชนจ์เจอร์ในพีวีซีออปโทด ตรวจวัดสัญญาณเชิงแสงด้วยกล้องถ่ายรูปดิจิตัลและคำนวณความเข้มสีด้วยโปรแกรม ImageJ ออปโทดกระดาษตอบสนองต่อไทโอไซยาเนตโดยเปลี่ยนสีจากชมพูเป็นเขียว ใช้ CCD กับ RSM ศึกษาความเข้มข้นของไอโอโนฟอร์และไอออนเอกซ์เชนจ์เจอร์ที่แสดงสีน้ำเงินต่ำที่สุด อีกทั้งออปโทดกระดาษตอบสนองต่อไทโอไซยาเนตเหนือกว่าแอนไอออนชนิดอื่น ที่ช่วงความเข้มข้น $1.00\times10^{-7} – 1.00\times10^{-2}$ โมลาร์ ขีดจำกัดการตรวจวัดของออปโทดกระดาษที่มีไอโอโนฟอร์ L2 และ L3 ต่อไทโอไซยาเนต เท่ากับ 7.00×10^{-6} และ 1.26×10^{-6} โมลาร์ ตามลำดับ นอกจากนี้ยังนำอุปกรณ์รับรู้ไปประยุกต์ใช้ตรวจวัดไทโอไซยาเนตในตัวอย่างปัสสาวะของกลุ่มตัวอย่างที่สูบบุหรี่และไม่สูบบุหรี่ได้สำเร็จและได้ผลอย่างน่าพอใจเมื่อเทียบกับเทคนิคไอออนโครมาโทกราฟี (IC)

สาขาวิชา เคมี ลายมือชื่อนิสิต .....
ปีการศึกษา 2562 ลายมือชื่อ อ.ที่ปรึกษาหลัก .....

5772849423 : MAJOR CHEMISTRY
KEYWORD: Ion-selective electodes, Paper-based optode, Perchlorate ion, thiocyanate ion, central composite design

Supacha Wirojsaengthong : DETERMINATION OF PERCHLORATE AND THIOCYANATE IONS BY ION-SELECTIVE MEMBRANE AND BULK OPTODE TECHNIQUES USING EXPERIMENTAL DESIGN APPROACH. Advisor: Assoc. Prof. Dr. WANLAPA AEUNGMAITREPIROM

This research aimed to develop the detection method for perchlorate and thiocyanate in aqueous solutions using potentiometric and colorimetric techniques. The optimum conditions were designed by the central composite design (CCD) with response surface methodology (RSM). The potentiometric response of perchlorate–selective electrode using di–tripodal amine calix[4]arene copper(II) complex (L1-Cu) in PVC membrane was studied. The optimized pH, ion exchanger and ionophore concentrations were found at pH 8.0, 3.25 mmol/kg and 13.25 mmol/kg, respectively. The optimized condition performed a Nernstian slope of –58.02 mV/decade with R^2=0.9994 in a working concentration range of 1.00×10^{-6} – 1.00×10^{-2} M, and the detection limit was 3.00×10^{-5} M. This membrane showed the highest selectivity toward perchlorate in comparison with other anions. Moreover, the paper–based optode sensing device was successfully developed for the determination of thiocyanate in aqueous solution based on colorimetric analysis. The metalloporphrin ionophores including 5,10,15,20–tetrakis(4–methoxyphenyl)porphyrine cobalt(II) complex (L2) and 5,10,15,20–tetrakis(4–octhyloxyphenyl)porphyrine cobalt(II) complex (L3) were used and coupled with ion exchanger in PVC optode. Optical responses were detected by a digital camera and color intensity was calculated by imageJ program. The paper–based optode were responded to thiocyanate by changing its color from pink to green. The CCD with RSM was also used to investigate the optimized concentration of ion exchanger and ionophore resulting in the lowest *Blue* value. In addition, the paper–based optode responses to thiocyanate with the highest selectivity among other anions with the dynamic range 1.00×10^{-7} – 1.00×10^{-2} M. The LOD of the paper–based optode containing L2 and L3 ionophore were 7.00×10^{-6} and 1.26×10^{-6} M of SCN^-, respectively. Furthermore, this study was successfully applied as a sensing device to detect thiocyanate in urine sample from smoker and non–smoker with favorable agreement with ion chromatography technique.

Field of Study:	Chemistry	Student's Signature .....
Academic Year:	2019	Advisor's Signature .....

ACKNOWLEDGEMENTS

My 10-year of B.Sc. and Ph.D. journey at the Department of Chemistry, Chulalongkorn University would not have been completed without the continuous encouragement from my advisor, Associate Professor Dr. Wanlapa Aeungmaitrepirom. She has been constantly given me numerous opportunities, understanding, guidance, and patience. I could not imagine having a better advisor than her. Also, I would like to express my gratitude to my dissertation committee members: Associate Professor Dr. Vudhichai Parasuk, Professor Dr. Thawatchai Tuntulani, Assistant Professor Dr. Passapol Ngamukot, and Assistant Professor Dr. Wanwisa Janrungroatsakul for their valuable ideas, comments, and suggestions.

I am grateful to Supramolecular Chemistry Research Unit for the synthesis of L1 ionophore, Dumrongsak Aryuwananon and Associate Professor Dr. Buncha Pulpoka for the synthesis of L3 ionophore. I also would like to thank Associate Professor Dr. Kanet Wongravee for his valuable comments and suggestion of experimental design part in this work.

My sincere thanks also go to Professor Eric Bakker for the great opportunity to join his group as intern at University of Geneva. He is a model scientist who given me experience to conceive the research in electrochemistry.

Also, I would like to thank everyone in the Environmental Analysis Research Unit (EARU) for their discussions, help and support. I gratefully acknowledge the financial support from Development and Promotion of Science and Technology Talents Project (DPST) throughout my study.

Finally, I am also grateful to have the continuous support from my family, my professors, and my friends. Especially, I am grateful for my Mom and Dad for love and support throughout my life.

Supacha Wirojsaengthong

TABLE OF CONTENTS

Page

TABLE OF FIGURES

Page

TABLE OF TABLES

Page

CHAPTER I

INTRODUCTION

1.1 Statement of the problem

Anions play a key roles in biochemical and physiological function in living species especially human such as hormone transportation, DNA regulation, protein synthesis, and the enzyme activity [1]. Therefore, the anion recognition and sensing field have become one of the most important areas of analytical chemistry in many application areas including clinical analysis [1], environmental monitoring [2], pharmacological study [3], food quantification [4] and industrial applications [5, 6]. Perchlorate (ClO_4^-) and thiocyanate (SCN^-) are one of the several anions that can competitively disrupt the iodide transportation into thyroid gland [7], thus inhibiting thyroid hormone production. Since iodide is essential for the production of thyroid hormones (THs), the blocking of iodide by perchlorate and thiocyanate is important effect. The thyroid hormones play an important activity in many physiologic functions in human body via nervous system development in children and endocrine system. These effects notice by the United States Environmental Protection Agency (USEPA) that perchlorate and thiocyanate consumption must be limited due to the potentially effects to normal thyroid function. Perchlorate and thiocyanate can enter the body through eating and smoking habits and can be found to exist at low concentrations in biological fluid such as serum, urine and saliva. These ions can be found in surface water [6, 8], groundwater [9], drinking water[10, 11], milk [12, 13], fish [14], soil [8], vegetable [15] and rice [11]. Perchlorate salt has been used in rocket and missile industries as an oxidizing agent in solid powder [10, 16]. Moreover, thiocyanate is a detoxification product degraded from inorganic cyanide in the liver. It is therefore the biomarker for inorganic cyanide which comes from tobacco smoke. Thiocyanate salt has been used in agriculture, dyeing and printing of photography, textiles and paints, gold mine [17] and petroleum field.

Several analytical methods can be used for anion determination such as spectrometric [18-21] and chromatographic [22] methods. Despite, the advantages of these methods are the low limit of detection and the multielemental analysis. These methods have some drawbacks such as complicated procedures, skilled operator requirement, time consuming and high cost. Thus, the low cost, easy and simple methods are required to overcome these disadvantages such as ion–selective electrodes (ISEs) and bulk optode technique. Additionally, an experimental design approach has many advantages which are used to investigate the maximum efficiency with the minimum number of the experiments.

1.2 Objective and scope of the research

This research aimed to develop a quantification method for perchlorate and thiocyanate in aqueous solutions using ion–selective electrodes (ISEs) and bulk optode technique. The potentiometric response of ion–selective electrode using poly(vinyl chloride) membrane was studied. The electrode membrane containing di–tripodal amine calix[4]arene (**L1**) in $CuCl_2$ were prepared. Meanwhile, the paper–based optode was developed for the determination of anions in aqueous solution based on colorimetric analysis using 5,10,15,20-tetrakis(4-methoxyphenyl)porphyrin cobalt(II) complex (**L2**) and 5,10,15,20-tetrakis(4-octhyloxyphenyl)porphyrin cobalt(II) complex (**L3**) as an ionophore. The structures of these ionophores are illustrated in **Figure 1.1**. Optical responses were detected by a scanner and the color intensity was calculated by imageJ program. Both ISE and bulk optode techniques were studied using the central composite design (CCD) with response surface methodology (RSM) to evaluate the optimum conditions of these methods.

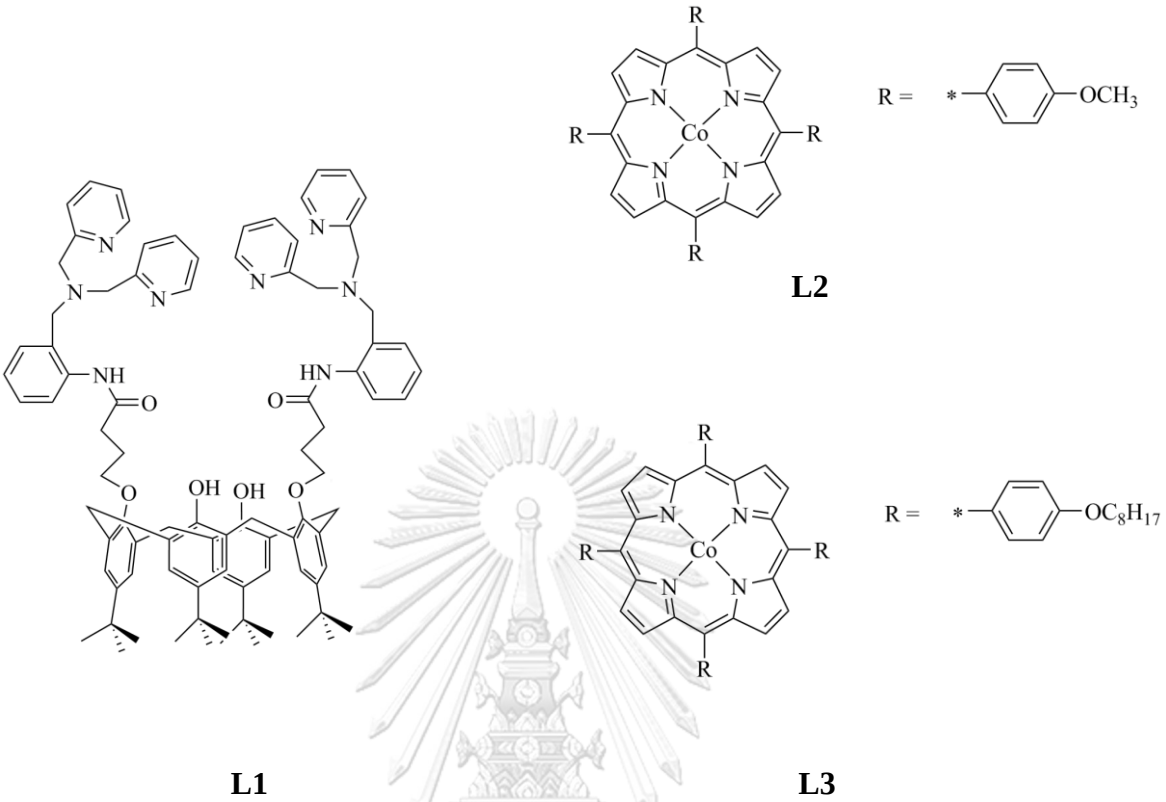

Figure 1.1 Structures of di–tripodal amine calix[4]arene (**L1**), 5,10,15,20–tetrakis (4–methoxyphenyl)porphyrin cobalt(II) complex (**L2**) and 5,10,15,20–tetrakis (4–octyloxyphenyl)porphyrin cobalt(II) complex (**L3**)

1.3 Benefits of this research

The determination of perchlorate and thiocyanate in aqueous solutions was achieved by ion–selective electrodes (ISEs) and bulk optode technique using the central composite design (CCD) with response surface methodology (RSM) approach.

CHAPTER II

THEORY AND LITERATURE REVIEW

2.1 Anions

A living organism's body contains a variety of ions to involve a various functions. In terms of body functioning, anions are a key which promotes system in body including contributing osmotic pressure gradient and maintaining the body's acid–base balance. Despite the anions are significant ions for human body system, the oversaturated anion concentration provides some toxicity. In the review of the physiological effects of anions, the first study was demonstrated by Hofmeister in 1888 [23] that neutral sodium salts of anions could differ to precipitate egg albumen. From the results, they obtained the sequence of the limiting molar concentrations at which the different salts effected the precipitation of that protein and also showed the same trend as lipophilicity of the ions known as Hofmeister series: $C_6H_5O_7^{3-} < SO_4^{2-} = C_4H_4O_6^{2-} < HPO_4^{2-} < CrO_4^{2-} < C_2H_3O_2^{-} < HCO_3^{-} < F^{-} < Cl^{-} < Br^{-} < I^{-} < NO_3^{-} < SCN^{-} < ClO_4^{-}$. As shown in the Hofmeister series, the most lipophilicity anions are perchlorate followed by thiocyanate which mean that the harmful of these two ions are need to be focus.

- Thiocyanate and perchlorate

One of the physiological effects in human body by thiocyanate and perchlorate is the reduced activity of thyroid hormone production via inhibit the iodide transportation into thyroid gland. Thyroid hormones are essential for normal growth, physical and mental development in human. Since iodine is a rate limiting substrate for thyroid hormone synthesis [7, 24]. The other anions such as thiocyanate and perchlorate which have similar size and charge to iodide can inhibit the accumulation of iodide in the thyroid gland.

Thiocyanate is anion which is normally found in the biological fluids of mammals such as blood, saliva, milk, and tears at a wide range of concentrations

[25-29]. Despite, thiocyanate has been used as a therapeutic agent for the treatment of hypertension [30] and lead to the observed thiocyanate values in plasma, the toxicity of thiocyanate are also presented. Thus, thiocyanate has been noticed both in host defense and as a detoxification product of cyanide. The thiocyanate toxicity shows as the symptoms that tended to be related to the nervous system, the thyroid, the kidneys, and the skin in patients. Thiocyanate enters the body through the diet or it is synthesized from cyanide by sulfurtransferase enzyme. The dietary intake of thiocyanate is based on the glucosidic cyanogen–rich plants and dairy product such as cauliflower, broccoli, kale, soybeans and cow milk [31]. Additionally, other sources of contamination of thiocyanate in human body include smoke from cigarettes, fires, plastic burning and vehicles via the body's utilization of sulfurtransferases to synthesis the resulting cyanide. For non–smoker, the normal concentration of thiocyanate in blood is in the range of 9.00×10^{-6} –2.40×10^{-5} M while smoker is in the range of 3.30×10^{-5} – 2.75×10^{-4} M [32]. The cyanide exposures are contributed from many ways for examples the use of cyanide in industrial including plastic manufacturing, electroplating, pesticides synthesis, paint processing and gold mining [17, 33].

Perchlorate is also in the similar size with iodide and can therefore be taken up in the thyroid gland resulting in the disruption of thyroid hormone production. Perchlorates can enter the body via ingestion, inhalation and skin contact of the contaminated substrates such as food and drinking water. Due to the toxicity of perchlorate, the US Environmental Protection Agency (US EPA) reported that perchlorate was contaminated ion in the final third Contamination Candidate List (CCL3) and existed in environment in various states in US [34]. Most of the perchlorate exposure found in environment is associated from both manmade and natural sources. The precipitation of trace level of perchlorate can be found from the naturally form in the atmosphere. Thus, perchlorate has been presented in soil, vegetation, groundwater, surface water and drinking water. It is typically found in the form of perchloric acid and salts such as sodium perchlorate, ammonium perchlorate, potassium perchlorate, and magnesium perchlorate. One of the perchlorate salts, ammonium perchlorate, is produced as an oxidizer in large amounts because it is used in rocket fuels, flares, vehicle airbags, batteries, and fertilizers.

Therefore, the necessity of the methods of perchlorate determination has been concerned. Several researches developed the methods for the detection of perchlorate and thiocyanate such as spectrophotometric and chromatographic methods. For thiocyanate detection, spectrophotometric method based on the complex formation with metal ions were investigated [18]. In addition, indirect spectrophotometric methods involving the precipitation and extraction for perchlorate detection were widely studied [20, 21]. The spectrophotometric and chromatographic techniques [35] have been widely demonstrated because of their various advantages such as good sensitivity. However, these methods provide some disadvantages including non–portable devices, high cost, required skilled operator, time consuming and complicated procedures. Therefore, the alternative techniques that can be used to determine cations and anions are investigated such as ion–selective electrodes (ISEs) and bulk optode technique.

2.2 Ion–selective electrodes (ISEs) [36]

Ion–selective electrodes are electrochemical sensors that response to one particular ion via the sensing part of electrode called ion–selective membrane. The response of particular ion in the solution is represented in term of the electrochemical potential across a ion–selective membrane and a solution of various concentration of analyte ion against a reference electrode as illustrated in **Figure 2.1**. The electrode potential is proportional to the logarithm of the activity of the analyte ion as described by the Nernst Equation as shown in **Eq. (2.1)**. In diluted solution, concentration can be used instead of activity without causing significant deviation.

$$E = E^{\circ} + \frac{2.303RT}{nF} + \log A \qquad \textbf{(2.1)}$$

where E is the measured potential,
E° is the standard electrode potential,
R is the gas constant ($J \cdot K^{-1} \cdot mol^{-1}$),
T is the absolute temperature (K),
n is the charge of ion,
F is the Faraday constant,
A is the activity of ion.

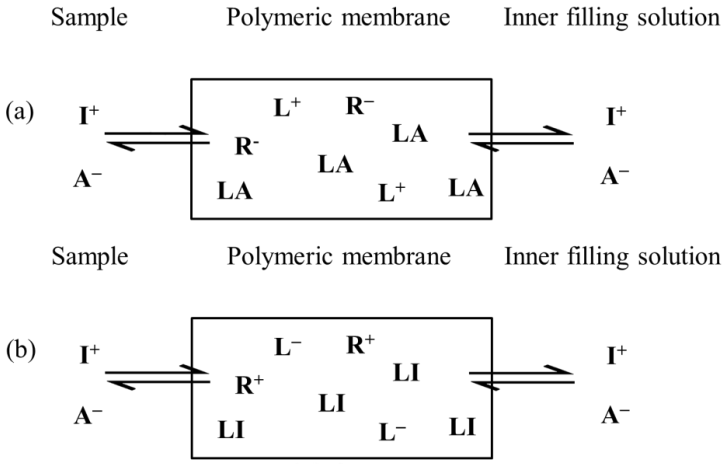

where L^+, L^- is the charged carrier, R^- is the anionic site, R^+ is the cationic site, I^+ is the target cation and A^- is the target anion.

Figure 2.1 Schematic views of the equilibria between sample, ion–selective membrane, and inner filling solution center (a) for the anion extraction, (b) for cation extraction.

The potentiometric devices compose of an ion selective membrane in ISE, a reference electrode and a potentiostat as shown in **Figure 2.2**.

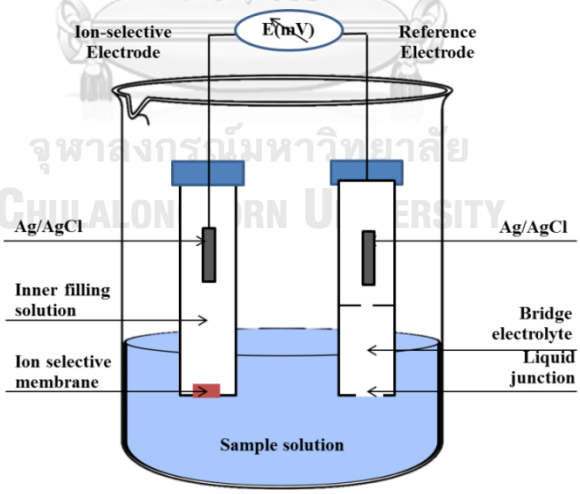

Figure 2.2 Electrochemical cell for potentiometric measurements using an ion–selective electrode and reference connected to a potentiostat electrode (modified from [37]).

2.2.1 Polymeric membrane of ISEs components

There are five categories of ISEs membranes: glass membrane electrodes, crystalline or solid–state electrodes, polymer membrane electrodes, gas sensing electrodes and enzyme membrane electrodes. The components of a selective membrane must selectively react or interact with the target ion.

The polymeric ion–selective membranes are composed of the components as shown below.

– Ionophore or ion carrier: the chemical that reacts with the target ion due to its lipophilic group. It is the key part of the polymeric membrane for transporting the particular ion across the hydrophobic membrane. Thus, the ionophore must have high selectivity to the target ion over the others to prevent the interference effect.

– Polymer matrix: the chemical that can mix all components to form homogenous membrane. The polymeric membranes are usually prepared with PVC, which has no interaction with the target ion.

– Plasticizer, which is used to form the membrane and transfer ion into the membrane.

– Ion exchanger: lipophilic salts containing anionic site (R^-) or cationic site (R^+) are used to maintain electroneutrality of membrane for cationaic and anionic analytes, respectively.

2.2.2 Electrode characteristics

2.2.2.1 Selectivity

One of the most significant characteristics of chemical sensor is the selectivity of the ion–selective membrane related to the strong complexation between ionophore and target ion. The key parameter related to the selectivity of membrane is called the selectivity coefficient ($\log K_{I,J}^{pot}$). It is associated to the equilibrium of the ionophore with primary ion (I) and interfering ion (J) between organic phase and aqueous phase. In theoretical, in a sample solution containing interfering ions as the same charge as the primary ion (analyte ion), those ions may be able to displace the primary ion from the ion selective membrane and lead to a deviation of potential from

the Nernst equation. An expanded Nernst equation may be used to describe this behavior which known as Nicolsky–Eisenman equation:

$$E = K_I + \frac{s}{Z_I}\log(a_I + \sum_{J \neq I} K_{I,J}^{pot} a_J^{Z_I/Z_J}) \qquad \textbf{(2.2)}$$

where $K_{I,J}^{pot}$ is the selectivity coefficient,

K_I is a constant potential value,

s is the Nernstian slope of 59.18 mV

Z_I and Z_J are charge of target ion (I) and interfering ion (J),

a_I and a_J are activity of target ion (I) and interfering ion (J).

From the equation, the zero value of $K_{I,J}^{pot}$ is an ideal value indicating no interference. However, there is no ion–selective membrane that absolutely specific for the particular ion. Then, the lower value of $K_{I,J}^{pot}$, the higher selective of membrane toward primary ion (I), is recommended.

Selectivity coefficients can be demonstrated experimentally by the separate solutions method (SSM) or the fixed interference method (FIM).

– Separate solutions method (SSM)

The potential in the solution is determined with each of two separate solutions, one containing primary ion while another one containing interfering ion. Then, the selectivity coefficience, $K_{I,J}^{pot}$ is calculated with the two obtained potential values by **Eq. (2.3)** as shown below and **Figure 2.3** illustrated the potentiometric response of primary ion (I) and interfering ion (J).

$$\log K_{I,J}^{pot} = \frac{Z_I F\{E(J) - E(I)\}}{2.303RT} + \log(a_I / a_J^{Z_I/Z_J}) \qquad \textbf{(2.3)}$$

where E(I) and E(J) are the measured potentials from the separate solutions for primary ion (I) and interfering ion (J) and a_I and a_J are the activities of I and J in the separate solutions.

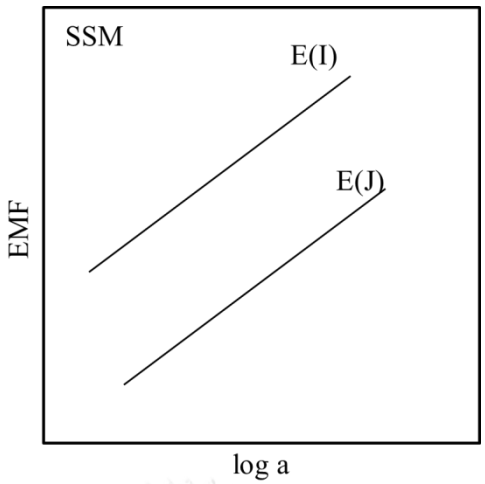

Figure 2.3 Schematic of the ion–selective membrane selectivity determined by SSM (modified from [36, 38]).

– Fixed interference method (FIM)

For this method, a Nernstian response for the primary ion is measured in a constant background of interfering ion. The selectivity coefficient, $K_{I,J}^{pot}$ is calculated using **Eq. (2.4)** which is shown the preferring of ISE to primary ion toward interfering ion in the same solution. As illustrated in **Figure 2.4**, a_J (BG) is the activity of the fixed interfering ion concentration in the solution as the background. a_I (DL) is the limit of detection obtained via the Nernstian response.

$$\log K_{I,J}^{pot} = \log(a_I(DL)/a_J(BG)^{z_I/z_J}) \qquad \textbf{(2.4)}$$

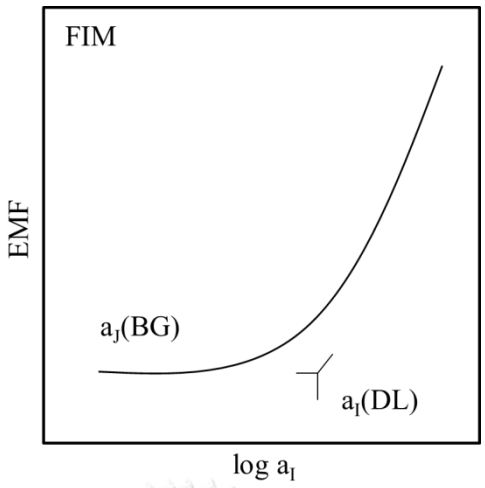

Figure 2.4 Schematic of the ion–selective membrane selectivity determined by FIM (modified from [36, 38]).

2.2.2.2 Limit of detection

The calibration curve of ion–selective electrode as the function of potential and the activity of ion also provides a lower and upper detection limit where the potentiometric response significantly deviates from a Nernstian electrode slope. According to the IUPAC recommendation in 1976, the detection limit is defined by the cross–section of the two extrapolated linear portions of the calibration curves [38] (see **Figure 2.5**).

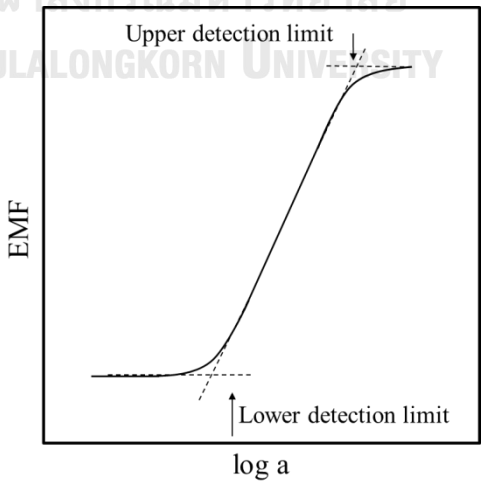

Figure 2.5 Schematic of definition of the upper and lower detection limits of an ion–selective electrode via the IUPAC recommendations (modified from [36, 38]).

There are two key possible factors for the loss of sensitivity or the deviation of Nernstian response slope at low primary ion activities. The first point is the interference of the competing ions or interfering ions. Another point is the leaching of the primary ions from the membrane phase into the sample lead to the perturbation of the interfacial sample activity of the membrane. In addition, the activity ratio of upper and lower detection limits is defined as the measuring range of ISEs.

2.2.2.3 Response time

Another important performance of the chemical sensors is the response time. Ideally, the response time for ion–selective membranes depends on the time required for the boundary concentrations in the diffusion layer to equilibrate with the sample bulk. The fast response time indicates the good sensitivity of the ISEs. According to the IUPAC recommendation in 1976 [38], the time when an ion–selective electrode and a reference electrode are brought into a first contact with a sample solution (or at which the activity of the analyte ion in a solution is changed) and the first point at which the emf/time slope (ΔE/Δt) becomes equal to its steady–state value within 1 mV, as illustrated in **Figure 2.6**.

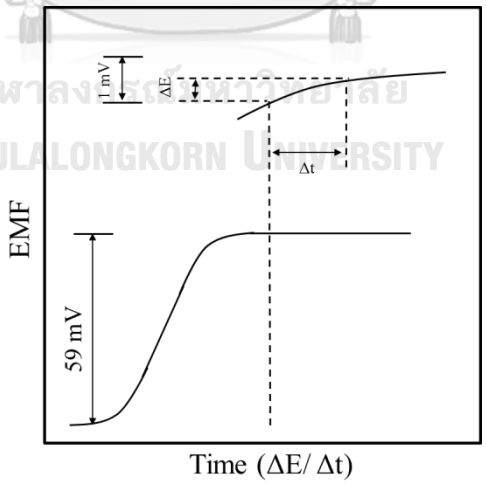

Figure 2.6 Schematic of definition of the response time of an ion–selective electrode via the IUPAC recommendations (modified from [38]).

2.3 Bulk optode technique [36]

Bulk optode technique or ion–selective optical sensor is one of the optical methods as the chemical sensors for determination an analyte by the change of the optical properties via the mass transfer of target ions in aqueous solution into optode membrane (**Figure 2.7**) as similar as the response mechanism of the ISEs. The optodes are also based on the equilibrium system between organic phase (polymeric membrane) and aqueous phase (sample solution). They consist of that necessary for extraction of the analyte ions such as ionophore, complexing agent, and ion carrier with the optical properties change.

The polymeric optode membranes are composed of the components found in ion selective membrane as described in the ion–selective electrode part, including chromoionophore (C) which is the chemical that has optical response to proton in the system. In case that the optical properties changing after ionophore react with the target ions, the chromoionophore is not necessary.

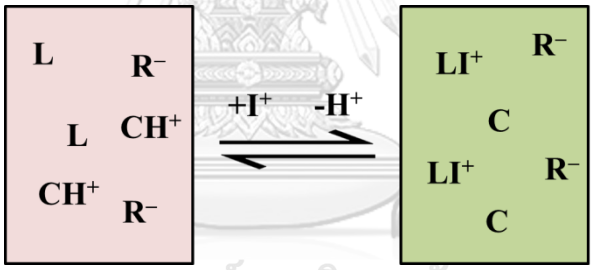

Figure 2.7 The equilibrium between the ionophore in the bulk optode membrane before and after forming complex with cation.

The equilibrium equation [39] is shown below.

$$zCH^{+}_{(org)} + nL_{(org)} + I^{z+}{}_{(aq)} \rightleftharpoons IL^{z+}_{n(org)} + zC_{(org)} + zH^{+}{}_{(aq)} \qquad \textbf{(2.5)}$$

where I^{Z+} is the target ion,

IL_n^{z+} is the ionophore–ion–complex,

L is the ionophore,

CH^+ is the protonated chromoionophore,

C is the deprotonated chromoionophore,

with the corresponding exchange constant:

$$K_{exch}^{IL_n} = \left(\frac{a_H[C]}{[CH^+]}\right)^z \frac{[IL_n^{z+}]}{a_I[L]^n} = \left(\frac{K_a}{k_H}\right)^z k_I \beta_{IL_n} \qquad \textbf{(2.6)}$$

To investigate a relationship between a signal S and ion activity a_I, **Eq. (2.6)** shows the activity of the analyte ion in the sample solution. Moreover, the signal has to be correlated with the protonation degree of the chromoionophore, which introduces another correlation:

$$1-\propto = \frac{[CH^+]}{C_T} \qquad \textbf{(2.7)}$$

where C_T is the total chromoionophore concentration in the optode from the membrane preparation. Therefore, the concentrations of protonated chromoionophore in the organic phase can be indicated in terms of the protonating degree 1−α and the total chromoionophore concentration. The remaining unknowns in the organic phase are the deprotonated chromoionophore [C], the uncomplexed ionophore concentration [L], and the ionophore–ion–complex concentration $[IL_n^{z+}]$. Mass and charge balances are therefore introduced to replace the unknown parameters. The total amount of chromoionophore or ionophore given by the mass balance is equal to the sum of all compounds containing the species:

$$C_T = [CH^+] + [C^0] \qquad \textbf{(2.8)}$$

$$L_T = n[IL_n^{z+}] + [L] \qquad \textbf{(2.9)}$$

Then, the charge balance is also presented resulting in the total positive charges which equal to the concentration of the anionic additive:

$$R_T = [CH^+] + n[IL_n^{z+}]. \qquad \textbf{(2.10)}$$

Finally, all terms have been inserted into the exchange constant in **Eq. (2.6)**, replace $[CH^+]$ with the protonation degree from **Eq. (2.7)**, and solve for the activity of the analyte ion a_I to obtain the response function:

$$a_I = \frac{1}{zK_{exch}^{CH^+,Ln I^{z+}}} \left(\frac{a_H \propto}{1-\propto}\right)^z \frac{R_T-(1-\propto)C_T}{\{L_T-z^{-1}n[R_T-(1-\propto)C_T]\}^n}, \qquad \textbf{(2.11)}$$

where the α is the relative portion of the deprotonated form of the chromoionophore (α = [C]/C_T). Because the optode membrane is in chemical equilibrium with the sample solution, the ratio of free sample ion activities (a_I/a_H^z) is measured. A sigmoidal response function is obtained by **Eq. (2.11)**. And, **Eq. (2.12)** described the experimental absorbance A at a given equilibrium can be correlated to α by measuring the absorbances of the fully protonated form (A_P) and deprotonated form (A_D) of the chromoionophore

$$\propto = \frac{A_P-A}{A_P-A_D} \qquad \textbf{(2.12)}$$

2.3.1 Ion–selective optode characteristics

2.3.1.1 Limit of detection

The limit of detection of ion–selective optodes is considered by various parameters, including interfering ions, the noise from the instrument, loss of sensitivity due to the sigmoidal response curve and response time. As shown in **Figure 2.8**, the detection limit can be predicted from the sigmoidal function of calibration curve.

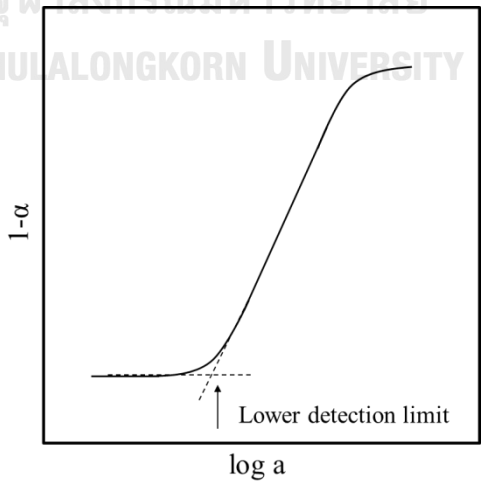

Figure 2.8 The sigmoidal response of the 1–α and the activities of analyte ion (modified from [38]).

2.3.1.2 Response time

Due to the ion–selective optodes are based on the quilibrium of extracting the analyte in the sample phase into the bulk of the membrane, the response time results in significantly longer than achieved via comparable interface–based techniques, including ionophore–based ion–selective electrodes. The response time of the ion–selective optode based on polymer with a thickness approximately around micrometers, is normally dominated by the diffusion time in the bulk of the membrane.

2.3.2 Quantitative analytical signal for optical sensors [40, 41]

According to the conventional basic of ion–selective optode, the sigmoidal responses of the optode are calculated by **Eq. (2.11)** with measured the optical response from the conventional optical signal including absorbance and fluorescence. The recent studies introduce the alternative optical detector such as camera and scanner provided the optical signal in term of color values. There are many types of color value: RGB(red–green–blue), HSVcolor space and etc. [42] where could be obtained by analysis the image with the ImageJ software. These color data have been presented as a quantitative analytical parameter for optical sensors instead of the protonating degree, 1−α as calculated follows Boltzmann equation [41, 43] as shown below:

$$\mathbf{H = \frac{A_1 - A_2}{1 + e^{\log[K(I)] - x_0/dx}} + A_2} \qquad \textbf{(2.13)}$$

where H denotes the color value, A_1, A_2, x_0 and dx are the data set for adjusting coefficients to give an excellent correlation. The sigmoidal response functions for quantitative colorimetric detection are demonstrated as **Figure 2.9**.

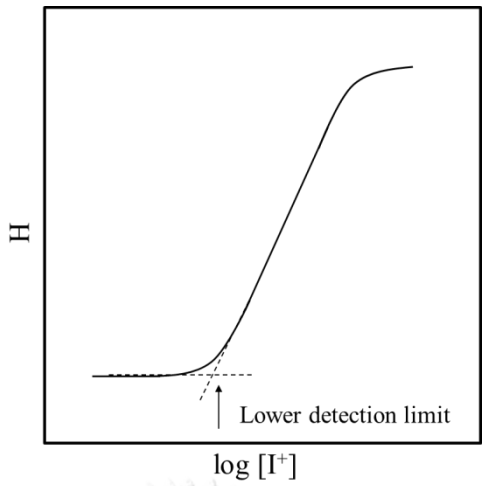

Figure 2.9 The sigmoidal response of the color detection and the concentration of analyte ion via Boltzmann equation (modified from [41]).

2.4 Metal complex as ionophore for anion–selective electrodes and anion–selective optodes

In order to focus on the sensitivity and the recognition ability of chemical sensor, the most important component of the polymeric membrane is the ionophore since the selectivity of chemical sensors including both ion–selective electrodes and ion–selective optode is based on the extraction of target ion with the ion carrier or ionophore. Various researches studied anion recognition via an ionophore or anion receptor development based on the interaction between their binding site including hydrogen-bonding groups, quaternary ammonium centers, Lewis acids, and cationic metal ions [44, 45]. The ionophores with the various functional groups have been widely developed, designed and applied to extract or form complex with the target anions. Due to the stability constant, steric effect and coordination of the central atom, capability of the ligand exchange, hydration and solvation energies, and spectral properties of metal coordinated complex, they are very popular ligand for anion recognition field. For example, **Figure 2.10** shows the structures of the ionophores that are organometallic compounds of palladium and cobalt. Besides, metal calixarene complexes and metalloporphyrins are interesting to use as anion hosts.

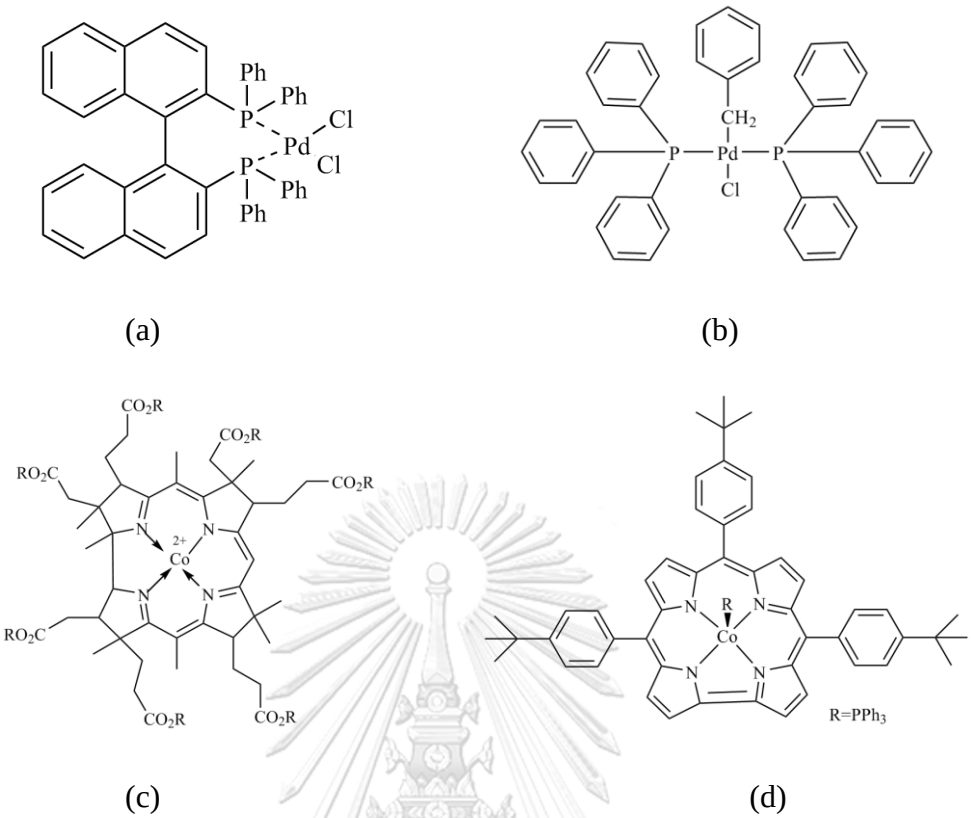

(a) (b)

(c) (d)

Figure 2.10 The structures of ionophores for anion detection (a) bis(diphenylphosphino)–1,1'–binaphthyl]palladium(II) dichloride [46], (b) benzylbis(triphenylphosphine)paltadium(II)–chloride [46], (c) Co(II) cobyrinate [47] and (d) Co(III) corrole [48].

2.4.1 Calix[4]arene based anion ionophores

Since the ionophore used for the ion–selective and optode membranes should has high lipophilic to immobilise in the organic phase or polymeric membrane which is hydrophobic, it is important that the ionophore must consist of the lipophilic part. Calixarene derivatives are macrocyclic compounds capable of forming a cup–liked shaped conformation and via their high lipophilicity, the stability of ligand is increased. Generally, the calixarenes are used as a building block. Not only the calixarenes provide high lipophilicity, but they can be created with the variety of the binding group. The cup–liked conformation of calixarene is stabilized by hydrogen–bonding interactions, and this allows the ligand to act as a host for a variety of suitably guests. Therefore, they are attractive ionophore due to they can be designed

with a various functional group as a binding site at the upper rim and the lower rim of the structure (see in **Figure 2.11**). One of the famous designs of the calixarene derivative ligand for anion recognition is to form complex with metal ion due to the electrostatic interaction between metal ion at the center of the calixarene containing a functional group as a binding site at the upper rim and target anion.

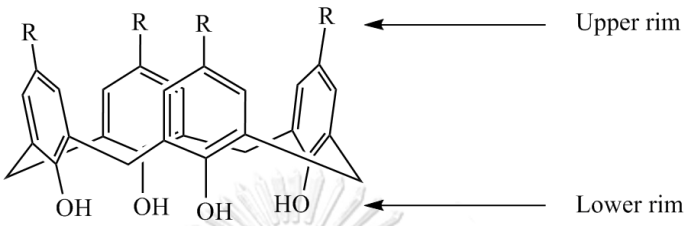

Figure 2.11 Cup–liked conformation of the calix[4]arene.

Although, the calix[n]arene has been widely used as the ionophore for anions sensing in several researches (shown in **Table 2.1** and their structures are illustrated in **Figure 2.12**), but the design and the development of the calix[n]arene–based ionophore are still challenging to improve the specificity and selectivity of our target anions.

Table 2.1 The calix[n]arene–based as an ionophore in anion–selective electrode.

Target anion	Ionophore	Slope (mV/decade)	Detection limit (M)	Ref.
$CH_3CO_2^-$	**A1**	ΔE = 155 mV (solid–state electrode)	–	[49]
CO_3^{2-}	**A2**	–22.9	1.2×10^{-4}	[50]
HPO_4^{2-}	**A3**	–33.0	5.0×10^{-5}	[51]
Cl^-	**A4**	–55.69	2.51×10^{-5}	[52]

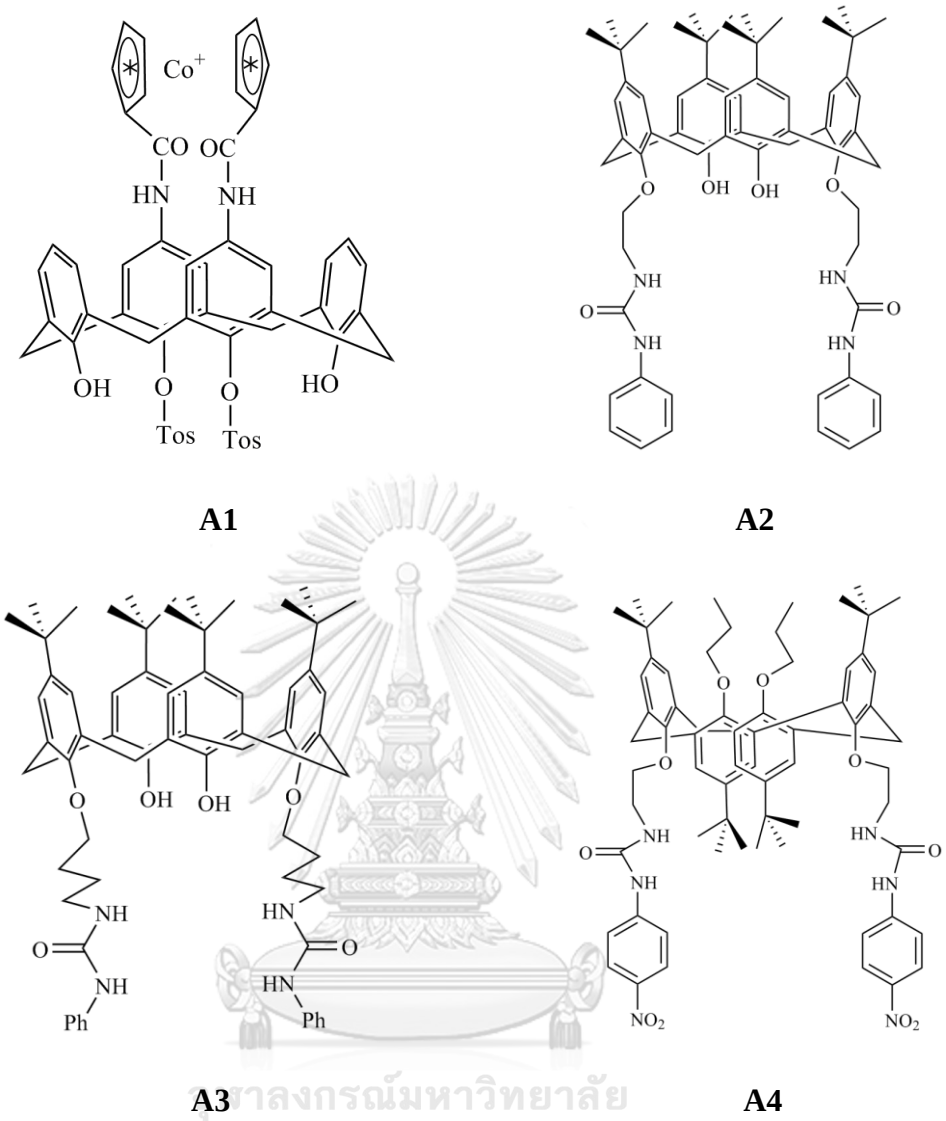

A1 **A2**

A3 **A4**

Figure 2.12 The structures of calix[4]arene derivatives.

2.4.2 Metalloporphyrin

The spectroscopic, lipophilic and chemical properties of porphyrin conjugates make them outstanding candidates used as the ionophore. Porphyrin consists of lipophilic structure which is favorable to use as the building block for ion recognition in chemical sensors. Besides, porphyrins also have the absorption and emission properties in the UV, visible, and near–infrared spectral regions which are the ability for optical sensors.

The form of porphyrin is a planar structure with four nitrogens which provides a vacant site at its center and can chelate strongly with metal ion in the center as a tetradentate ligand with metal ions called a metalloporphyrin (**Figure 2.13**). The metal ions behave as Lewis acids, obtaining lone pairs electrons from the porphyrin ligand. Their colors are originated from the absorption within the porphyrin ligand associated the excitation of electrons from π to π* porphyrin ring orbitals. Each metalloporphyrin complex has different spectroscopic properties via the various metal ions in the center as illustrated in **Figure 2.14**.

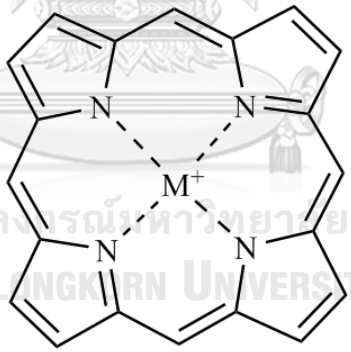

Figure 2.13 The structure of metalloporphyrin.

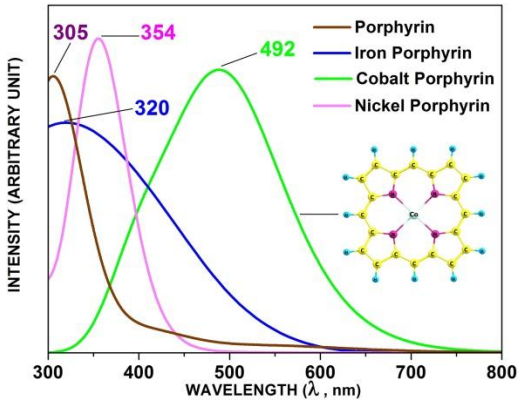

Figure 2.14 Optical absorption spectra of metalloporphyrin with different metal ions (reprinted from Publication [53] with permission from Elsevier).

Depend on the metal ions coordinated with porphyrin, the selectivity of metalloporphyrin ionophores behave differently with exhibit varied interactions with anions as can been seen in **Table 2.2** and some structures of metalloporphyrin ionophores are illustrated in **Figure 2.15**.

Table 2.2 The metalloporphyrins –based as an ionophore in anion–selective sensor.

Target anion	Ionophore	Method	Ref.
F^-	Zr(IV)–tetraphenyl porphyrins (**A5**)	Ion–selective electrode	[54]
	Al(III)– picket–fence porphyrin Ga(III)–octaethylporphyrin (**A6**)	Ion–selective electrode	[55]
	Al(III)–octaethylporphyrin	Ion–selective electrode	[56]
	Sc(III)–octaethylporphyrin	Optical sensor	[57]
		Flow–injection optical sensor	[58]
Cl^-	In(III)–octaethylporphyrin	Flow–through optical ion/gas sensors	[59]
	In(III)–octaethylporphyrin	Anion–selective optical sensors	[60]
	In(III)–octaethylporphyrin	Fluorescent nano–optical probes	[61]
	In(III)–octaethylporphyrin	Potentiometric and optical determination with flow system	[62]
NO_3^-	Co(II)–tetraphenylporphyrin	Ion–selective electrode	[63]
	Co(II)–deuteroporphyrin (**A7**)	Ion–selective electrode	[64]
SCN^-	Co(II)–methoxyphenyl porphyrin (**A8**)	Ion–selective electrode	[65]
	Mn(III)–triphenylphenyl porphyrin	Flow injection ion–selective electrode	[66]
$C_7H_5O_3^-$	Sn(IV)–tetraphenyl porphyrins	Ion–selective electrode	[67]
	Cr(III)–tetraphenyl porphyrin	Ion–selective electrode	[68]

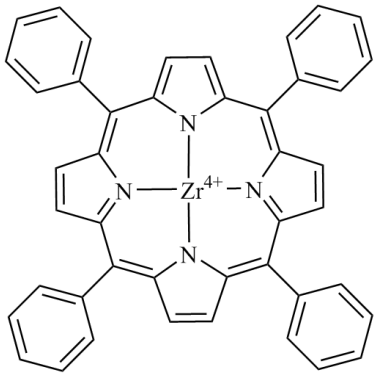

A5

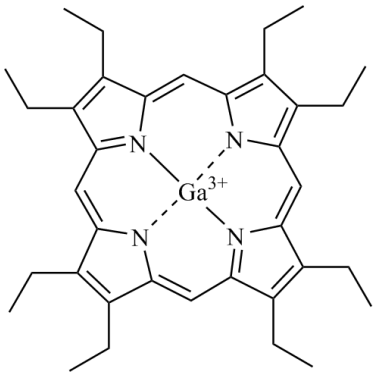

A6

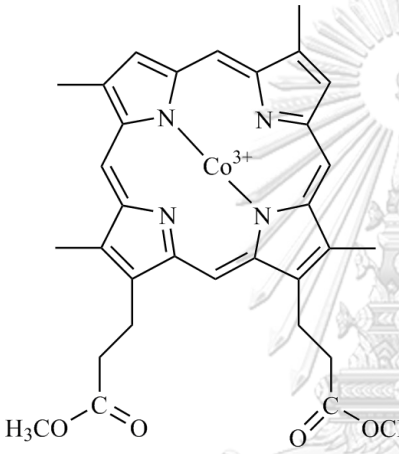

A7

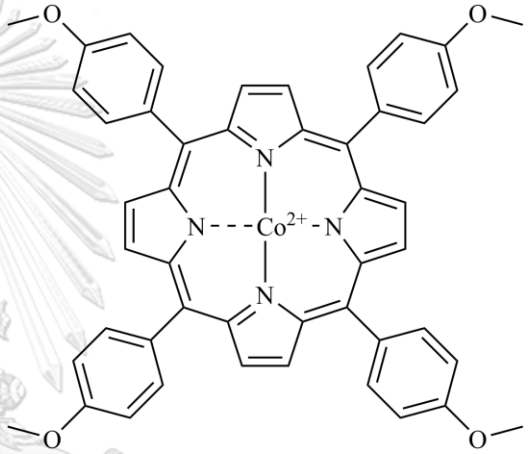

A8

Figure 2.15 The structures of metalloporphyrin ionophores.

2.5 Experimental design

To improve the analytical performance of chemical sensors, the optimization of the related factors in detection condition in the chemical reaction and the experiment is investigated. Basically, the optimization of the experiments is monitoring the maximum efficiency response which effected from single factor at the time while the other factors are a constant value called one factor at a time method. This method is used in a system when the factors do not interact with other factors. This means that if an interaction among the factors is relevant such as temperature, reaction time and synthetic yield, the experiments are the various temperatures with one level of reaction time. However, the effect of the temperature is dependent on the reaction time. It means that the result optimized condition from one factor at a time method is not the best condition to give the highest efficiency.

2.5.1 Central composite design (CCD) [69]

The experimental design is another approach to optimize the experimental conditions which is the alternative method that monitoring the relationship between multiple factors and obtain the maximum response condition using the minimum amount of experiments. Thus, there are many advantages of the experimental design approach, i.e. screening (obtain the strongly influencing factor), optimization (investigate the optimized condition with the highest efficiency), saving time and quantitative modeling (predict the response from experiment without laboratory). The experimental design approach has many design methods such as full factorial design, fractional factorial design and CCD. Choosing the experimental design approach depends on the number of the interest effected variables and the chemical system. Even though the experimental design is to reduce the number of the experiments, some design i.e. full factorial design cannot be used to demonstrate high number of factors because the design still will be included high number of experiments. Therefore, the CCD is an another design to indicate the best response.

To obtain the model in quadratic term, the CCD experimental design methods with 3 factors are studied which consists of three parts illustrated in **Figure 2.16**.

The CCD experiment can be divided into three parts:

- The first part (experiment 1–8 in **Table 2.3**) containing 8 experiments (three factors with two levels). The number of experiments is calculated by

$$N = l^k \quad \textbf{(2.14)}$$

where N is the number of experiment,

l is the number of level,

k is the number of independent variables.

- The second part (experiment 9–14 in **Table 2.3**) is the star points. The each star point value depends on the number of experiment.

- Last, the third part (experiment 15–20 in **Table 2.3**) is the replication of the experiment.

Table 2.3 The experiment using CCD with 3 factors

Experiment	Factor 1	Factor 2	Factor 3
1	–1	–1	–1
2	1	–1	–1
3	–1	1	–1
4	1	1	–1
5	–1	–1	1
6	1	–1	1
7	–1	1	1
8	1	1	1
9	–1.68	0	0
10	1.68	0	0
11	0	–1.68	0
12	0	1.68	0
13	0	0	–1.68
14	0	0	1.68
15	0	0	0
16	0	0	0
17	0	0	0
18	0	0	0
19	0	0	0
20	0	0	0

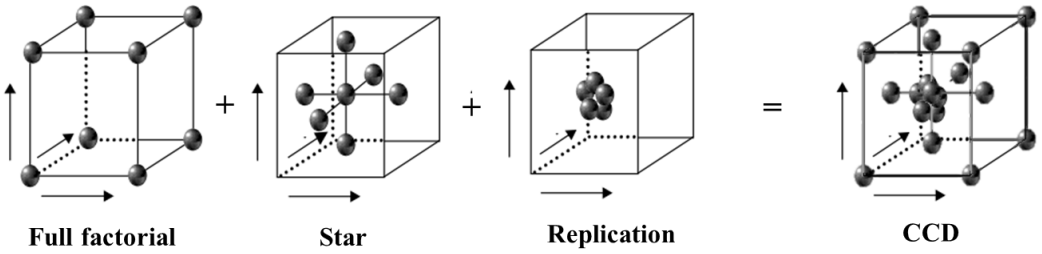

Figure 2.16 The experiment points with 3 factors using CCD shown in 3D box (modified from Ref. [69]).

2.5.2 Response surface methodology (RSM)

An alternative technique to present the model and analyze a process which can be calculated with various experimental design such as factorial design, the Box–Behnken design, the central composite design and Doehlert's design is called response surface methodology (RSM) [70]. The role advantage of RSM is to represent the relavant effects of the primary factors correspond to the response. It is highly effective for improving and optimizing the experimental conditions in order to obtain the most significant responses of the process. The experimental factors are considered as X_1, X_2, …,X_n of the individual independent parameter and y is the response. The regression model of these parameters with the individual, interaction and second order polynominal terms can be optimized an approximation of the function as following equation.

$$y = b_0 + \sum b_i X_i + \sum b_{ii} X_i^2 + \sum b_{ij} X_i X_j \qquad \textbf{(2.15)}$$

where b_0 is the constant coefficient, b_i, b_{ii}, and b_{ij} are the coefficients for linear, quadratic, and interaction effects, respectively, and X_i, X_j indicate the dependent variables.

To evaluate RSM of the experiment, it consists of three main steps [70]:

First step: the experiment is statistically designed using central composite design.

Second step: obtaining the coefficients of the mathematical regression model using multiple linear regression (MLR) technique [69] was used to calculated the

coefficients of each terms in the regression model by written in matrix form **Eq. (2.16)** as following **Eq. (2.17)**;

$$\begin{bmatrix} y_1 \\ y_2 \\ \vdots \\ \vdots \\ \cdot \\ y_n \end{bmatrix} = \begin{bmatrix} 1 & x_{11} & x_{12} & \cdot & \cdot & x_{1k} \\ 1 & x_{21} & x_{22} & \cdot & \cdot & x_{2k} \\ \vdots & \vdots & \vdots & \vdots & \vdots & \vdots \\ \vdots & \vdots & \vdots & \vdots & \vdots & \vdots \\ \cdot & \cdot & \cdot & \cdot & \cdot & \cdot \\ 1 & x_{n1} & x_{n2} & \cdot & \cdot & x_{nk} \end{bmatrix} \begin{bmatrix} \propto_0 \\ \propto_1 \\ \vdots \\ \cdot \\ \propto_k \end{bmatrix} + \begin{bmatrix} \varepsilon_1 \\ \varepsilon_2 \\ \vdots \\ \cdot \\ \varepsilon_n \end{bmatrix}, \qquad \textbf{(2.16)}$$

where all factors are square matrixes, y is the (n, 1) vector of measured responses, x is the (n, p) matrix of the mathematical model of factor levels, and α is the (p, 1) vector of unknown coefficients.

$$b = (D^T \cdot D)^{-1} \cdot D^T \cdot y \qquad \textbf{(2.17)}$$

where b is coefficients (M×1), D is design matrix (N×M), and y is response (N×1). And, M and N represent factors and samples amount, respectively.

Third step: evaluate the predicted responses using the observed regression model to calculate the response surface in order to optimize the optimum condition.

Finally, a surface response can be stimulated by plotting with the obtained equation which contains first order, quadratic, and interaction relationships as illustrated in **Figure 2.17**.

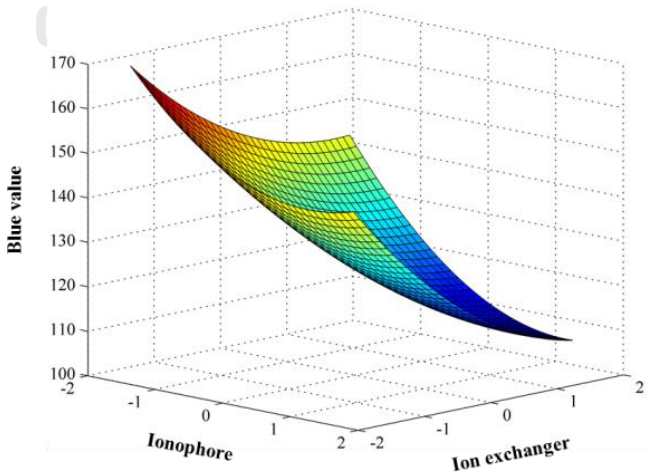

Figure 2.17 Example of surface responses of thiocyanate determination as the Blue value level in this work.

2.6 Literature review of thiocyanate and perchlorate determinations

Many analytical methods have been presented for thiocyanate and perchlorate detections. Ion selective electrode and bulk optode technique are one of the well-known techniques that can be used for determination of cations and anions. The recent studies investigated perchlorate and thiocyanate determinations by these two techniques. For both ion–selective and bulk optode methods, an ionophore is the key factor. Metal complex has been widely used as the ionophore via their electrostatic interaction between them and anion. For example, Abdel–Haleem and Rizk [71] developed the optical sensors using optode technique based on Mn(III)–salophen complex as an ionophore to detect thiocyanate in human saliva and spiked saliva sample. Vlascici and co–worker [65] presented the potentiometric response characteristics of a Co(II) porphyrin based electrode for thiocyanate determination. And, Kunthadee and co–worker [72] synthesized an ion carrier called di–tripodal amine calix[4]arene (**Figure 1.1**), which was applied as an anion sensors for thiocyanate, the results showed the highest selectivity towards perchlorate.

Table 2.4 The comparison of the proposed sensors with other works.

Target ion	Response mechanism/reagent	Detection instrument/method	LOD (M)	Ref.
SCN^-	Forming complex with Fe(III) sulfate	Photometer	1.79×10^{-6}	[19]
	Forming complex with Ag(I) catalyst	Visible spectrophotometer	2.00×10^{-9}	[18]
	Chromatography	HPLC-MS-MS	5.00×10^{-8}	[73]
	Film-based optode based on Mn(III)-salophen ionophore	UV-visible spectrophotometer	1.90×10^{-6}	[71]
	Flow injection with optode based on 5-octadecanoyloxy-2-(4-nitrophenylazo)phenol	UV-visible spectrophotometer	2.00×10^{-6}	[74]
	ISEs based on 5,10,15,20-tetrakis-(4-methoxyphenyl)-porphyrin-Co(II)	Potentiometric measurement	6.00×10^{-6}	[65]
	ISEs based on zinc(II)-tris(*N-tert*-butyl-2-thioimidazolyl)hydroborate complex	Potentiometric measurement	3.16×10^{-7}	[75]
ClO_4^-	Chromatography	Ion chromatography	4.97×10^{-5}	[76]
	Chromatography	Ion chromatography	1.49×10^{-5}	[77]
	ISEs based on Co(II) phthalocyanine complex	Potentiometric measurement	1.00×10^{-5}	[78]
	Flow-optode based on 5-octadecanoyloxy-2-(4-nitrophenylazo) phenol	UV-visible spectrophotometer	6.20×10^{-5}	[79]

As mentioned in **Table 2.4**, the ion selective electrode and bulk optode techniques have been demonstrated for the thiocyanate and perchlorate determinations. However, the sensitivity in term of the limits of detection of ISEs and optode methods showed lower that of the spectroscopy and chromatography techniques.

To improve the analytical characteristic performance, the development of the substrate for optode-based sensors is interesting. Generally, the material of the sensor using conventional bulk optode membrane is polymeric film while the other materials of the sensors have been developed to improve the advantages of the sensor such as paper and thread. The paper–based devices which are low cost, high surface to volume ratio and high ability to immobilize chemicals were studied. Pena–Pereira and co-worker [80] demonstrated the paper–based analytical devices based on bulk optode as the biomarker of thiocyanate in saliva from tobacco smoke. The results showed that the detection limit was 0.6 mM and the average thiocyanate levels found in non–smokers and smokers were 0.28–0.87 and 0.78–4.28 mM, respectively. The paper–based devices are focused not only for the enhancement of the sensitivity, but color change responses of the paper substrates are also easy to measure for example captured by camera or scanner.

CHAPTER III

EXPERIMENTAL

3.1 Chemicals

All chemicals were of analytical reagent grade listed in **Table 3.1**.

Table 3.1 Chemicals lists.

Chemicals	Companies
2–Nitrophenyl octyl ether (*o*–NPOE)	Sigma–Aldrich
4–*n*–Octyloxybenzaldehyde	TCI Japan
5,10,15,20-Tetrakis(4-methoxyphenyl)porphyrin cobalt(II) complex (**L2**)	Sigma–Aldrich
5,10,15,20-Tetrakis(4-octhyloxyphenyl)porphyrin cobalt(II) complex (**L3**)	Synthesized from SCRU*
Calcium chloride	Aldrich
Copper(II) chloride	Sigma–Aldrich
di-Tripodal amine calix[4]arene	Synthesized from SCRU* [72]
Hydrochloric acid	Merck
Magnesium chloride	Sigma–Aldrich
Magnesium sulfate	Sigma–Aldrich
Methanol	Merck
Nitric acid	Merck
Polyvinylchloride (PVC)	Sigma–Aldrich
Potassium chloride	Sigma–Aldrich
Potassium tetrakis(4–chlorophenyl)borate (KT*p*ClPB)	Sigma–Aldrich

Table 3.1 Chemicals lists (continue).

Chemicals	Companies
Propionic acid	Merck
Pyrrole	TCI Japan
Sodium (meta)arsenite	Aldrich
Sodium arsenate	Sigma–Aldrich
Sodium arsenite	Sigma–Aldrich
Sodium bicarbonate	Sigma–Aldrich
Sodium bromide	Sigma–Aldrich
Sodium chloride	Sigma–Aldrich
Sodium dihydrogen phosphate	Sigma–Aldrich
Sodium fluoride	Sigma–Aldrich
Sodium hydroxide	Sigma–Aldrich
Sodium iodide	Sigma–Aldrich
Sodium nitrate	Sigma–Aldrich
Sodium nitrite	Sigma–Aldrich
Sodium perchlorate	Sigma–Aldrich
Sodium sulfate	Sigma–Aldrich
Sulfuric acid	Merck
Tetrahydrofuran (THF)	Sigma–Aldrich
Toluene	Merck
Tridodecyl–methylammonium chloride (TDMACl)	Sigma–Aldrich

*SCRU = Supramolecular Chemistry Research Unit, Department of Chemistry, Faculty of Science, Chulalongkorn University

3.2 Ion–selective electrode (ISE) based on di–tripodal amine calix[4]arene copper(II) complex ionophore

3.2.1 Preparation of materials and experiment set up

3.2.1.1 Fabrication of polymeric membrane electrode

To prepare the polymeric membrane, a cocktail solution consists of di–tripodal amine calix[4]arene (**L1**), ion exchanger (KT*p*ClPB), and polymer (PVC) : plasticizer (*o*–NPOE); 1: 2 w/w in the total amount of 220 mg were dissolved in 2 mL of THF and stirred for an hour. Then, the cocktail solution was poured into a glass ring (22 mm in diameter). The solution was allowed to evaporate overnight to form transparent membrane (0.2–0.3 mm thickness). The membranes were cut by a hole puncher into 8 mm diameter. Before measurement, the membranes were conditioned in 1.00×10^{-2} M of $CuCl_2$ overnight and the sodium salt of primary ion for overnight. The scheme of the membrane preparation is illustrated in **Figure 3.1**.

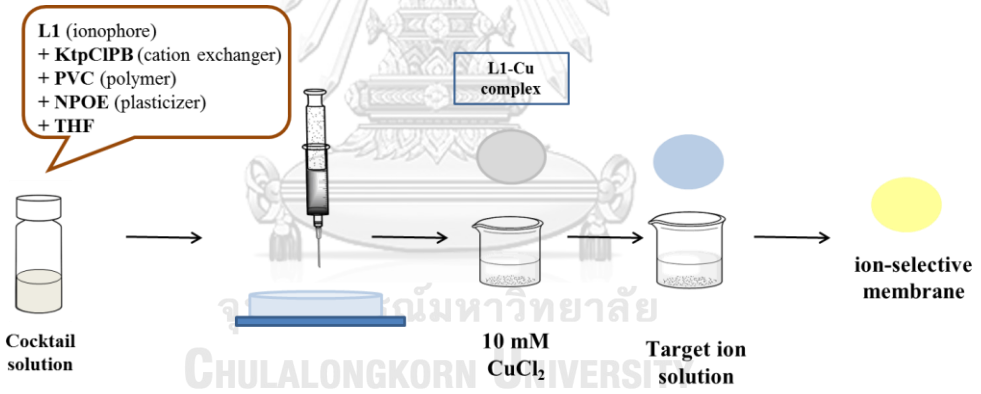

Figure 3.1 Schematic illustration of the fabrication of the ion-selective membrane.

3.2.1.2 EMF measurement

Potentiometric measurement were performed using a high impedance input 16–channels EMF monitor (Lawson Laboratories, Inc., Malvern, PA) with Ag/AgCl/3M KCl/1 M LiOAc as a reference electrode (Metrohm, Switzerland). The conditioned membrane was fitted into an electrode body. The mixed solution of 1.00×10^{-2} M primary anion and 1.00×10^{-3} M NaCl was filled into the electrode body as the internal filling solution. The potentials of ion–selective membrane were

measured at room temperature with the following set up (galvanic cell, two electrodes):

Ag, AgCl | 3 M KCl || 1 M LiOAc || sample solution | ion–selective membrane | inner filling solution (IFS) | AgCl, Ag

The potentiometric measurement was performed in the concentrations of target anion from 1.00×10^{-7} M to 1.00×10^{-2} M with stirring. In order to investigate the performance of prepared ion–selective membrane with the analyte anions, the activities of anions and the measured EMF were fitted according to **Eq. (2.1)**. The analytical performances including detection limit and working range were demonstrated with the IUPAC recommendations.

3.2.2 Central composite experimental design (CCD)

In this research, central composite design (CCD) was used as an experimental design. CCD was a box–like design covered with a spherical shape which used to optimize the amounts of ion exchanger and ionophore for electrode composition and pH of the sample solution. Next, each parameter was coded to avoid analytical bias from using different levels of each parameter. The code values of each parameter are shown in **Table 3.2**.

Table 3.2 Code values for pH and the amounts of ion exchanger (KT*p*ClPB) and ionophore (**L1**).

factor	**code**				
	–1.68	–1	0	1	1.68
pH	5.06	6.25	8.00	9.75	10.94
KT*p*ClPB (mmol/kg)	0.80	2.50	5.00	7.50	9.20
L1 (mmol/kg)	5.80	7.50	10.00	12.50	14.20

The following conditions of the ion–selective membranes was studied and optimized.

– The amount of ionophore in ion–selective membranes: 5.00–15.00 mmol/kg.

– The amount of ion exchanger in ion–selective membranes: 1.00–10.00 mmol/kg.

– The pH of sample solution from 4.0 – 10.0 (**Table 3.3**).

Table 3.3 Various buffer solutions at different pH.

pH	Type of buffer
4.0, 5.0, 6.0	0.01 M citric acid/citrate
7.0	0.01 M NaH_2PO_4/ Na_2HPO_4
8.0, 9.0, 10.0	0.01 M boric acid/borate

In order to design the experiment by CCD, 20 experiments were performed which represent each point inside a simulation box and sphere of all factor, as shown in **Table 2.3**. All experiments in the box were investigated for construction of a surface response plot.

For each point, the potentiometric measurement was performed in the concentration of target anion from 1.0×10^{-7} M to 1.0×10^{-2} M resulting in the response between the logarithm of anion activity and EMF. Then, the slope via Nernst equation was calculated from the relationship of the logarithm of anion activity and EMF and used to obtain the calculation in CCD process which provided the equation for prediction of the optimum value.

3.2.3 Selectivity

For selectivity study, the selectivity coefficients are the parameter which generally used to descript the selectivity performance of the ion–selective membrane toward the primary ion over other interfering ions. In order to calculate the selectivity coefficient, the experiment was demonstrated followed the detail in **section 2.2.2.1** in chapter 2.

In this work, the selectivity of purposed ion–selective membrane electrode towards primary anions (i) was determined by the separate solution method (SSM) by measuring in separate solutions of sodium salts of AsO_4^{3-} , SO_4^{2-}, $H_2PO_4^-$, NO_3^-, F^-, I^-, Br^-, Cl^-, SCN^- and ClO_4^- (1.00×10^{-7} M to 1.00×10^{-2} M) follows the Hofmeister selectivity pattern. The membranes were conditioned in 1.00×10^{-2} M $CuCl_2$ solution

for overnight and then conditioned in the solution of 10 mM Na_2SO_4 for overnight. The EMF measurements were performed in 10 mM separate solution containing SO_4^{2-}, followed by the other containing anions.

3.3 Paper–based optode

3.3.1 Fabrication of the paper–based optode

For the paper-based optode preparation (see **Figure 3.2**), a cocktail solution consisted of ionophore (**L2** or **L3**), tridodecyl–methylammonium chloride (TDMACl), and polymer (PVC) : plasticizer (*o*–NPOE); 1: 2 w/w in the total amount of 90 mg were dissolved in 2 mL of THF and stirred for an hour. Then, 4 µL of the cocktail solution was pipetted and drop–casted onto a filter paper with the diameter of 10 mm. The paper-beased optode was allowed to evaporate THF for 10 minutes to form optode.

3.3.2 Measurement of anion using paper–based optode

The color measurements of the proposed paper–based membrane were performed by dipping the paper-based optode in a solution containing an anion with different concentrations. Then, the paper–based optode was observed by capturing the photographs with DSLR camera (Nikon D5200) under a studio lightbox (Udiobox, Thailand). The color value (RGB value) was fitted with Boltzmann equation as shown in **Eq. (2.13)** in **section 2.3.2**. The scheme of the fabrication, detection and analysis methods are illustrated in **Figure 3.2**.

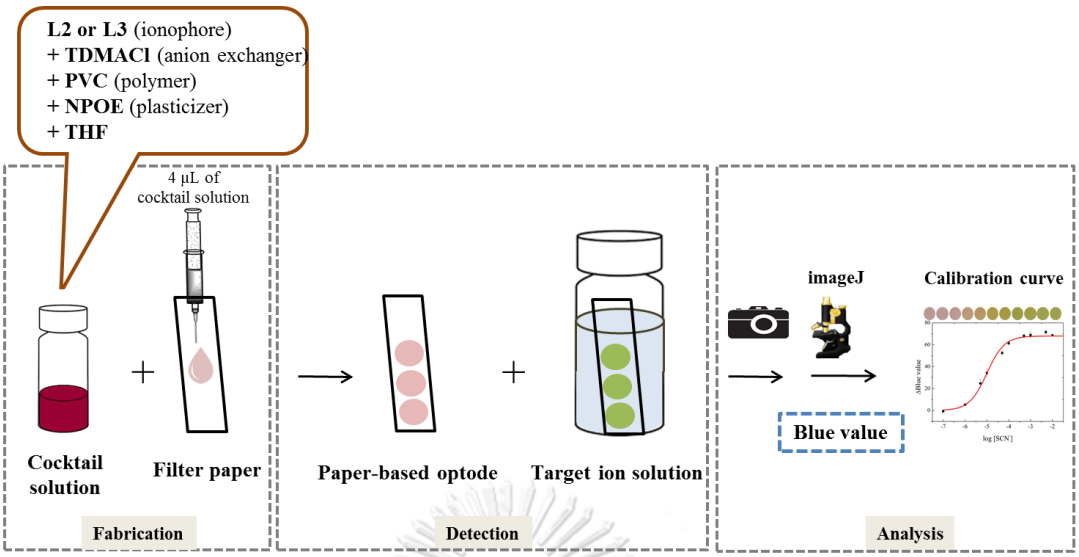

Figure 3.2 Schematic illustration of the fabrication, the detection and analysis methods for thiocyanate determination.

3.3.3 Types of paper filter and plasticizer

The filter papers studied in this work were Whatman no.1 (pore size: 11 µm) and Whatman no.42 (pore size: 2.5 µm). The second parameter was the type of plasticizers which were DOS and *o*–NPOE. The color measurements of the proposed paper–based optode were performed by dipping the paper-based optode in a solution containing 1.00×10^{-4} M SCN^- and captured the photographs with DSLR camera under a studio lightbox.

3.3.4 Response time

The response time was determined for paper–based optode in the different concentrations of target anions solutions prepared in 0.01 M tris–HCl buffer, pH 7.4. The concentration of the sample solution was studied from 1.00×10^{-7} to 1.00×10^{-2} M in the varied of time from initial to 30 minutes.

3.3.5 Effects of the solution of pH

The effect of sample solution pH on the color change of paper–based optode was examined by investigating the color change of the optimized paper–based optode with the various pH of the analyte anion solution. The pH of the sample solution was

varied from 4.0 to 10.0 with the different buffer as illustrated in **Table 3.4**. The concentration of the sample solution was studied from 1.00×10^{-7} to 1.00×10^{-2} M.

Table 3.4 Various buffer solutions at different pH.

pH	Type of buffer
4.0, 5.0	0.01 M CH_3COOH/CH_3COONa
6.0	0.01 M NaH_2PO_4/Na_2HPO_4
8.0	0.01 M boric acid/borate
7.4, 8.4, 9.0	0.01 M Tris–HCl
10.0	0.01 M $NaHCO_3/Na_2CO_3$

3.3.6 Central composite experimental design (CCD)

For this experiment, central composite design (CCD) was used as an experimental design. The amounts of ion exchanger and ionophore for paper–based optode composition were considered as the factor effected to the color change response. And, each parameter was coded to avoid analytical bias from using different levels of each parameter. The code values of each parameter are shown in **Table 3.5**.

Table 3.5 Code values for the amounts of ion exchanger and ionophore.

factor	code level				
	–1.414	–1	0	1	1.414
TDMACl (X_1)	0.76	2.50	5.00	8.00	9.24
Ionophore (X_2)	6.47	7.50	10.00	12.50	13.54

In order to design the experiment by CCD, 13 experiments were performed which represent each point inside a simulation box and sphere of all factor, as shown in **Table 3.6**. All experiments in the box were investigated for construction of a surface response plot.

For each point, the color measurement was performed in the concentration of target anion from 1.00×10^{-7} M to 1.00×10^{-2} M resulting in the response between the logarithm of anion activity and color values. Then, the color values were used to obtain the calculation in CCD process which provided the equation for prediction of the optimum condition.

Table 3.6 Central composite design for optimization of the amounts of ion exchanger and ionophore.

Experiment	Code level	
	Factor 1	Factor 2
1	–1	–1
2	1	–1
3	–1	1
4	1	1
5	–1.414	0
6	1.414	0
7	0	–1.414
8	0	1.414
9	0	0
10	0	0
11	0	0
12	0	0
13	0	0

3.3.7 Selectivity

In order in determine the selectivity of the prepared paper–based optode toward the target anion among interfering anions, the selectivity of the purposed paper–based optode was investigated by dipping the paper–based optode in separate 10 mM solutions of sodium salt of AsO_3^{3-}, AsO_4^{3-}, SeO_4^{2-} SO_4^{2-}, $H_2PO_4^-$, NO_2^-, NO_3^-, F^-, I^-, Br^-, Cl^-, SCN^- and ClO_4^- in boric/borate buffer at pH 8.0 or in tris-HCl buffer at pH 7.4. Then, optode was observed by capturing the photographs with DSLR camera (Nikon D5200) under a studio lightbox. The color value (RGB value) was fitted with Boltzmann equation as shown in **Eq. (2.13)** in **section 2.3.2**.

3.3.8 Real sample

The purposed paper–based optode was applied to determine the concentration of analyte anion in real sample solutions. In this work, urine samples were employed as the real sample for thiocyanate determination. The urine samples were collected from a non–smoker and two smokers. The samples were centrifuged at 3000 rpm for 2 minutes and stored at 4°C until analysis before measurement. The scheme of the sample preparation, detection and analysis methods are illustrated in **Figure 3.3**.

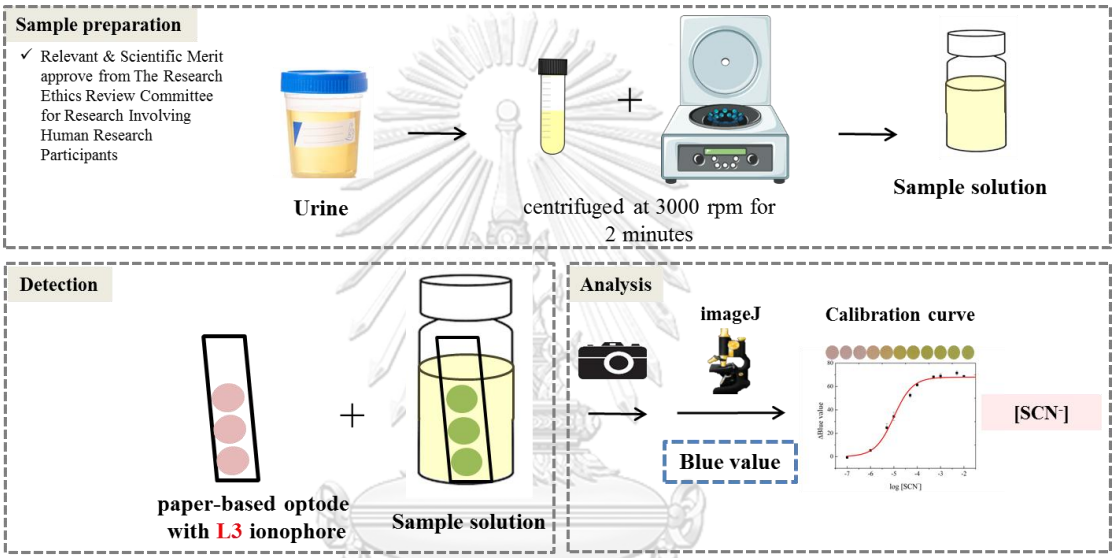

Figure 3.3 Schematic illustration of the sample preparation, the detection and analysis methods for thiocyanate determination in real sample.

Then, the determination of thiocyanate in urine sample was measured using spiking technique. For accuracy test, the various concentrations of thiocyanate ion were added. In order to validate the performance of the purposed paper–based optode, the ion chromatography, IC (Thermo Scientific, MA, USA) was applied to measure the thiocyanate concentration in the urine samples and compared with the results using the purposed method.

The ion chromatographic analysis was demonstrated on a Dionex Integrion HPIC (Thermo Scientific, MA, USA) with a suppressed conductivity detector. The mobile phase gradients were generated online from milliQ water using the Dionex EGC-KOH eluent generator cartridge (Thermo Scientific, Waltham, MA, USA) and

then polished off from the contaminants using continuously regenerating trap column. Data analysis and instrumental control were evaluated through a Chromeleon Client (7) software (Thermo Scientific, Waltham, MA, USA). The optimized ion chromatographic conditions for thiocyanate ion detection: The eluent gradient was 0-20 minutes 36 mmol/L KOH isocratic. The suppressor current was 90 mA. Column compartment temperature and detector cell temperature were kept stable with a thermostate at 30 and 30°C, respectively. The flow rate was 1.000 mL/min and the sample loop was 25 μL.

CHAPTER IV

RESULTS AND DISCUSSION

This research aimed to develop the quantification method for perchlorate and thiocyanate in aqueous solutions using potentiometric and colorimetric techniques. The potentiometric method of perchlorate-selective electrode using di–tripodal amine calix[4]arene copper(II) complex (**L1-Cu**) in poly(vinyl chloride) membrane was studied. Moreover, the optode sensor was successfully developed as paper-based for the determination of thiocyanate in aqueous solution based on colorimetric analysis. The metalloporphrin ionophores including 5,10,15,20-tetrakis(4-methoxyphenyl) porphyrin cobalt(II) complex (**L2**) and 5,10,15,20-tetrakis(4-octhyloxyphenyl) porphyrin cobalt(II) complex (**L3**) were used as ionophore.

4.1 Ion–selective electrode (ISE) based on copper (II) di–tripodal amine calix[4]arene ionophore

4.1.1 Fabrication of ion–selective membrane for ISEs

The di–tripodal amine calix[4]arene copper(II) complex (**L1-Cu**) has been previously synthesized and reported for thiocyanate determination using ISEs method [72]. Thus, we have been interested in investigating the anion sensing properties of **L1-Cu** via the potentiometric sensors with the ion–selective membrane using the experimental design approach.

In this work, the **L1** was synthesized by SCRU. The **L1-Cu** was first dissolved in THF in the presence of cation exchanger (potassium tetrakis(4–chloro phenyl)borate, KT*p*ClPB), plasticizer (1–(2–nitrophenoxy)octane, *o*–NPOE) and polymer (PVC) to fabricate the polymeric membrane as ion–selective membrane for ISEs. To optimize the sensing characteristic of the prepared ISEs, pH, the concentrations of ionophore and ion exchanger were examined using CCD method.

4.1.2 Central composite experimental design (CCD) for ISEs

The CCD approach was used to optimize the effected factors of potentiometric response including the amounts of ion exchanger and ionophore for electrode composition and pH of the sample solution while all of the parameters were coded to avoid analytical bias from using different levels of each parameter. The code values of each parameter are shown in **Table 3.2**. All experiments (20 experiments) in the box were investigated for construction of a surface response plot.

According to the experimental results, all variables were considered as quadratic terms via more accurate results. Moreover, the relevant between three variables was also investigated to determine the effect of each interaction as shown in **Table 4.1**. In order to show the optimum point of each parameter, the linear regression was calculated resulting in the coefficients of the equation, as shown in **Eq. (4.1)** which was responded as 3D surface plots to figure out the optimum points for each parameter.

$$y_{slope} = -57.51 + 1.93X_1 + 0.89X_2 - 0.90X_3 + 2.04X_1^2 \\ -1.16X_2^2 - 0.13X_3^2 + 0.52X_1X_2 - 0.81X_1X_3 - 0.54X_2X_3 \qquad \textbf{(4.1)}$$

Figure 4.1 shows the relationship between the amount of ion exchanger and pH of the working solution. The highest and lowest experimental slopes from Nernst equation were represented in red and blue colors, respectively. As shown in the x–axis, the effect of pH on the slope via Nernst equation, in the results, the blue areas (slope around –59 mV/decade) were on the middle sides of the figure, which corresponded to pH values of lower than 9.75 and higher than 5.06. And, the results indicated that the optimum amount of ion exchanger was in the range of 0.80–9.20 mmol/kg (blue).

Table 4.1 Three parameters with three levels of CCD experiments for optimization of pH (Factor X_1) and the amounts of KT*p*ClPB (Factor X_2) and **L1** (Factor X_3) for perchlorate determination using ISEs.

Experiment	b_0	Factor									Slope	
		b_1	b_2	b_3	b_1^2	b_2^2	b_3^2	b_{12}	b_{13}	b_{23}	experiment	predict
1	1	–1	–1	–1	1	1	1	1	1	1	–58.78	–59.50
2	1	1	–1	–1	1	1	1	–1	–1	1	–54.80	–55.06
3	1	–1	1	–1	1	1	1	–1	1	–1	–58.01	–57.69
4	1	1	1	–1	1	1	1	1	–1	–1	–50.59	–51.18
5	1	–1	–1	1	1	1	1	1	–1	–1	–59.22	–58.61
6	1	1	–1	1	1	1	1	–1	1	–1	–57.10	–57.41
7	1	–1	1	1	1	1	1	–1	–1	1	–59.22	–58.95
8	1	1	1	1	1	1	1	1	1	1	–56.41	–55.68
9	1	–1.68	0	0	2.82	0	0	0	0	0	–54.70	–54.99
10	1	1.68	0	0	2.82	0	0	0	0	0	–48.78	–48.51
11	1	0	–1.68	0	0	2.82	0	0	0	0	–62.68	–62.27
12	1	0	1.68	0	0	2.82	0	0	0	0	–58.87	–59.30
13	1	0	0	–1.68	0	0	2.82	0	0	0	–57.11	–56.36
14	1	0	0	1.68	0	0	2.82	0	0	0	–58.62	–59.39
15	1	0	0	0	0	0	0	0	0	0	–57.61	–57.51
16	1	0	0	0	0	0	0	0	0	0	–57.11	–57.51
17	1	0	0	0	0	0	0	0	0	0	–57.61	–57.51
18	1	0	0	0	0	0	0	0	0	0	–57.61	–57.51
19	1	0	0	0	0	0	0	0	0	0	–58.02	–57.51
20	1	0	0	0	0	0	0	0	0	0	–57.11	–57.51

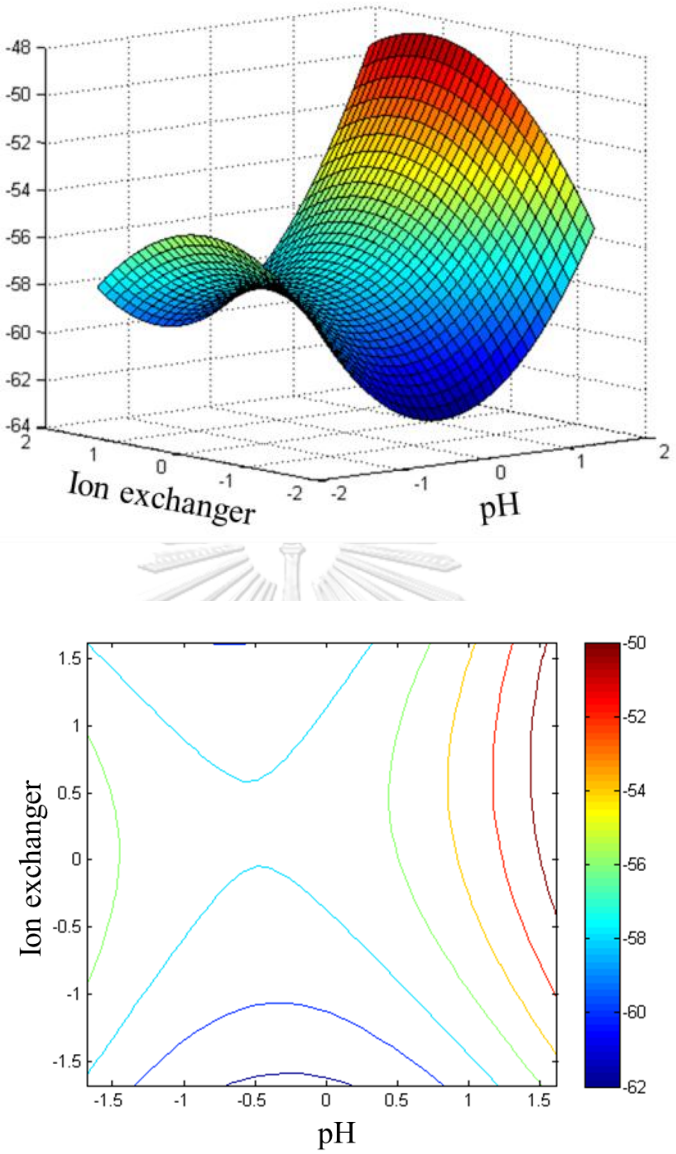

Figure 4.1 Effect of the amount of ion exchanger and pH on the slope via Nernst equation.

In addition, the relationship between the amount of ionophore and pH was also considered. Results from **Figure 4.2** demonstrated a 3D surface plot and contour plot showing the relationship beteween the amount of ionophore and pH. Low slope form Nernst equation (–59 mV/decade) was obtained when using higher pH values than 5.06 or lower pH values than 8.88. The optimum amount of ionophore was obtained in the range of 5.80–14.20 mmol/kg (blue). In addition, results from both **Figures 4.1**

and **Figure 4.2** indicated that –59 mV/decade slope was observed from either lower pHs than 8.88 or higher pHs than 5.06.

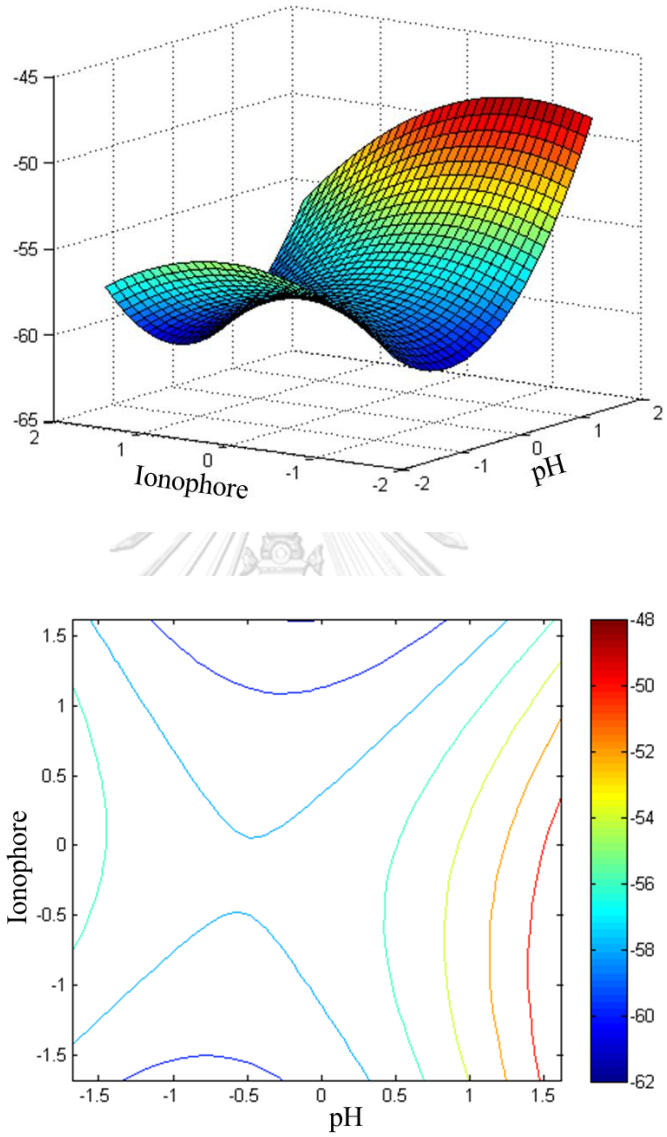

Figure 4.2 Effect of the amount of ionophore and pH on the slope via Nernst equation.

However, the relationships between the amounts of ion exchanger and ionophore were also demonstrated as illustrated in **Figure 4.3**. From results, a green area is located at the middle of the figure, the optimum amount of ion exchanger was considered to be in the range of 2.50–7.50 mmol/kg while the amount of ionophore was in the range of 11.25–14.20 mmol/kg.

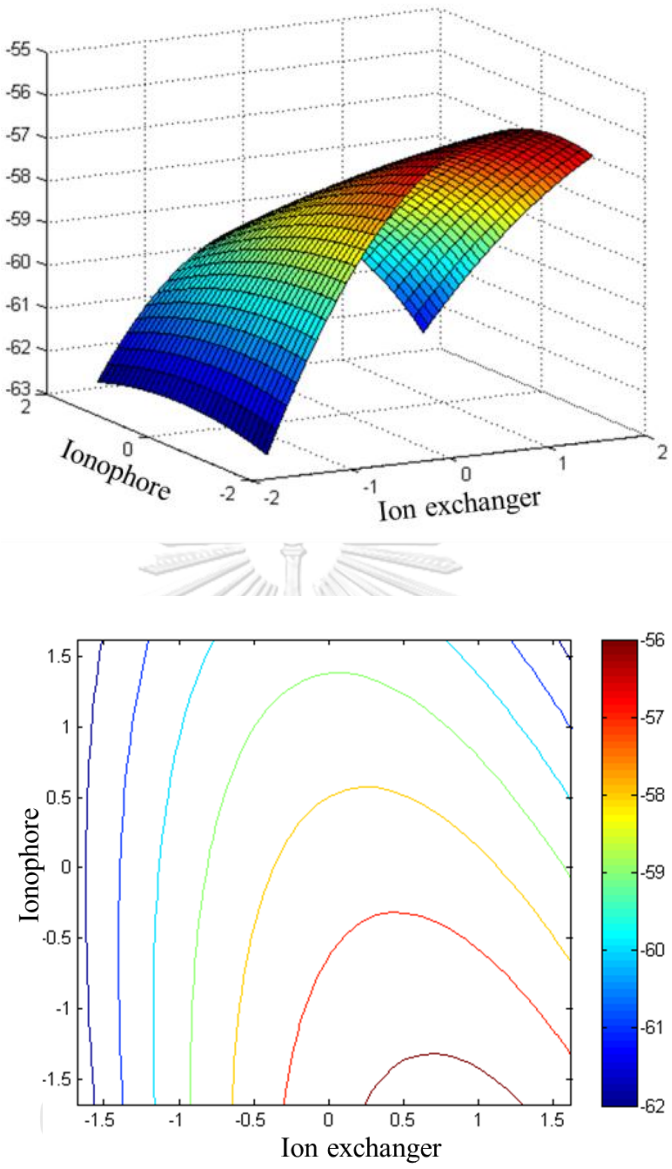

Figure 4.3 Effect of the amounts of ion exchanger and ionophore on the slope via Nernst equation.

All of the surface plots and contours plot showed the optimum condition of three parameters (pH, the amounts of ion exchanger and ionophore) which was related to the good sensitivity via the extraction of ionophore (**L1-Cu**) and perchlorate via the purposed ISEs. From **Figure 4.1, Figure 4.2** and **Figure 4.3**, they indicated the optimum values for all parameters that the optimum pH was considered to be in the range of 5.06–8.88, the optimum amount of ion exchanger was considered to be in the

range of 2.50–7.50 mmol/kg while the amount of ionophore was determined to be in the range of 11.25–14.20 mmol/kg.

Using the multiple linear regressions, a regression model was calculated from the responsive surface plots, as shown in the **Eq. (4.1)**. The linear relationship from the equation was plotted and shown in **Figure 4.4** with $R^2 = 0.9747$.

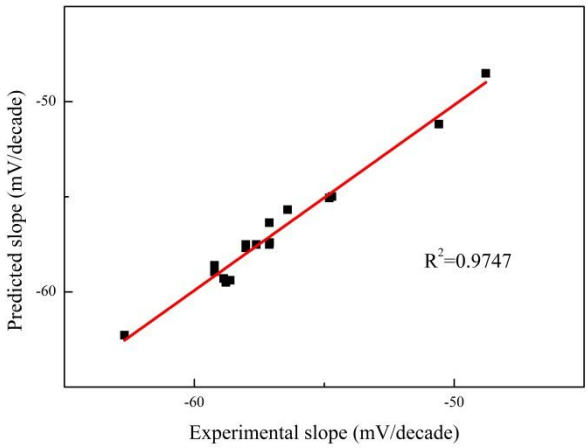

Figure 4.4 Correlation of the experimental (observed) slope and the predicted slope via Nernst equation.

Each coefficient in **Eq. (4.1)** was indicated the significance of the parameters in terms of either an isolated term or a related term. The coefficients of two parameters (pH, the amount of ion exchanger) were posititive whlie the coefficient of the amount of the ionophore was negative. It can be implied that the slope increased when the pH and the amount of ion exchanger increased. However, the slope decreased when the amount of ionophore increased. The optimized values of the parameters were figured out using the first derivative method from the constructed equation. It was found that the optimized pH, the amounts of ion exchanger (KT*p*ClPB) and ionophore (**L1-Cu**) were found to be 8.0, 3.25 mmol/kg and 13.25 mmol/kg, respectively. Therefore for the futher experiment, these conditions was used as the optimum condition to determine perchlorate by ISEs.

4.1.3 Selectivity

In order to study the performance of the proposed ion–selective membrane based on **L1**, the potentiometric selectivity is a key characteristic of the development of ISEs. Generally, the potentiometric selectivity represents the preferance of ionophore toward primary ion over interfering ions. In this study, the selectivity coefficients ($\log K_{i,j}^{pot}$) of the ion–selective membrane for perchlorate were demonstrated using the separate solution method (SSM).

In this work, the selectivity of purposed ion–selective membrane electrode was measured in separate solutions of sodium salt of AsO_4^{3-}, SO_4^{2-}, $H_2PO_4^-$, NO_3^-, F^-, I^-, Br^-, Cl^-, SCN^- and ClO_4^- (1.00×10^{-7} to 1.00×10^{-2} M) in boric/borate buffer pH 8.0 follows the Hofmeister selectivity pattern resulting in the response between the logarithm of anion activity and EMF. Then, the selectivity coefficients were calculated followed the detail in **section 2.2.2.1**.

The results in **Table 4.2** showed that the EMF responses of various anions gave the negative EMF response except $H_2PO_4^-$ showed the positive EMF response. It indicated that the optimized membrane with **L1-Cu** did not show the negatively EMF response trough the $H_2PO_4^-$. Although, the other anions showed the negatively EMF response, AsO_4^{3-}, F^-, Cl^-, NO_2^-, NO_3^- and SO_4^{2-} gave the EMF response different from the Nernstian slope (–59.2 mV/decade). On the other hand, I^-, and SCN^- responded to the ISEs with super–Nernstian slope and Br^- responded to the ISEs with sub–Nernstian slope. It is suggested that the optimized membrane with **L1-Cu** did not show good selectivity with these anions while performed good selectivity with ClO_4^- resulting in near–Nernstian slope of –58.02 ± 0.01 mV/decade.

Table 4.2 Potentiometric responses of optimized membrane with **L1-Cu** ionophore towards the various of anions.

Samples (10 mM)	**Slope (mV/decade)**	**Linear range (M)**
ClO_4^-	–58.02 ± 0.01	$1.00\times10^{-6} – 1.00\times10^{-2}$
I^-	–70.66 ± 6.12	$1.00\times10^{-5} – 1.00\times10^{-2}$
SCN^-	–67.45 ± 0.20	$1.00\times10^{-6} – 1.00\times10^{-2}$
AsO_4^{3-}	–19.97 ± 0.30	$1.00\times10^{-6} – 1.00\times10^{-2}$
F^-	–6.02 ± 1.00	$1.00\times10^{-3} – 1.00\times10^{-2}$
Br^-	–51.63 ± 0.05	$1.00\times10^{-5} – 1.00\times10^{-2}$
Cl^-	–35.88 ± 0.25	$1.00\times10^{-4} – 1.00\times10^{-2}$
NO_2^-	–41.15 ± 0.10	$1.00\times10^{-5} – 1.00\times10^{-2}$
NO_3^-	–38.54 ± 2.71	$1.00\times10^{-5} – 1.00\times10^{-2}$
SO_4^-	–7.48 ± 2.66	$1.00\times10^{-4} – 1.00\times10^{-2}$
$H_2PO_4^-$	2.85 ± 1.35	$1.00\times10^{-3} – 1.00\times10^{-2}$

The results in **Figure 4.5** demonstrated that the ion–selective membrane containing **L1−Cu** as an ionophore exhibited high selectivity toward perchlorate over all interfering anions. The selectivity coefficient of purposed ion–selective membrane electrode was determined using the separate solution method (SSM) by measuring EMF in separate solutions of each interfering anions (j), followed by primary anions (j), ClO_4^- and illustrated in **Figure 4.6**. The selectivity sequence obtained with ISEs was as follows: $ClO_4^- > SCN^- > H_2PO_4^- > I^- > SO_4^{2-} > AsO_4^{3-} > NO_3^- > Br^- > NO_2^- > Cl^- > F^-$. As illustrated, the anion selectivity sequence exhibited by ion–selective membrane deviated significantly from the Hofmeister sequence with high perchlorate selectivity. This deviation from the Hofmeister pattern ensures the existence of a selective interaction between **L1−Cu** and perchlorate.

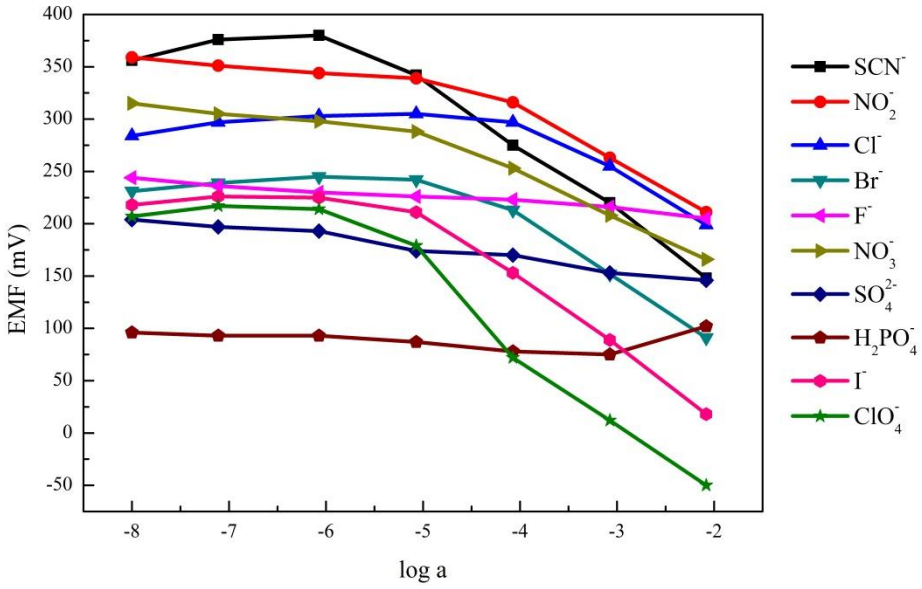

Figure 4.5 EMF responses of ISEs based on the **L1−Cu** toward the different anions.

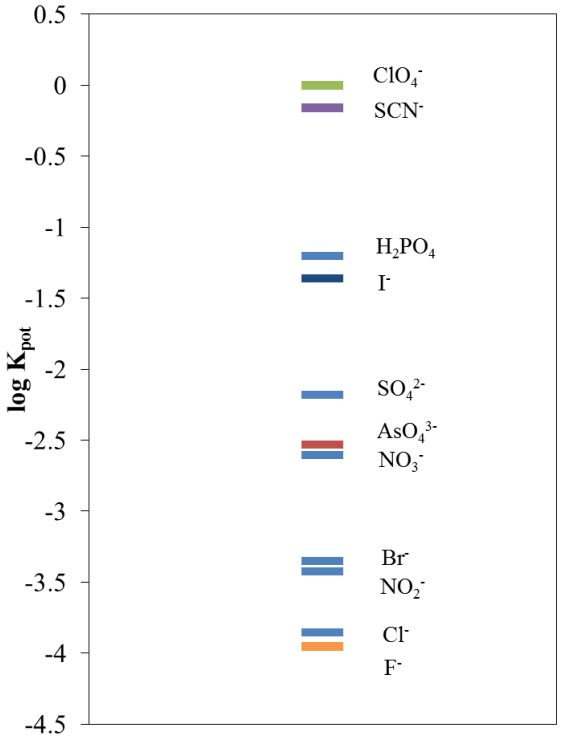

Figure 4.6 Comparison of the selectivity coefficients of anions in the polymeric membrane containing the **L1-Cu**.

4.1.4 Potentiometric responses of perchlorate

In order to further evaluate the electrochemical behavior of the copper di–tripodal amine calix[4]arene membrane, the potentiometric responses of perchlorate were demonstrated. The membrane composed of 3.25 and 13.25 mmol/kg of ion exchanger (KT*p*ClPB), and **L1**, respectively, the amount of polymer (PVC) : plasticizer (*o*–NPOE) was 1: 2 w/w in the total amount of 220 mg and then applied to detect perchlorate in boric/borate buffer solution at pH 8.0. Before measurement, the membranes were conditioned in 10 mM $CuCl_2$ solution for overnight and 10 mM of sodium perchlorate solution for overnight, respectively. Potentiometric measurements were performed in the concentration of perchlorate ions from 1.00×10^{-8} to 1.00×10^{-2} M.

The results in **Figure 4.7** and **Figure 4.8** showed that the negative potentiometric responses for perchlorate yielded a near–Nernstian slope (–58.02 ± 0.01 mV/decade) in the working range of 1.00×10^{-6} to 1.00×10^{-2} M which suggested that the **L1−Cu** membrane exhibited the perchlorate responses with the limit of detection of 3.00×10^{-5} M defined by using the cross–section of the two extrapolated linear portions of the calibration curves and showed an excellent correlation with a correlation coefficient (R^2=0.9994).

Furthermore, the response time, one of the important performances of ISEs, was determined. As can be seen in **Figure 4.7**, the fabricated perchlorate–selective electrodes with **L1−Cu** performed a fast response time to reach its steady–state EMF value which performing as the stable and smooth potential signal after changing the perchlorate concentration in sample solution.

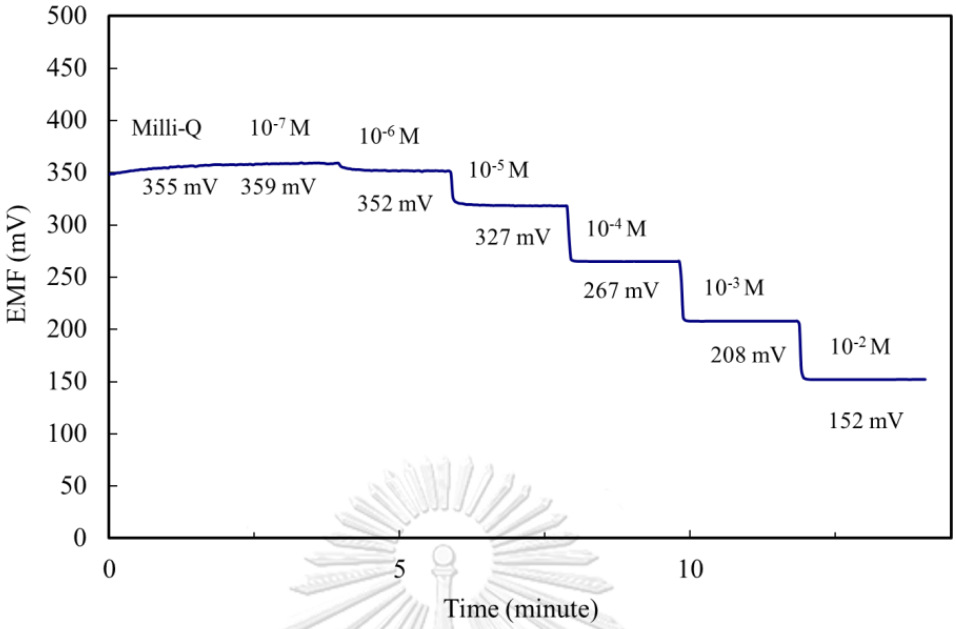

Figure 4.7 Time–dependent response of the optimized membrane towards perchlorate in the concentration range from 1.00×10^{-7} to 1.00×10^{-2} M at pH 8.0.

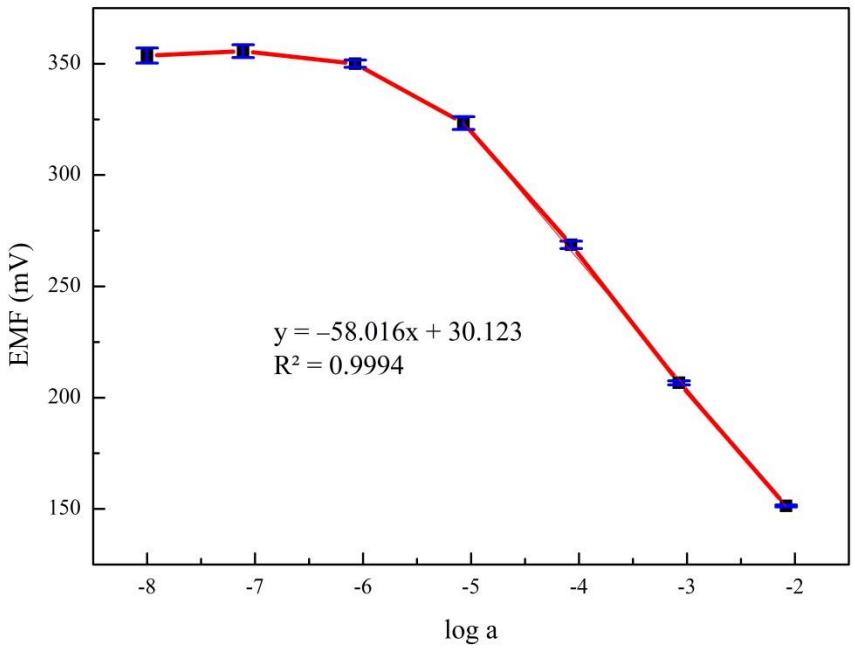

Figure 4.8 EMF responses of ISEs based on the **L1−Cu** toward perchlorate in the concentration range from 1.00×10^{-7} to 1.00×10^{-2} M at pH 8.0.

The di–tripodal amine calix[4]arene copper(II) complex (**L1−Cu**) showed the anion sensing properties as the potentiometric sensors for perchlorate determination. Moreover, the optical sensor using bulk optode techniques was also interesting. Since **L1** is colorless, the chromoionophore is necessary to the extraction of analyte ions to the membrane. The composition of cocktail solution was **L1**, chromoionophore I, TDMACl, *o*-NPOE and PVC. From the results, membrane showed color change towards the pH increasing as seen in **Figure 4.9(a).** There was no color difference of the membrane between immersing in the blank and 1 mM AsO_4^{3-} in buffer pH 8.0 **Figure 4.9(b)**. This poor sensitivity was purposed that **L1** ionophore was not suitable for the anion sensing with bulk optode technique.

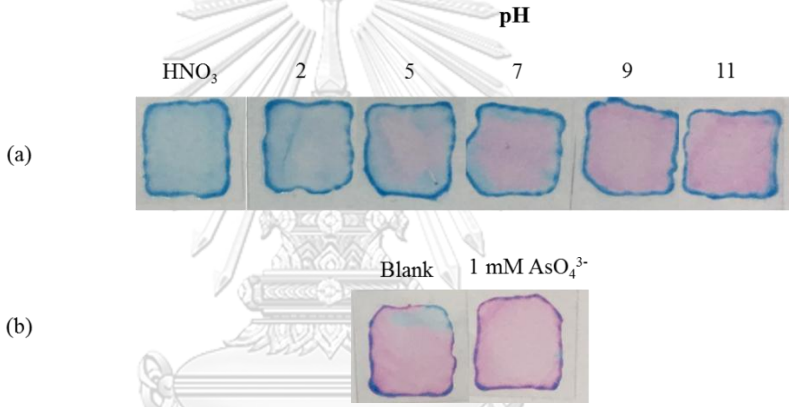

Figure 4.9 Colors of film-based optode with **L1** toward (a) the various pH with the immersing time of 20 minutes, and (b) 1 mM AsO_4^{3-} in buffer pH 8.0 with the immersing time of 20 minutes.

4.2 Bulk optode technique based on metalloporphyrin ionophores

According to the absorption of porphyrin compound, the porphyrins were interesting to use as ionophore for anion sensing with bulk optode technique. Thus, this part was performed to detect thiocyanate using bulk optode technique based on metalloporphyrin ionophores. The metalloporphyrin ionophores in this work were 5,10,15,20-tetrakis(4-methoxyphenyl)porphyrin cobalt(II) complex (**L2**) and 5,10,15,20-tetrakis(4-octhyloxyphenyl)porphyrin cobalt(II) complex (**L3**). These two ionophores consist of cobalt(II) porphyrin but different alkyl chain substitutions at *meso*-position. Thus, these ionophores provided the different lipophilicity.

4.2.1 5,10,15,20–Tetrakis(4–methoxyphenyl)porphyrin cobalt(II) complex (L2) as an ionophore

4.2.1.1 Measurement of thiocyanate using the solution of L2 ionophore

For the preparation, 1 mg of **L2** was dissolved in 2 mL of THF and stirred for an hour. Then, the color measurements of the proposed cocktail solution were performed by adding 0.1 mL of cocktail solution into 1.9 mL of the solution containing thiocyanate with different concentrations in the range from 1.00×10^{-7} to 1.00×10^{-2} M at pH 8.0. The mixed solution was observed by measuring the absorption spectra with UV–visible spectrophotometer and capturing the photographs.

The colors of the solution after mixing and the absorbance are shown in **Figure 4.10** and **Figure 4.11**, respectively. From these results, the color of the **L2** ionophore was changed from orange to green when the concentration of thiocyanate in the sample solution was increased. From the absorption spectra, the absorbance at 525 nm was decreased and the absorbance at 550 nm was increased with the increasing of the thiocyanate concentration. It may confirm the complexation of **L2** ionophore and thiocyanate. The characteristic color of the coordination complex is exhibited by splitting of an electron from a lower-energy d orbital to a higher-energy d orbital. Thus, the deviation of the energy gap of two levels of d orbital results the color change of the complex. The color change of **L2** may purposed by distortion of the structure of **L2** after attaching SCN^- as a ligand from the planar of metal-pyrrole unit to the octahedral. Thus to apply the **L2** ionophore as the thiocyanate sensors, the analytical performances were further investigated.

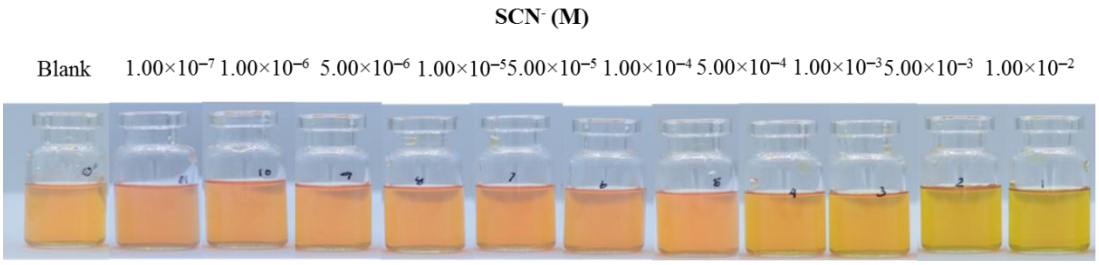

Figure 4.10 Colors of **L2** solution in the various concentrations of SCN^- solution at pH 8.0 with the mixing time of 15 minutes.

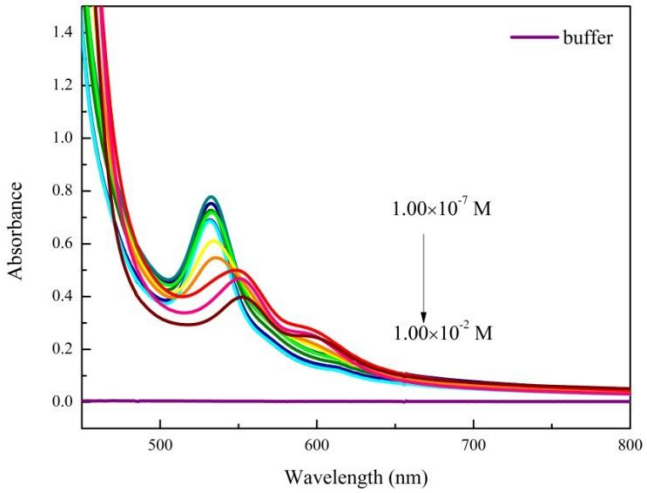

Figure 4.11 Absorption spectra of **L2** ionophore solution in the presence of various concentrations of SCN^- standard solutions from 1.00×10^{-7} to 1.00×10^{-2} M in 0.01 M boric/borate buffer at pH 8.0 with the mixing time of 15 minutes.

The sigmoidal curve was demonstrated with the **L2** ionophore solution in the presence of various concentrations of SCN^- standard solutions from 1.00×10^{-7} to 1.00×10^{-2} M in 0.01 M boric/borate buffer at pH 8.0. The sample solution was mixed into the ionophore solution for 15 minutes. The sigmoidal response of the solution with logarithm of SCN^- concentrations was fitted with the sigmoidal relationship given by the Boltzman equation [41] as expressed in **Eq. (2.13)** where the A_1, A_2, x_0, and dx are parameters given in **Table 4.3**. The sigmoidal curve illustrated the relationship between the ΔBlue values and logarithm of SCN^- concentrations is shown in **Figure 4.12**. Because green was the combination of yellow and blue, the Blue value was chosen for the quantitative analysis. The results provided an excellent correlation coefficient (R^2 = 0.9789). The limit of detection (LOD) was 7.94×10^{-5} M of SCN^- which expressed from the cross-section of the two extrapolated linear portions of the calibration curves [36]. The **L2** solution showed the working range from 1.00×10^{-4} to 1.00×10^{-2} M.

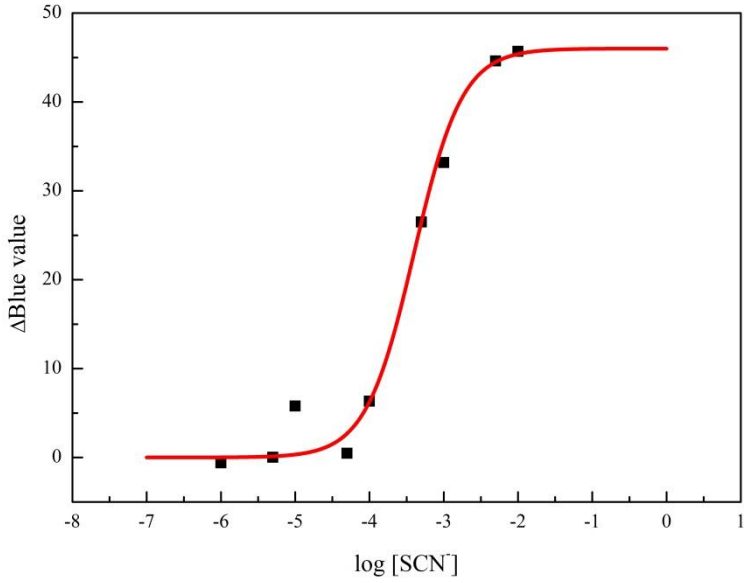

Figure 4.12 Sigmoidal curve of **L2** ionophore solution in the presence of various concentrations of SCN^- standard solutions from 1.00×10^{-7} to 1.00×10^{-2} M in 0.01 M boric/borate buffer at pH 8.0 with the mixing time of 15 minutes.

Table 4.3 Parameters of Boltzmann equation for SCN^- determination in the **L2** solution.

Parameters	Values
A_1	0.00
A_2	46.00
x_0	–3.40
dx	0.33

4.2.1.2 Measurement of thiocyanate using the paper–based optode containing L2 ionophore

The **L2** ionophore has been previously shown as an ionophore for thiocyanate determination via the color change of the ionophore after mixing into the thiocyanate solutions. Thus, to improve the sensitivity of method for thiocyanate determination, these analytical approaches have been implemented in the paper–based couple with bulk optode technique [43]. The cellulose papers are widely used as the

substrate to create colorimetric sensors for the improvement of the analytical performance due to the increase of surface contact between analysis area and an aqueous solution [81]. Thus, we have been interested in investigating the anion sensing properties of **L2** ionophore via paper–based optode sensor using the experimental design approach to improve sensitivity.

From the preliminary study of solution method, the color change of the paper–based platform based on **L2** ionophore with thiocyanate was shown obviously by naked–eye from pink to green as illustrated in **Figure 4.13**. In addition, the color values were performed by capturing the photographs with DSLR camera under a studio lightbox. The color values in term of Blue values were fitted with Boltzmann equation as the quantitative model shown in sigmoidal response which provided the excellent correlation (R^2 > 0.99). The blue value was used to do the quantitative analysis because green is the combination of yellow and blue. It was found that the paper–based optode provided the obvious color change of **L2** ionophore with lower concentration of SCN^- (5.00×10^{-4} M) than the solution of **L2** ionophore (1.00×10^{-4} M).

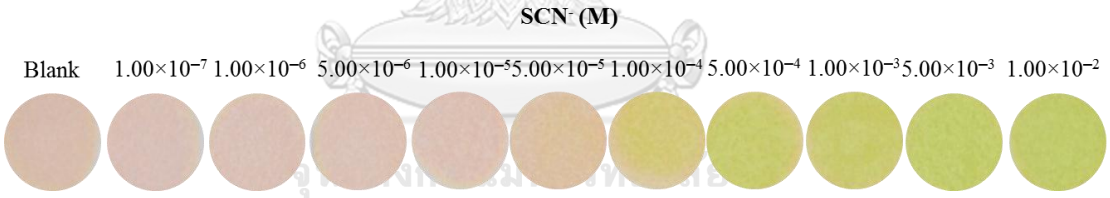

Figure 4.13 Colors of the paper–based optode with **L2** ionphore in various concentrations of SCN^- solution.

4.2.1.3 Types of filter paper and plasticizer on the response of paper-based optode containing L2 ionophore

According to the effect of the composition of optode, the first two factors studied were the plasticizer and the filter paper because their properties may lead to the efficiency of the color change detection. The filter papers studied in this work were Whatman no.1 (pore size: 11 µm) and Whatman no.42 (pore size: 2.5 µm). The second parameter was the type of plasticizers which were DOS and *o*–NPOE. The color measurements of the proposed paper–based optode were performed by

dipping the paper-based optode in a solution containing 1.00×10^{-4} M SCN^- and captured the photographs with DSLR camera under a studio lightbox.

The results are shown in the **Table 4.4** and plotted as the stacked graph to compare the relationship of the color change among SCN^- in **Figure 4.14** which were illustrated the Blue values of the paper–based optode in the buffer solution as blank condition as shown in blue area. Then, the paper–based optode was dipped into 1.00×10^{-4} M of thiocyanate solution and the color of the paper–based optode changed as shown in term of ΔBlue value (red area) calculated as followed: ΔBlue value = Blue $value_{blank}$ − Blue $value_{SCN^-}$. To simplify the color change of the paper–based optode in buffer solution and anion solution, the percentage of Blue value was calculated as follows:

$$\%\Delta Blue\ value = \frac{\Delta Blue\ value}{Blue\ value_{blank}} \times 100. \qquad \textbf{(4.2)}$$

As can be seen in **Figure 4.14**, the filter paper no.1 and *o*–NPOE plasticizer (second column) showed the highest %ΔBlue value and indicating that the filter paper no.1 and *o*–NPOE plasticizer were the better composition for the thiocyanate determination using paper–based optode.

Table 4.4 Blue values of the paper–based optode with **L2** ionophore in buffer pH 8.0 as blank and after dipping in 1.00×10^{-4} M thiocyanate solution.

Filter paper	**Plasticizer**	**Blue value**		**ΔBlue value**	**%ΔBlue value**
		Blank	**SCN^-**		
No.1	DOS	184.15	135.08	49.07	27
	o–NPOE	170.68	96.76	73.91	43
No.42	DOS	155.51	122.30	33.51	21
	o–NPOE	153.45	100.78	52.67	34

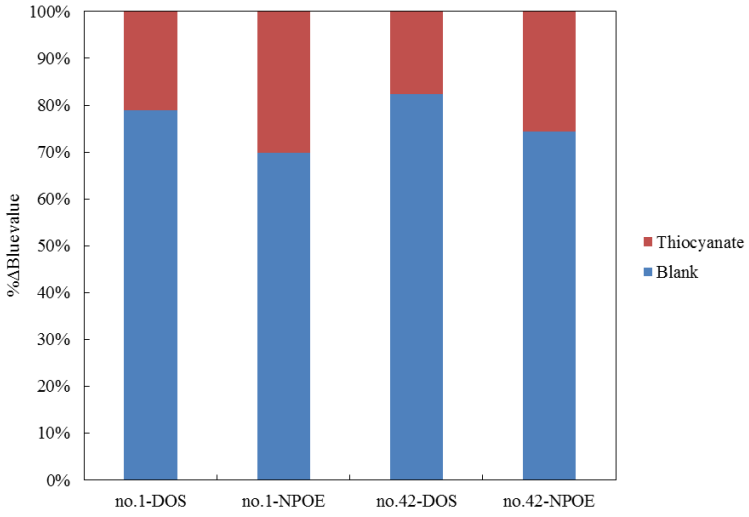

Figure 4.14 Percentage of color change of the paper–based optode with **L2** ionophore in buffer solution (blank, blue area) and in the 1.00×10^{-4} M thiocyanate solution (red area).

4.2.1.4 Effect of immersing time on the response of paper-based optode containing L2 ionophore

The effect of immersing time for the paper–based optode to determine SCN^- in the solutions was also demonstrated. The paper–based optode was dipped in 1.00×10^{-4} M of thiocyanate solution. The results as shown in **Figure 4.15** and **Figure 4.16** indicated that the Blue value was decreased with a function of time. The optimized time required to obtain a constant response for SCN^- detection was found to be 10 minutes. However for the further experiment, 15 minutes was applied to be the immersing time.

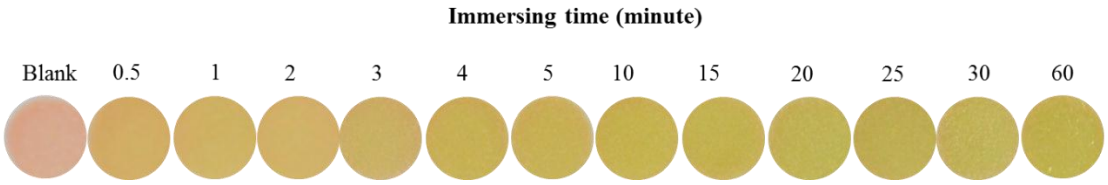

Figure 4.15 Colors of the paper–based optode with **L2** ionophore obtained from 1.00×10^{-4} M SCN^- solution at different immersing times.

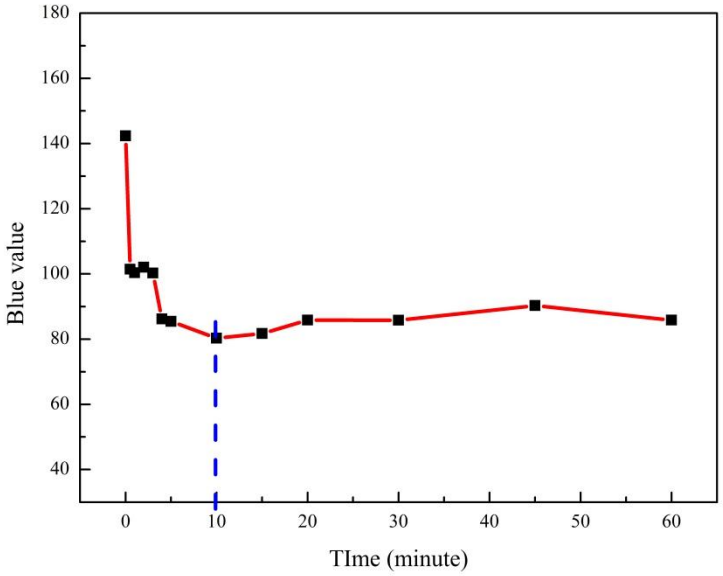

Figure 4.16 Effect of immersing time of the paper–based optode with **L2** ionophore. Blue values were obtained from 1.00×10^{-4} M SCN^- solution at different immersing times.

To optimize the other sensing characteristic of the prepared paper–based optode, the concentration of ionophore and ion exchanger were examined using CCD method.

4.2.1.5 Central composite experimental design (CCD) for paper–based optode with L2 ionophore

The CCD approach was used to optimize the effected factors of color response including the amounts of ion exchanger and ionophore for paper-based optode composition while all of the parameters were coded to avoid analytical bias from using different levels of each parameter. The code values of each parameter are shown in **Table 3.6**. All experiments (13 experiments) in the box were investigated for construction of a surface response plot.

For each point, the Blue values measurement was performed in the concentration of SCN^- from 1.00×10^{-7} M to 1.00×10^{-2} M at pH 8.0 with the immersing time of 15 minutes resulting in the response between the logarithm of

activity of anion and Blue value. Then, the Blue value was used to obtain the calculation in CCD process which provided the equation for prediction of the optimum values.

According to the experimental results, all variables were considered as quadratic terms via more accurate results. Moreover, the relevant between two variables were also investigated to determine the effect of each interaction as shown in **Table 4.5**. In order to show the optimum point of each parameter, the linear regression was calculated resulting in the coefficients of the equation, as shown in **Eq. (4.3)** which responded as 3D surface plots to figure out the optimum points for each parameter.

$$y_{blue\ value} = 124.39 - 8.72X_1 - 9.72X_2 + 3.52X_1^2 + 2.75X_2^2 - 1.22X_1X_2 \qquad \textbf{(4.3)}$$

Figure 4.17 shows the relationship between the amount of ion exchanger and ionophore of the working solution. The highest and lowest experimental Blue values from experiments were represented in red and blue, respectively.

Table 4.5 Two parameters with three levels of CCD experiments for optimization of the amounts of ion exchanger (Factor X_1) and **L2** (Factor X_2) for thiocyanate determination using paprer–based optode.

Experiment	b_0	factor					Blue value	
		b_1	b_2	b_1^2	b_2^2	b_{12}	experiment	predict
1	1	–1	–1	1	1	1	148.28	147.88
2	1	–1	1	1	1	–1	131.23	130.89
3	1	1	–1	1	1	–1	132.33	132.59
4	1	1	1	1	1	1	110.10	111.01
5	1	–1.414	0	1.999	0	0	143.20	143.76
6	1	1.414	0	1.999	0	0	119.89	119.11
7	1	0	–1.414	0	1.999	0	143.71	143.63
8	1	0	1.414	0	1.999	0	116.29	116.15
9	1	0	0	0	0	0	124.12	124.39
10	1	0	0	0	0	0	124.08	124.39
11	1	0	0	0	0	0	124.57	124.39
12	1	0	0	0	0	0	124.92	124.39
13	1	0	0	0	0	0	124.27	124.39

As shown in the x–axis of **Figure 4.17**, the effect of the concentration of the ion exchanger (TDMACl) on the Blue value of the paper–based optode, in the results, the blue areas (Blue value below 120) were on the corner of the figure, which corresponded to the concentration of the ion exchanger values higher than 6.50 mmol/kg. And, the results indicated that the optimum amount of ionophore was higher than 12.50 mmol/kg (blue).

Both of the surface plots and contours plot showed the optimum condition of two parameters (the amount of ion exchanger and ionophore) which was

related to the good sensitivity via the extraction of ionophore (**L2**) and thiocyanate via the purposed paper–based optode. From **Figure 4.17**, it indicated the optimum values for all parameters that the optimum amount of ion exchanger was considered to be higher than 6.50 mmol/kg while the amount of ionophore was determined to be higher than 12.50 mmol/kg.

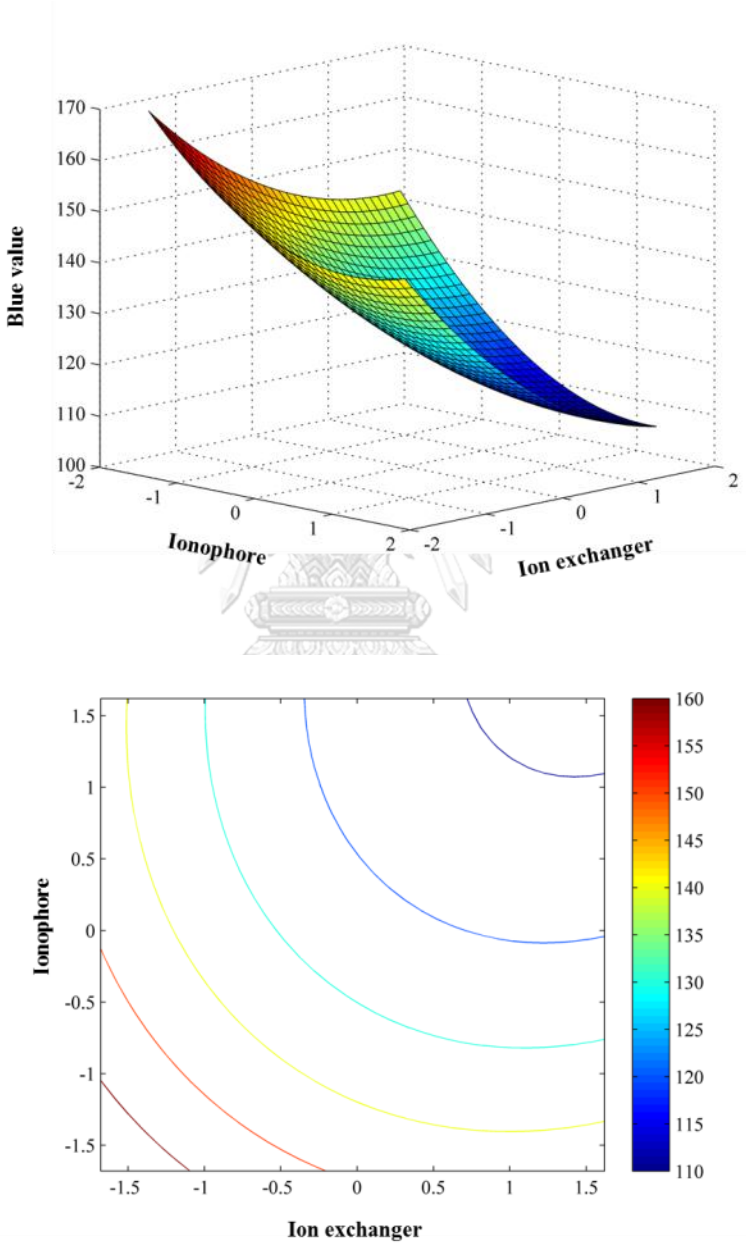

Figure 4.17 Effects of the amount of ion exchanger and **L2** ionophore on Blue value.

Using the multiple linear regressions, a regression model was calculated from the responsive surface plots, as shown in the **Eq. (4.3)**. The linear relationship from the equation was ploted and shown in **Figure 4.18** with R^2 was 0.9984.

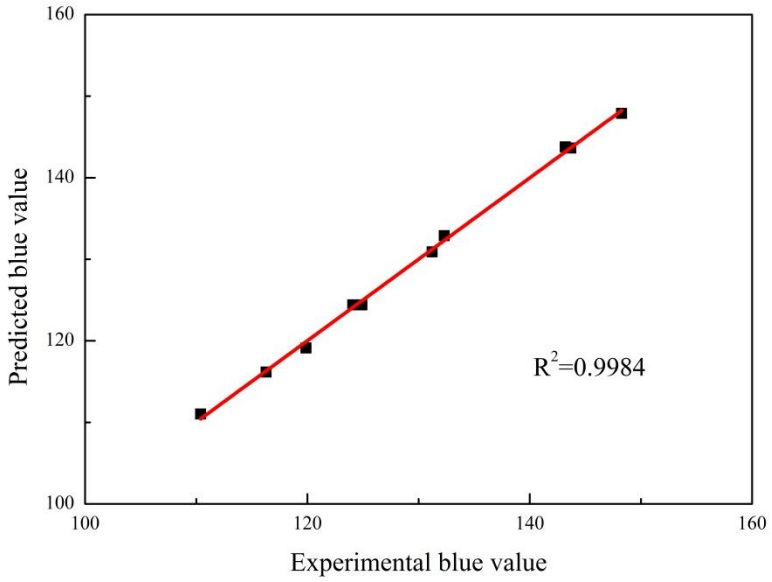

Figure 4.18 Correlation of the experimental (observed) Blue value and the predicted Blue value of the paper–based optode with **L2** ionophore.

Each coefficient in **Eq. (4.3)** was indicated the significance of the parameters in terms of either an isolated term or a related term. The coefficient of both the amount of ion exchanger and ionophore were negative which implied that the Blue value was decrease when the amount of ion exchanger and ionophore were increased. The optimized values of the parameters were figured out using the first derivative method from the constructed equation. It was found that the optimized amounts of ion exchanger and ionophore were found to be 10.10 mmol/kg and 13.88 mmol/kg, respectively. Therefore for the futher experiment, these conditions were used as the optimum condition to determine thiocyanate by paper–based optode.

4.2.1.6 Selectivity

In order to determine the selectivity of the prepared paper–based optode toward the target anions among interfering anions, the selectivity of purposed paper–based optode was investigated by dipping the paper–based optode in the separate 10 mM solutions of sodium salts of AsO_3^{3-}, AsO_4^{3-}, SO_4^{2-}, $H_2PO_4^-$, NO_2^-, NO_3^-, F^-, I^-, Br^-, Cl^-, SeO_4^{2-}, SCN^- and ClO_4^- at pH 8.0. Then, the optode was observed by capturing the photographs with a DSLR camera (Nikon D5200) under a studio lightbox.

For selectivity behavior of the proposed paper–based optode based on **L2**, the results are shown in **Figure 4.19** and **Figure 4.20** The thiocyanate showed lowest Blue value compared to the Blue value of the paper–based optode in the blank condition. It can be concluded that the **L2** showed highest selectivity toward thiocyanate over all interfering anions. The selectivity coefficient ($\log K_{IJ}^{opt}$) of optimized paper–based optode towards the various anions was calculated and showed in **Table 4.6**. The selectivity sequence obtained with optode was as follows: SCN^- > NO_2^- > I^- > AsO_3^{3-} > SeO_4^{2-} > NO_3^- > Br^- > AsO_4^{3-} > ClO_4^- > SO_4^{2-} > F^- > Cl^- > $H_2PO_4^-$. Generally, the anion selectivity sequence is mostly followed the Hofmeister sequence which presented the lipophilicity of the target ions lead to the selectivity pattern of the optode [36]. As can be seen, the proposed paper–based optode exhibited the anion optical selectivity sequence that deviates significantly from the Hofmeister sequence and intimated high thiocyanate selectivity.

Table 4.6 Color responses and selectivity coefficients ($\log K_{IJ}^{opt}$) of optimized paper–based optode membrane with **L2** ionophore towards the several anions.

Samples (1.00×10^{-4} M)	Blue value	ΔBlue value	$\log K_{IJ}^{opt}$
Boric/borate buffer	166.25 ± 10.37	0	0
SCN^-	84.32 ± 2.21	66.93 ± 2.21	0
NO_2^-	125.13 ± 10.09	49.22 ± 11.86	–0.15 ± 0.11
I^-	163.10 ± 0.22	11.16 ± 0.23	–0.83 ± 0.03
AsO_3^{3-}	162.42 ± 0.41	10.73 ± 0.08	–0.84 ± 0.02
SeO_4^{2-}	159.93 ± 0.08	7.94 ± 0.09	–0.98 ± 0.02
NO_3^-	164.45 ± 6.26	6.38 ± 2.47	–1.11 ± 0.22
Br^-	162.55 ± 6.25	5.73 ± 0.68	–1.12 ± 0.06
ClO_4^-	156.58 ± 0.40	4.46 ± 0.48	–1.23 ± 0.04
AsO_4^{3-}	156.25 ± 0.62	4.44 ± 0.20	–1.23 ± 0.04
SO_4^{2-}	162.13 ± 8.58	3.43 ± 1.24	–1.37 ± 0.17
F^-	161.17 ± 8.88	2.79 ± 0.22	–1.43 ± 0.05
Cl^-	159.71 ± 9.09	2.10 ± 1.10	–1.60 ± 0.20
$H_2PO_4^-$	160.89 ± 10.16	1.50 ± 0.44	–1.72 ± 0.14

Figure 4.19 Colors of the paper–based optode with **L2** ionophore toward various anions in 0.01 M boric/borate buffer solution at pH 8.0 with the immersing time of 15 minutes.

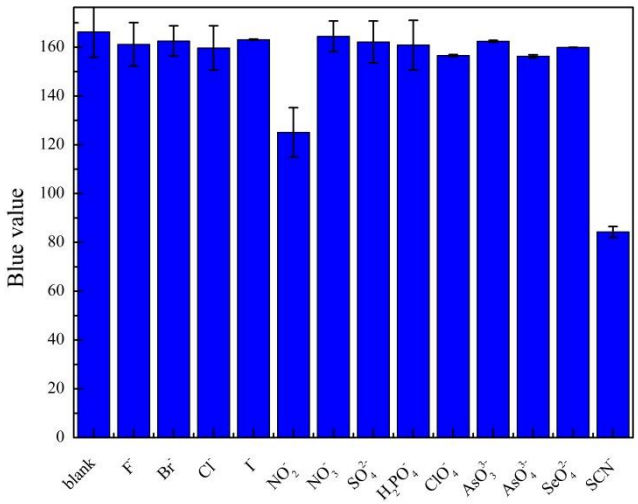

Figure 4.20 Blue values of paper-based with **L2** ionophore responses of the sensor toward various anions in 0.01 M boric/borate buffer solution at pH 8.0 with the immersing time of 15 minutes.

4.2.1.7 Analytical performance of paper-based optode containing L2 ionophore

In order to further investigate the color change behavior of the paper–based optode, the optimized conditions were applied to detect thiocyanate in the solution. The optode composed of 10.10 and 13.88 mmol/kg of ion exchanger (TDMACl), and **L2**, respectively. The amount of polymer (PVC): plasticizer (*o*–NPOE) was 1: 2 w/w in the total amount of 90 mg and then applied to detect thiocyanate in boric/borate buffer solution pH 8.0. The measurements were performed in the concentration of thiocyanate ions from 1.00×10^{-7} to 1.00×10^{-2} M.

The calibration curve was demonstrated on the paper–based optode with the **L2** ionophore in the presence of various concentrations of SCN^- standard solutions from 1.00×10^{-7} to 1.00×10^{-2} M in 0.01 M boric/borate buffer at pH 8.0. The paper–based optode was dipped into the thiocyanate solution for 15 minutes. The color change of the paper–based optode with **L2** ionophore with thiocyanate ions was observed by naked–eye from pink to green as shown in **Figure 4.21**. The sigmoidal response of the paper-based optode with logarithm of SCN^- concentrations was fitted with the sigmoidal relationship given by the Boltzman equation as expressed in **Eq.**

(2.13) where the A_1, A_2, x_0, and dx are parameters given in **Table 4.7**. The calibration curve shown the relationship between the ΔBlue values and logarithm of SCN^- concentrations is illustrated in **Figure 4.22** and provided an excellent correlation coefficient (R^2 = 0.9988). The limit of detection (LOD) was 7.00×10^{-6} M of SCN^- defined using the cross–section of the two extrapolated linear portions of the calibration curves. The proposed paper–based optode showed the working ranges from 1.00×10^{-6} M to 1.00×10^{-3} M.

It was found that the paper–based optode provided the color change of **L2** ionophore with lower LOD than the solution of **L2** ionophore indicating that the developed paper–based optode was successfully improve the analytical characteristic features for thiocyanate determination.

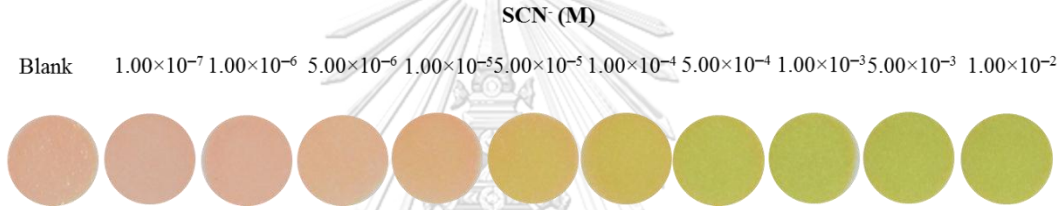

Figure 4.21 Colors of paper–based optode with **L2** ionphore in various concentration of SCN^- solution under the optimized conditions.

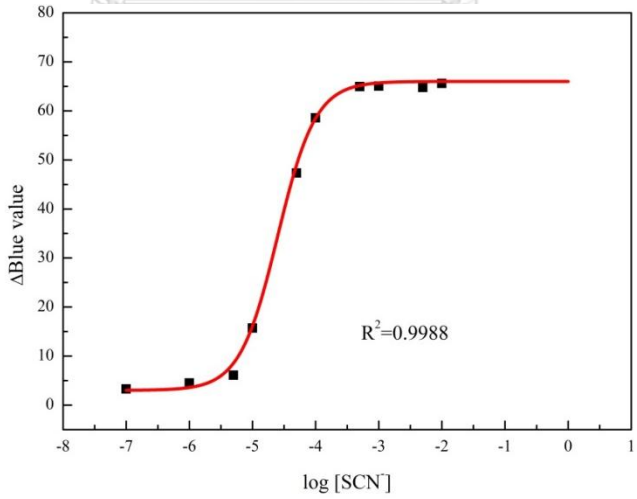

Figure 4.22 Sigmoidal calibration curve of the paper-based optode with **L2** ionophore in the presence of various concentrations of SCN^- standard solutions from 1.00×10^{-7} to 1.00×10^{-2} M in 0.01 M boric/borate buffer at pH 8.0 with the mixing time of 15 minutes.

Table 4.7 Parameters of Boltzmann equation for the SCN^- determination of paper–based optode with **L2** ionphore.

Parameters	Values
A_1	3.00
A_2	66.00
x_0	–4.60
dx	0.30

4.2.2 5,10,15,20–Tetrakis(4–octyloxyphenyl)porphyrin cobalt(II) complex (L3) as an ionophore

L3 ionophore was synthesized by SCRU. The **L3** ionophore has been designed to contain longer aliphatic hydrocarbon chain than **L2** ionophore. The longer aliphatic chain of hydrocarbon in metalloporphyrin ionophore provided the higher lipophilicity of the ionophore which increased the solubility of ionophore in organic phase. The leaking of the ionophore out of the organic phase may lead to the poor sensitivity of the optode sensors. Thus, we expected that the **L3** would be performed better sensitivity among **L2** ionophore.

4.2.2.1 Measurement of thiocyanate using the solution of L3 ionophore

First, the study of the color change of **L3** and thiocyanate was considered. 1 mg **L3** was dissolved in 2 mL of THF and stirred for an hour. Then, the color measurements of the proposed cocktail solution were performed by adding 0.1 mL of cocktail solution into 1.9 mL of the solution containing thiocyanate with different concentrations in the range from 1.00×10^{-7} to 1.00×10^{-2} M at pH 8.0. After 15 minutes, the mixed solution was observed by capturing the photographs with DSLR camera under a studio lightbox.

As shown in **Figure 4.23** there was no response of color change from the different thiocyanate concentrations. Compared to **L2**, the aliphatic chain of **L3** in porphyrin complex is longer than **L2** which leads to the poor sensitivity of the detection of target ion in an aqueous solution. Then, the film-based optode containing **L3** was prepared and immersed in 10 mM SCN^- solution. The blue shift of **L3** was

illustrated in **Figure 4.24**. Moreover, to improve the sensitivity of method for thiocyanate determination, these analytical approaches have been implemented in paper–based couple with bulk optode technique [43].

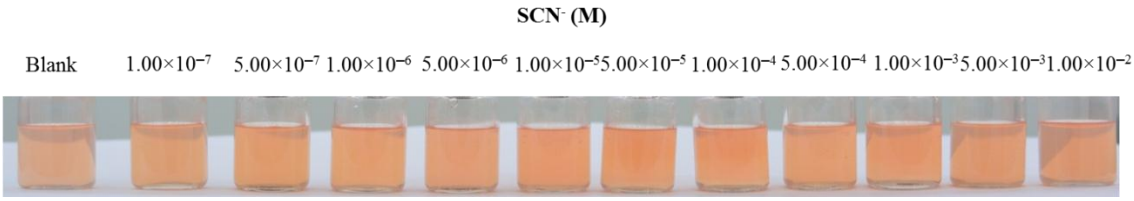

Figure 4.23 Color of **L3** in the various concentration of SCN^- solution at pH 8.0 with the mixing time of 15 minutes.

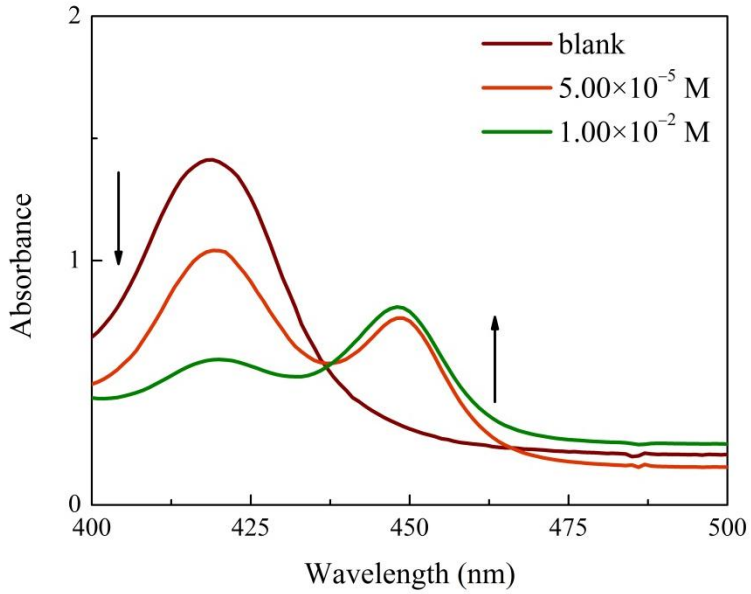

Figure 4.24 Absorption spectra of film-based optode with **L3** ionophore toward SCN^- with the immersing time of 15 minutes.

4.2.2.2 Measurement of anion using the paper–based optode with L3 ionophore

For preliminary study, the paper–based optode was dipped into the SCN^- solution for 15 minutes. The color change of the paper–based platform based on **L3** with thiocyanate was shown obviously by naked–eye from pink to green as illustrated in **Figure 4.25**. In addition, the color values were performed by capturing the photographs with DSLR camera under a studio lightbox. The color values in term of Blue values were fitted with Boltzmann equation as the quantitative model shown in sigmoidal response which provided the excellent correlation ($R^2 > 0.99$). It was clearly shown that the paper–based optode provided the color change of **L3** while the solution of **L3** showed no color change indicating that the developed paper–based optode was successfully improve the analytical characteristic features of the thiocyanate determination.

Figure 4.25 Colors of the paper–based optode contained **L3** ionophore toward the various concentration of SCN^- at pH 8.0 with the immersing time of 15 minutes.

4.2.2.3 Types of filter paper and plasticizer on the response of paper-based optode containing L3 ionophore

According to the effect of the composition of optode, the first two factors studied were the plasticizer and the filter paper because their properties may lead to the efficiency of the color change detection. The filter papers studied in this work were Whatman no.1 (pore size: 11 µm) and Whatman no.42 (pore size: 2.5 µm). The second parameter was the type of plasticizers which were DOS and *o*–NPOE. The color measurements of the proposed paper–based optode were performed by dipping the paper-based optode in a solution containing 1.00×10^{-4} M SCN^- and captured the photographs with DSLR camera under a studio lightbox.

The results are shown in the **Table 4.8** and plotted as the stacked graph to compare the relationship of the color change among SCN^- in **Figure 4.26** which were illustrated the Blue values of the paper–based optode in the buffer solution as blank condition as shown in blue area. Then, the paper–based optode was dipped into 1.00×10^{-4} M of thiocyanate solution and the color of the paper–based optode was changed as shown in term of ΔBlue value (red area). To simplify the color change of the paper–based optode in buffer solution and anion solution, the percentage of blue value was calculated follows **Eq.(4.2)**.

As can be seen in **Figure 4.26**, the filter paper no.1 and *o*–NPOE plasticizer (second column) showed the highest %ΔBlue value indicating that the filter paper no.1 and *o*–NPOE plasticizer were the better composition for the thiocyanate determination using paper–based optode.

Table 4.8 Blue values of the paper–based optode with **L3** ionophore in buffer solution as blank and after dipping in 1.00×10^{-4} M thiocyanate solution.

Filter paper	**Plasticizer**	**Blue value**		**ΔBlue value**	**%ΔBlue value**
		Blank	**SCN^-**		
No.1	DOS	180.05	129.77	50.28	28
	o–NPOE	187.55	96.84	90.71	48
No.42	DOS	169.46	156.66	12.8	8
	o–NPOE	165.62	99.71	65.91	40

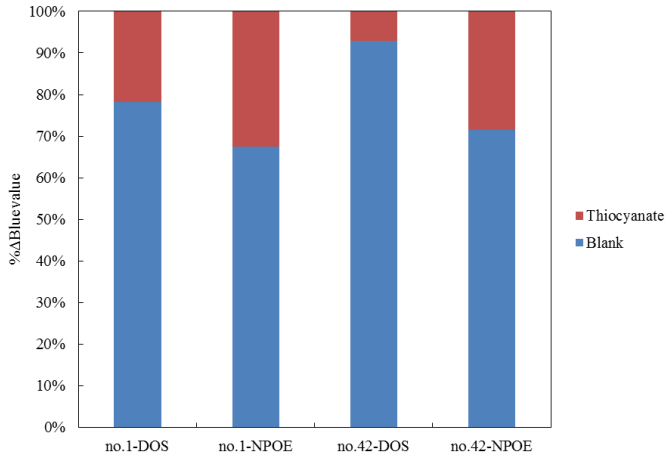

Figure 4.26 Percentage of color change of the paper–based optode with **L3** ionophore in buffer solution (blank, blue area) and in the 1.00×10^{-4} M thiocyanate solution (red area).

4.2.2.4 Effect of immersing time on the response of paper-based optode containing L3 ionophore

The other interesting parameter was the effect of immersing time using the paper–based optode to determine SCN^- in the solutions. The paper–based optode was immersed in the various concentrations obtained from the 1.00×10^{-7} M to 5.00×10^{-3} M of thiocyanate solution. The results were shown in **Figure 4.27**. Moreover, the sigmoidal response curves and ΔBlue values were presented in **Figure 4.28** indicating that the ΔBlue value was increased with a function of time. In addition, the ΔBlue values were stabled with the immersing time more than 10 minutes for the concentration of thiocyanate below 1.00×10^{-5} M while the concentration of thiocyanate higher than 5.00×10^{-5} M, the constant ΔBlue values were observed to be 5 minutes as can be seen as two groups of concentration in **Figure 4.28**. Thus, the optimized immersing time required to achieve a constant response for SCN^- detection was found to be 10 minutes. However in this work, 15 minutes was applied to be the immersing time.

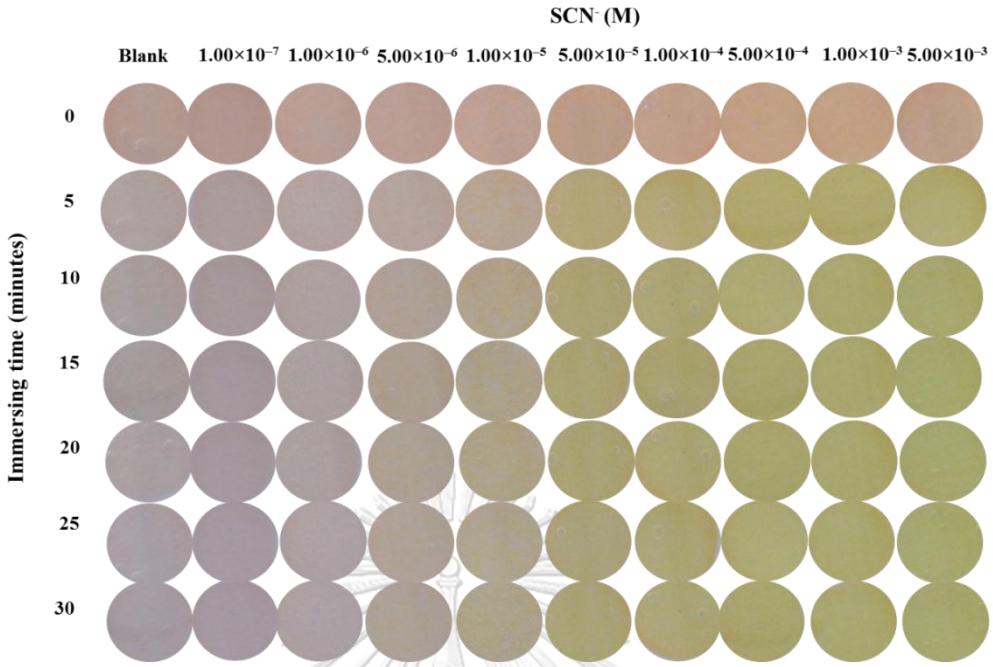

Figure 4.27 Colors of the paper–based optode contained **L3** ionophore toward the various concentrations of SCN^- at the different immersing times.

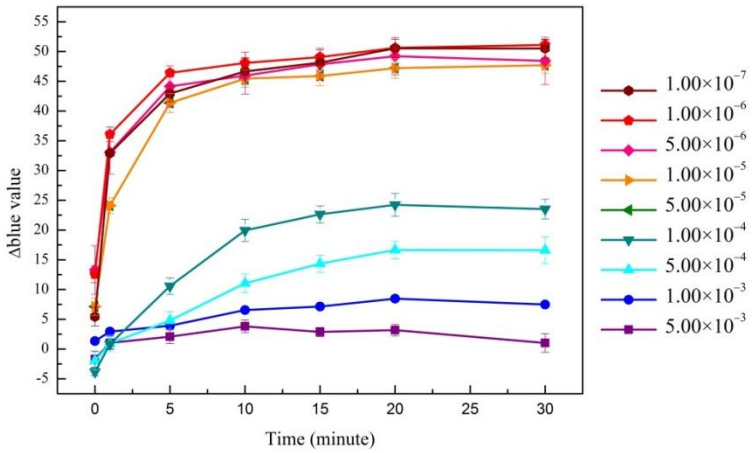

Figure 4.28 Effect of immersing time on ΔBlue values of the paper-based optode with **L3** ionophore toward the various concentrations obtained from the 1.00×10^{-7} to 5.00×10^{-3} M SCN^-.

4.2.2.5 Effect of pH of the sample solution on the response of paper-based optode containing L3 ionophore

The color change of **L3** ionophore and thiocyanate may affect by pH of the sample solution due to the protonation and deprotonation behavior on metalloporphyrin ionophore. Therefore, the pH effect was also studied by measuring the color change of **L3** ionophore and thiocyanate in various pH buffer solutions. The different pH of solutions was prepared in different buffer types (shown in **Table 3.4**).

The colors of the paper–based optode contained **L3** ionophore toward the various concentrations of SCN^- at different pH with the immersing time of 15 minutes were shown in **Figure 4.29.** The response ΔBlue values were then measured and plotted the sigmoidal curve in **Figure 4.30**. From the results, the response ΔBlue values curves were shifted after the pH increased from 4.0 to 10.0. The ΔBlue values curves were shifted to the right when the pH was increased. The sigmoidal curve of the ΔBlue values in the pH from 4.0 to 8.4 were approximately nearby each other apart from the curves of pH 9.0 and 10.0. The results can be assumed that at pH 9.0 and 10.0, the **L3** was disturbed the complexation of **L3** and thiocyanate by hydroxide ions. Therefore, pH 7.4 was chosen as the optimized pH for further experiments with the expected a good detection limit.

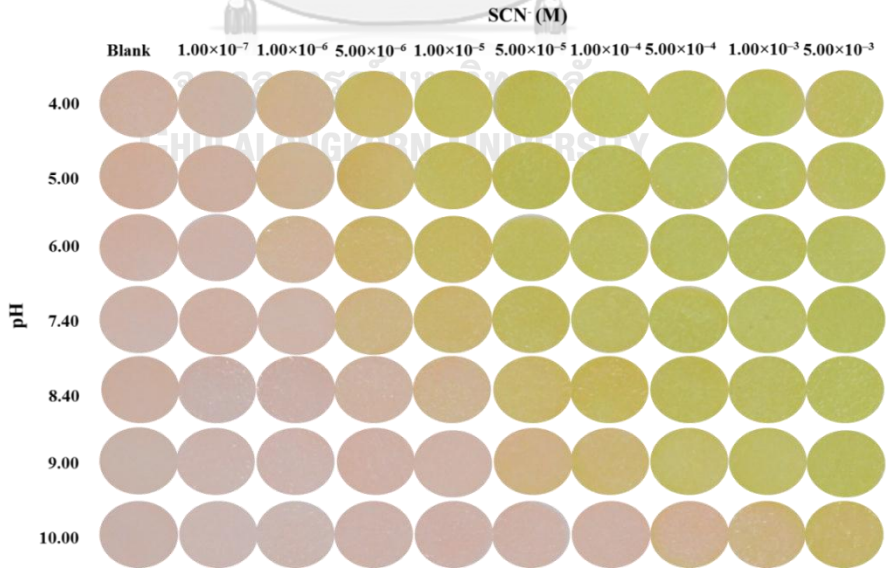

Figure 4.29 Colors of the paper–based optode with **L3** ionophore toward the various concentrations of SCN^- at different pH with the immersing time of 15 minutes.

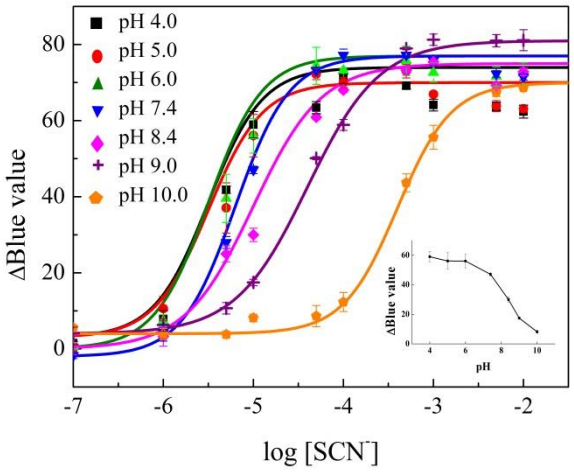

Figure 4.30 Effect of pH on the sigmoidal response curves of paper-based optode with **L3** ionophore. ΔBlue values were obtained from various concentrations of SCN^- solutions in 0.01 M buffer at different pH values with the immersing time of 15 minutes. Inset graph showed the plot of pH and ΔBlue values-based responses.

To optimize the other sensing characteristic of the prepared paper–based optode, the concentration of ionophore and ion exchanger were examined using CCD method.

4.2.2.6 Central composite experimental design (CCD) for paper–based optode with L3 ionophore

The CCD approach was again applied to optimize the effected factors of color response including the amounts of ion exchanger (TDMACl) and **L3** for composition of the paper-based optode while all of the parameters were coded to avoid analytical bias from using different levels of each parameter. The code values of each parameter are shown in **Table 3.6**. All experiments (13 experiments) in the box were investigated for construction of a surface response plot.

According to the experimental results, all variables were considered as quadratic terms via more accurate results. Moreover, the relevant between two variables were also investigated to determine the effect of each interaction as shown in **Table 4.9**. In order to show the optimum point of each parameter, the linear regression was calculated resulting in the coefficients of the equation, as shown in **Eq.**

(4.4) which was responded as 3D surface plots to figure out the optimum points for each parameter.

$$y_{blue\ value} = 96.46 - 9.45X_1 - 8.82X_2 + 4.87X_1^2 + 2.80X_2^2 + 6.87X_1X_2 \qquad \textbf{(4.4)}$$

Figure 4.31 shows the relationship between the amount of ion exchanger and ionophore of the working solution. The highest and lowest experimental Blue values from experiments were represented in red and blue, respectively.

As shown in the x–axis, the effect of the concentration of the ion exchanger (TDMACl) on the Blue value of the paper–based optode, in the results, the blue areas (Blue value below 100) were on one side of the figure, which corresponded to the concentration of the ion exchanger values in the range lower than 6.50 mmol/kg and higher than 3.50 mmol/kg. And, the results indicated that the optimum amount of ionophore was higher than 12.50 mmol/kg (blue).

Both of the surface plots and contours plot (**Figure 4.31**) showed the optimum condition of two parameters (the amount of ion exchanger and ionophore) which was related to the good sensitivity via the extraction of ionophore (**L3**) and thiocyanate using the purposed paper–based optode. From **Figure 4.31**, it can be indicated the optimum values for all parameters that the optimum amount of ion exchanger was considered to be in the range of lower than 6.50 mmol/kg and higher than 3.50 mmol/kg while the amount of ionophore was determined to be higher than 12.50 mmol/kg.

Table 4.9 Two parameters with three levels of CCD experiments for optimization of the amounts of TDMACl (Factor X_1) and **L3** (Factor X_2) for thiocyanate ions determination using paprer–based optode.

Experiment	b_0	factor					Blue value	
		b_1	b_2	b_1^2	b_2^2	b_{12}	experiment	predict
1	1	–1	–1	1	1	1	128.34 ± 0.78	129.26
2	1	–1	1	1	1	–1	91.81 ± 0.80	96.63
3	1	1	–1	1	1	–1	99.51 ± 2.30	97.89
4	1	1	1	1	1	1	90.45 ± 2.87	92.73
5	1	–1.414	0	1.999	0	0	123.85 ± 0.50	119.55
6	1	1.414	0	1.999	0	0	91.74 ± 1.47	92.83
7	1	0	–1.414	0	1.999	0	112.48 ± 1.72	114.53
8	1	0	1.414	0	1.999	0	94.84 ± 0.68	89.59
9	1	0	0	0	0	0	96.47 ± 1.45	96.46
10	1	0	0	0	0	0	97.03 ± 0.28	96.46
11	1	0	0	0	0	0	96.02 ± 0.58	96.46
12	1	0	0	0	0	0	96.07 ± 0.31	96.46
13	1	0	0	0	0	0	96.70 ± 0.64	96.46

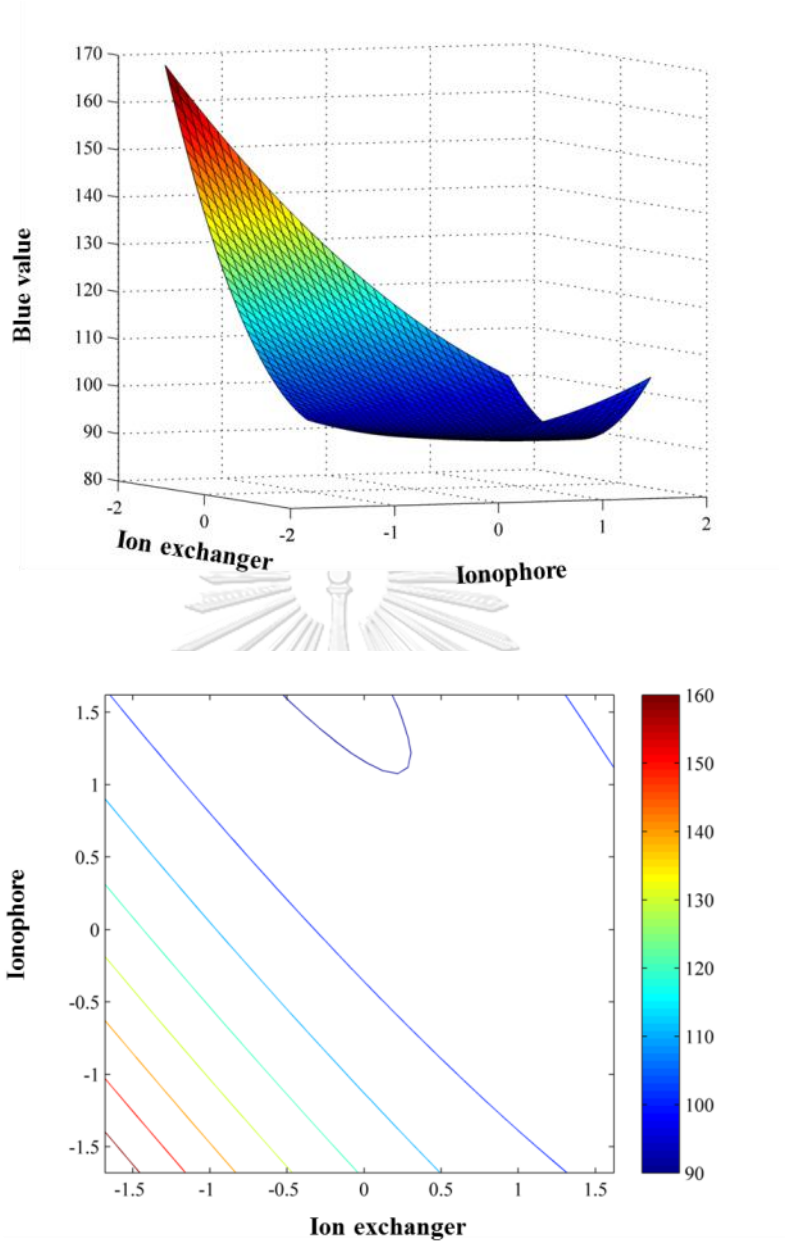

Figure 4.31 Effects of the amount of TDMACl and **L3** on Blue value.

Using the multiple linear regressions, a regression model was calculated from the responsive surface plots, as shown in the **Eq. (4.4)**. The linear relationship from the equation was ploted and shown in **Figure 4.32** with $R^2 = 0.9382$.

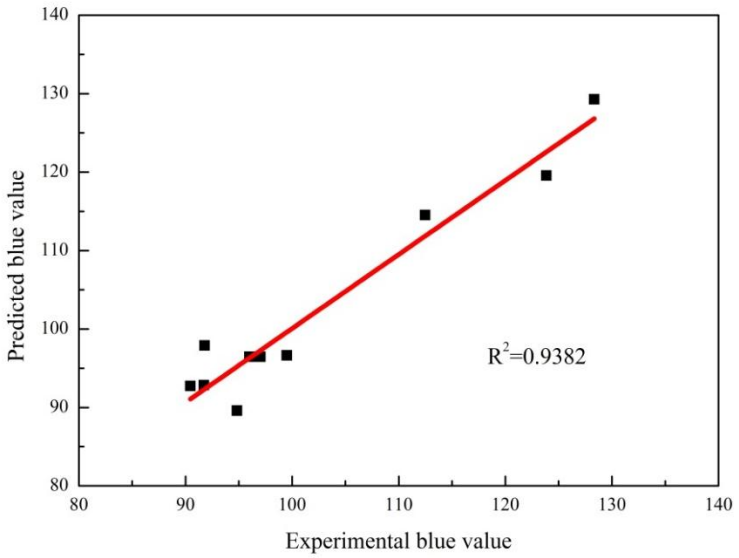

Figure 4.32 Correlation of the experimental (observed) Blue value and the predicted Blue value of the paper–based optode with **L3** ionophore.

Each coefficient in **Eq. (4.4)** was indicated the significance of the parameters in terms of either an isolated term or a related term. The coefficients of both the amount of ion exchanger and ionophore were negative which implied that the Blue value decrease when the amount of ion exchanger and ionophore increased. The optimized values of the parameters were figured out using the first derivative method from the constructed equation. It was found that the optimized amounts of ion exchanger and ionophore were found to be 4.70 mmol/kg and 13.75 mmol/kg, respectively. Therefore for the futher experiment, these conditions were used as the optimum condition to determine thiocyanate by paper–based optode.

4.2.2.7 Selectivity

In order to determine the selectivity of the the prepared paper–based optode toward the target anions among interfering anions, the selectivity of purposed paper–based optode was investigated by dipping the paper–based optode in the separate 10 mM solutions of sodium salt of AsO_3^{3-}, AsO_4^{3-}, SO_4^{2-}, $H_2PO_4^-$, NO_2^-, NO_3^-, F^-, I^-, Br^-, Cl^-, SCN^- and ClO_4^- at pH 7.4. Then, optode was observed by capturing the photographs with a DSLR camera under a studio lightbox.

For selectivity behavior, the proposed paper–based optode based on **L3** was performed and the results are shown in **Figure 4.33** and **Figure 4.34**. The thiocyanate showed lowest Blue value compared to the Blue value of the paper–based optode in the blank condition. It can be concluded that the **L3** showed highest selectivity toward thiocyanate over all interfering anions. The selectivity coefficient ($\log K_{IJ}^{opt}$) of optimized paper–based optode towards the various anions was calculated and showed in **Table 4.10**. The selectivity sequence obtained with optode was as follows: $SCN^- > NO_2^- > AsO_3^{3-} > AsO_4^{3-} > ClO_4^- > NO_3^- > Br^- > Cl^- > H_2PO_4^- > I^- > SO_4^{2-} > F^-$. Generally, the anion selectivity sequence is mostly followed the Hofmeister sequence which presented the lipophilicity of the target ions lead to the selectivity pattern of the optode [36]. As can be seen, the proposed paper–based optode exhibited the anion optical selectivity sequence that deviates significantly from the Hofmeister sequence and intimated high thiocyanate selectivity.

Table 4.10 Color responses and selectivity coefficient ($\log K_{IJ}^{opt}$) of optimized paper–based optode membrane with **L3** ionophore towards the several of sodium salt of anion.

Samples (1.00×10^{-4} M)	**Blue value**	**ΔBlue value**	**$\log K_{IJ}^{opt}$**
Tris–HCl buffer	174.63 ± 0.39	0	0
SCN^-	127.25 ± 1.01	47.37 ± 1.01	0
NO_2^-	141.92 ± 1.37	32.71 ±1.37	–0.16 ± 0.01
AsO_3^{3-}	163.08 ± 1.86	11.54 ± 1.86	–0.62 ± 0.07
AsO_4^{3-}	164.02 ± 1.67	10.60 ± 1.67	–0.66 ± 0.06
ClO_4^-	164.18 ± 1.67	10.45 ± 1.67	–0.66 ± 0.06
NO_3^-	164.87 ± 0.93	9.75 ± 0.93	–0.69 ± 0.05
Br^-	166.13 ± 0.97	8.49 ± 0.97	–0.75 ± 0.04
Cl^-	167.23 ± 0.34	7.40 ± 0.34	–0.81 ± 0.01
$H_2PO_4^-$	167.32 ± 1.18	7.31 ± 1.18	–0.82 ± 0.06
I^-	168.06 ± 0.46	6.56 ± 0.46	–0.86 ± 0.02
SO_4^{2-}	168.13 ± 0.83	6.50 ± 0.83	–0.87 ± 0.05
F^-	167.87 ± 2.17	6.75 ± 2.17	–0.87 ± 0.14

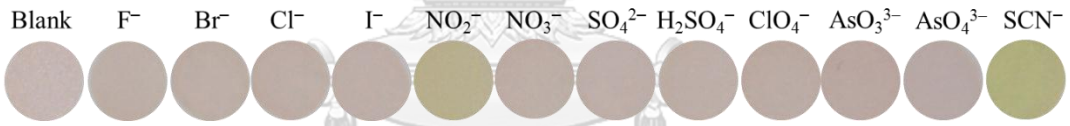

Figure 4.33 Colors of paper–based optode with the **L3** toward different 1 mM of anions in 0.01 M tris–HCl buffer solution at pH 7.4 with the immersing time of 15 minutes.

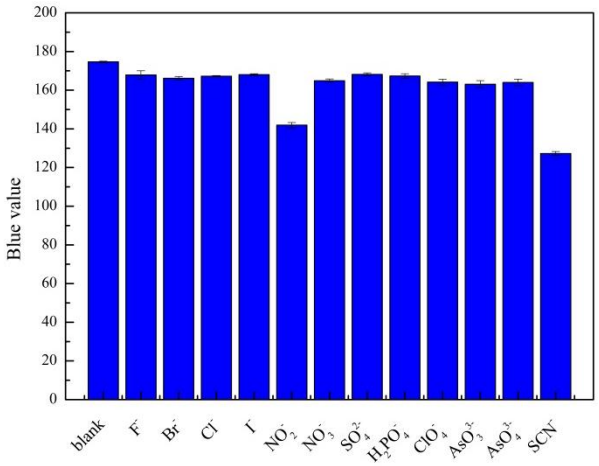

Figure 4.34 Blue values responses of the paper-based optode with **L3** ionophore toward various anions in 0.01 M tris–HCl buffer solution at pH 7.4 with the immersing time of 15 minutes.

4.2.2.8 Analytical performance of paper-based optode containing L3 ionophore

In order to further investigate the color change behavior of the **L3** ionophore paper–based membrane, the optimized condition were applied to detect thiocyanate in the solution. The membrane was composed of 4.70 and 13.75 mmol/kg of ion exchanger (TDMACl), and **L3**, respectively, the amount of polymer (PVC) : plasticizer (*o*–NPOE) are 1: 2 w/w in the total amount of 90 mg and then applied to detect thiocyanate in tris–HCl buffer solution at pH 7.4. The paper–based sensors were fabricated from the filter paper Whatman no.1. The measurements were performed in the concentration of thiocyanate from 1.00×10^{-7} to 5.00×10^{-3} M with the immerse time of 15 minutes.

The optimized parameters were applied to determine the thiocyanate in the solutions. The calibration curve was demonstrated on the paper–based optode with the **L3** in the presence of various concentrations of SCN^- standard solutions from 1.00×10^{-7} to 1.00×10^{-2} M in 0.01 M tris–HCl buffer at pH 7.4 and each concentration was evaluated in triplicate. The paper–based optode was dipped into the thiocyanate solution for 15 minutes. As a result in **Figure 4.35**, the color change of the paper–based optode was obviously seen by naked–eye from pink to green. The sigmoidal

response of the paper-based optode with logarithm of SCN^- concentrations was fitted with the sigmoidal relationship given by the Boltzman equation as expressed in **Eq. (2.13)** where the A_1, A_2, x_0, and dx are parameters given in **Table 4.11**. The calibration curve shown the relationship between the ΔBlue values and logarithm of SCN^- concentrations are illustrated in **Figure 4.36** and provided an excellent correlation coefficient (R^2 = 0.9915). The limit of detection (LOD) was 1.26×10^{-6} M of SCN^- defined by using the cross–section of the two extrapolated linear portions of the calibration curves. The proposed paper–based optode showed the working ranges from 1.00×10^{-6} M to 5.00×10^{-3} M.

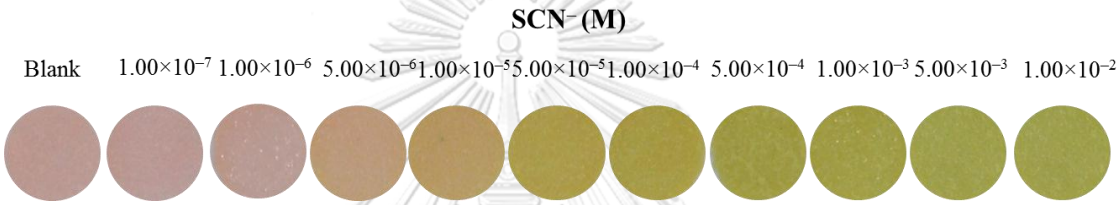

Figure 4.35 Colors of paper–based optode with **L3** in the various concentration of SCN^- solution with optimized condition.

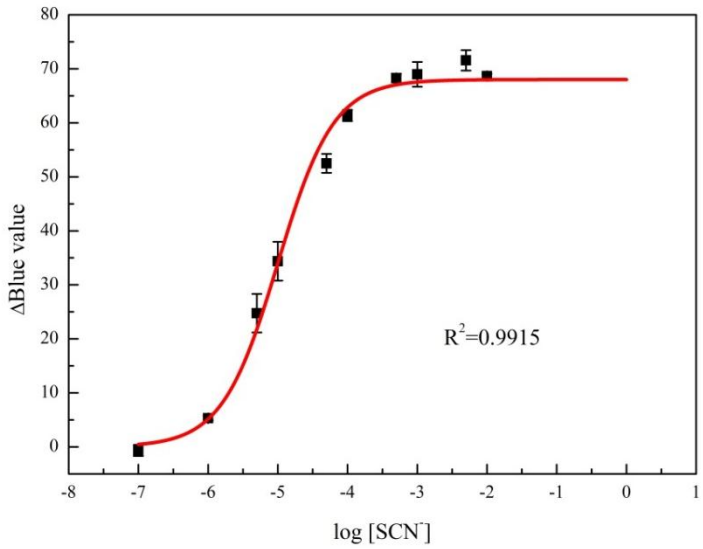

Figure 4.36 Sigmoidal calibration curve of paper-based optode with **L3** ionophore toward the various concentrations of SCN^- standard solutions from 1.00×10^{-7} to 1.00×10^{-2} M in 0.01 M tris–HCl buffer solution at pH 7.4 with the mixing time of 15 minutes.

Table 4.11 Parameters of Boltzmann equation for the SCN^- determination of paper–based optode with **L3** ionophore.

Parameters	Values
A_1	–0.66 ± 1.03
A_2	68.65 ± 0.41
x_0	–5.00
dx	0.40

To confirm the development of analytical performance of the synthesized ionophore (**L3**) with the purchased ionophore **L2**, the **L3** containing longer aliphatic hydrocarbon chain was investigated. The comparison of the sigmoidal calibration curves of the paper–based optode containing **L2** and **L3** ionophores indicated that the **L3** ionophore gave better sensitivity toward thiocyanate resulting in the LOD and working range.

4.2.2.9 Reproducibility

According to the reproducibility is one of the necessary characteristic performances, the reproducibility of the proposed paper–based optode was explored. The paper–based optodes were fabricated and measured with the range of concentration of thiocyanate from 1.00×10^{-7} M to 1.00×10^{-2} M in 0.01 M tris–HCl buffer solution at pH 7.4 with the immersing time of 15 minutes. The paper–based doped with **L3** exhibited a stable and a reproducible responses to thiocyanate, the colors of the paper–based optode and the comparison of the sigmoidal curve (as illustrated in **Figure 4.37** and **Figure 4.38**) were shown to yield reproducible analytical results during short–term experiments.

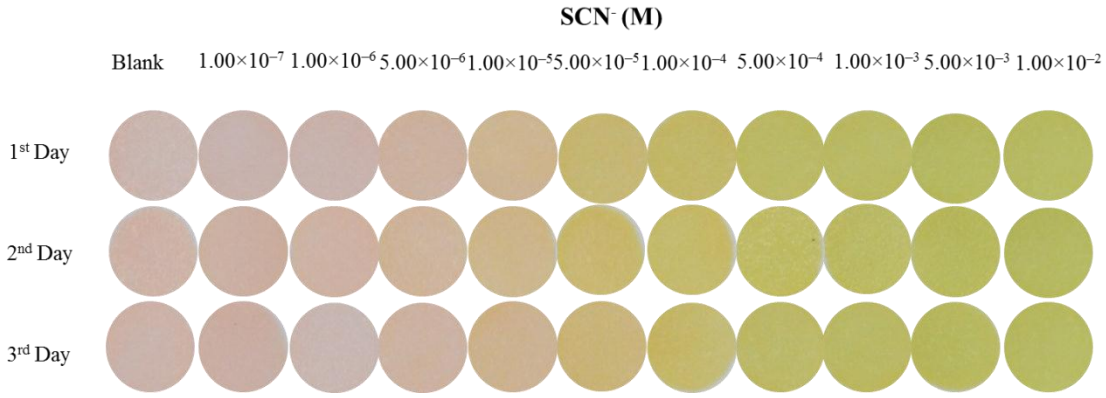

Figure 4.37 Colors of the paper–based optode with **L3** in the various concentrations of SCN^- solution which were demonstrated in different working days.

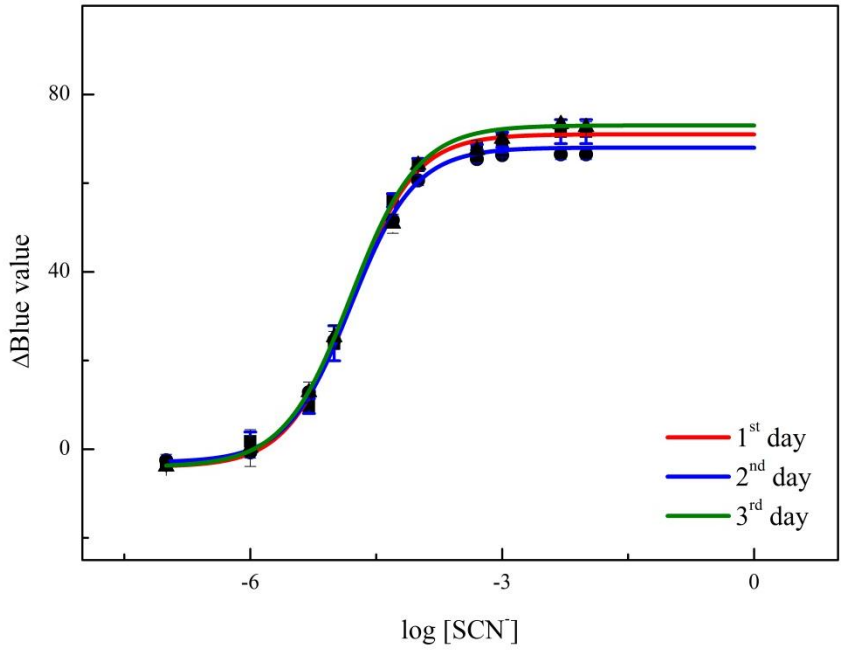

Figure 4.38 Comparison of the sigmoidal calibration curves of **L3** in the paper–based optode with the various concentrations of SCN^- standard solutions from 1.00×10^{-7} to 1.00×10^{-2} M in 0.01 M tris–HCl buffer solution at pH 7.4 with the immersing time of 15 minutes in three working day.

4.2.2.10 Real sample analysis

The promising results for proposed paper–based optode sensors based on **L3** for thiocyanate detection have led to apply the proposed paper–based optode to determine the concentration of thiocyanate in real sample solution under the optimized condition. The relevant & scientific merit had been approved from the research ethics review committee for research involving human research participants of Chulalongkorn university (COA No. 281/2019) as shown in appendix.

The urine samples were utilized as the real sample for thiocyanate determination. The urine samples were collected from a non–smoker and two smokers in Faculty of Science, Chulalongkorn University operated under the research ethics approval for research involving human. For the sample preparation, each urine sample was diluted with the different dilution steps via the different concentrations of thiocyanate in urine samples to fit with the working range of the proposed method. The urine samples no.1 and no.2 were diluted 4 in 5 with buffer solution to adjust the pH to pH 7.4 while the urine sample no.3 was diluted 1 in 5 with tris–HCl buffer solution.

As illustrated in **Table 4.12**, the concentrations of thiocyanate in the urine samples were successfully evaluated by analyzing ΔBlue values of the optimized paper–based optode. The concentration of thiocyanate of urine from non–smoker (urine no.1) was not detectable due to the concentration of thiocyanate in this sample was below the working range while the concentration of thiocyanate in urine sample from smokers (urine no.2 and 3) calculated with the dilution factor were 2.22 ± 0.13 and 6.65 ± 0.14 mg/L, respectively. These were reasonable agreement with the concentration obtained from ion chromatography (IC) on the same sample (urine no.1 : $t_{critical}$ 2.78 > t_{exp} 2.45–2.57, urine no.2 : $t_{critical}$ 2.78 > t_{exp} 0.74–1.04 and urine no.3 : $t_{critical}$ 4.30 > t_{exp} 0.85–1.23 with n = 3 at 95% of confidence level).

Table 4.12 Comparison of measured concentration of thiocyanate from proposed method and IC.

Urine	Spike (mg/L)	Paper–based optode			IC		
		concentration (mg/L)	% RSD	% recovery	concentration (mg/L)	% RSD	% recovery
no.1[b]	–	N.D.[a]			N.D.[a]		
	1	0.86 ± 0.06	7	86	0.75 ± 0.01	2	75
	3	2.38 ± 0.18	8	79	2.73 ± 0.09	3	91
no.2[b]	–	1.79 ± 0.08	5	-	1.73 ± 0.02	1	-
	1	2.79 ± 0.01	5	100	2.86 ± 0.03	1	113
	3	4.64 ± 0.15	3	95	4.75 ± 0.04	1	101
no.3[c]	–	1.32 ± 0.02	2	-	1.28 ± 0.05	4	-
	1	2.32 ± 0.14	6	99	2.44 ± 0.03	1	116
	3	4.64 ± 0.21	4	111	4.77 ± 0.02	1	116

[a] N.D. = not detectable
[b] dilution factor = 0.8
[c] dilution factor = 0.2

CHAPTER V

CONCLUSION

The di–tripodal amine calix[4]arene copper(II) complex (**L1**–**Cu**), 5,10,15,20–tetrakis(4–methoxyphenyl)porphyrin cobalt(II) complex or arsenite ionophore (**L2**) and 5,10,15,20–tetrakis(4–octyloxyphenyl)porphyrin cobalt(II) complex (**L3**) were successfully applied as an ionophore for anion determination using ISEs and paper–based optode method. The **L1-Cu** demonstrated great sensitivity and selectivity toward perchlorate ions while the **L2** and **L3** show the appropriate sensitivity and selectivity toward thiocyanate ions. These results proposed that the amine calix[4]arene could bind strongly with copper(II) and led to be used as the anions carrier. In addition, cobalt(II) porphyrin complex were found to form complex with thiocyanate ions showing good selectivity. The optimized conditions were successfully evaluated using CCD approach including the other effective parameters were also studied.

The ISEs based on di–tripodal amine calix[4]arene complex copper(II) complex (**L1**–**Cu**) was achieved using the membrane prepared from 3.25 and 13.25 mmol/kg of ion exchanger (KT*p*ClPB), and **L1**, respectively, the amount of polymer (PVC) : plasticizer (*o*–NPOE) are 1: 2 w/w in the total amount of 220 mg and the sample solution of perchlorate ion was prepared in boric/borate buffer solution pH 8. As a result, the negative potentiometric responses for perchlorate ions yielded a near–Nernstian slope (–58.02 ± 0.01 mV/decade) in the working range of concentration from 1.00×10^{-6} to 1.00×10^{-2} M, the limit of detection was 3.00×10^{-5} M and showed an excellent correlation with a correlation coefficient (R^2=0.9994).

The development of the platform for bulk optode sensor into the paper–based optode was clearly found that the paper–based optode provided the color change with lower which can be indicated that the developed paper–based optode was successfully improve the analytical characteristic performance of the thiocyanate determination.

The paper–based optode with the **L2** and **L3** ionophore were demonstrated in the various concentrations of SCN^- standard solutions from 1.00×10^{-7} M to 1.00×10^{-2} M with the immerse time 15 minutes. The color of paper–based optode was changed from pink to green which could be observed by naked–eye. The factors that affected the color change including types of paper substrate and composition of cocktail solution were evaluated. The CCD with RSM was also used to perform the optimized concentration of the component of cocktail solution: ion exchanger and ionophore resulting in the lowest *Blue* value and illustrated the acceptable correlation coefficients ($R^2 > 0.93$). In addition, the paper–based optode based of both **L2** and **L3** responded to thiocyanate with the highest selectivity among other anions .The calibration curves which shown the relationship between the ΔBlue values and logarithm of SCN^- concentrations provided an excellent correlation with a correlation coefficient. According to the results, the limit of detection (LOD) of the paper–based containing **L2** and **L3** were 7.00×10^{-6} and 1.26×10^{-6} M of SCN^-, respectively. The proposed paper–based optode of **L3** showed the wider working ranges from 1.00×10^{-6} to 5.00×10^{-3} M among **L2**. The **L3** was used in the paper–based optode to determine the concentration of thiocyanate ions in urine sample from smoker and non–smoker with favorable agreement with IC technique.

Suggestion for further work

For the further study, the stability and robustness of the developed sensor are the interesting factors. The stability and robustness of the polymeric membrane can be partially associated by their structures. Therefore, the polymeric material should be investigated. The role characteristic of the materials is that they should not interfere the interaction between ionophores and analytes ions. The materials have been developed for the polymeric membrane such as polyurethane [82], polymethylmethacrylate [83, 84] and silicone rubber [85].

REFERENCES

[1]. Chohan, Z. H.; Praveen, M., Biological role of anions (sulfate, nitrate , oxalate and acetate) on the antibacterial properties of cobalt (II) and nickel(II) complexes with pyrazinedicarboxaimide derived, furanyl and thienyl compounds. *Met.-Based Drugs* **1999,** *6* (2), 95-99.

[2]. Suk, J.-m.; Jeong, K.-S., Indolocarbazole-based foldamers capable of binding halides in water. *J. Am. Chem. Soc.* **2008,** *130* (36), 11868-11869.

[3]. Chohan, Z. H.; Rauf, A., Pharmacological role of anions (sulphate, nitrate, oxalate and acetate) on the antibacterial activity of cobalt(II), copper(II) and nickel(II) complexes with nicotinoylhydrazine-derived ONO, NNO and SNO Ligands. *Met.-Based Drugs* **1996,** *3* (5), 211-217.

[4]. Lavigne, J. J.; Anslyn, E. V., Teaching old indicators new tricks: a colorimetric chemosensing ensemble for tartrate/malate in beverages. *Angew. Chem. Int. Ed.* **1999,** *38* (24), 3666-3669.

[5]. Rajbanshi, A.; Moyer, B. A.; Custelcean, R., Sulfate separation from aqueous alkaline solutions by selective crystallization of alkali metal coordination capsules. *Cryst. Growth Des.* **2011,** *11* (7), 2702-2706.

[6]. Mohammad, A.; Chahar, J. P. S., Thin-layer chromatographic separation, colorimetric determination and recovery of thiocyanate from photogenic waste, river and sea waters. *J. Chromatogr. A* **1997,** *774* (1), 373-377.

[7]. Carrasco, N., Iodide transport in the thyroid gland. *Biochim. Biophys. Acta, Biomembr.* **1993,** *1154* (1), 65-82.

[8]. Calderón, R.; Palma, P.; Parker, D.; Molina, M.; Godoy, F. A.; Escudey, M., Perchlorate levels in soil and waters from the atacama desert. *Arch. Environ. Contam. Toxicol.* **2014,** *66* (2), 155-161.

[9]. Spurr, L. P.; Watts, M. P.; Gan, H. M.; Moreau, J. W., Biodegradation of thiocyanate by a native groundwater microbial consortium. *PeerJ* **2019,** *7:e6498*, 1-17.

[10]. Blount, B. C.; Alwis, K. U.; Jain, R. B.; Solomon, B. L.; Morrow, J. C.; Jackson, W. A., Perchlorate, nitrate, and iodide intake through tap water. *Environ. Sci. Technol.* **2010,** *44* (24), 9564-9570.

[11]. Shi, Y.; Zhang, P.; Wang, Y.; Shi, J.; Cai, Y.; Mou, S.; Jiang, G., Perchlorate

in sewage sludge, rice, bottled water and milk collected from different areas in China. *Environ. Int.* **2007,** *33* (7), 955-962.

[12]. Yong, L.; Wang, Y.; Yang, D.; Liu, Z.; Abernethy, G.; Li, J., Investigation of concentration of thiocyanate ion in raw cow's milk from China, New Zealand and the Netherlands. *Food Chem* **2017,** *215*, 61-66.

[13]. Benito, S.-B.; Silvana, L. G., Milk transfer of cyanide and thiocyanate: Cyanide exposure by lactation in goats. *Vet. Res.* **2003,** *34* (2), 213-220.

[14]. Theodorakis, C.; Rinchard, J.; Anderson, T.; Liu, F.; Park, J.-W.; Costa, F.; McDaniel, L.; Kendall, R.; Waters, A., Perchlorate in fish from a contaminated site in east-central Texas. *Environ. Pollut.* **2006,** *139* (1), 59-69.

[15]. Felker, P.; Bunch, R.; Leung, A. M., Concentrations of thiocyanate and goitrin in human plasma, their precursor concentrations in brassica vegetables, and associated potential risk for hypothyroidism. *Nutr. Rev.* **2016,** *74* (4), 248-258.

[16]. Urbansky, E. T.; Brown, S. K.; Magnuson, M. L.; Kelty, C. A., Perchlorate levels in samples of sodium nitrate fertilizer derived from Chilean caliche. *Environ. Pollut.* **2001,** *112* (3), 299-302.

[17]. Akcil, A., Destruction of cyanide in gold mill effluents: biological versus chemical treatments. *Biotechnol. Adv.* **2003,** *21* (6), 501-511.

[18]. Naik, R. M.; Kumar, B.; Asthana, A., Kinetic spectrophotometric method for trace determination of thiocyanate based on its inhibitory effect. *Spectrochim. Acta A* **2010,** *75* (3), 1152-1158.

[19]. Basova, E. M.; Ivanov, V. M.; Apendeeva, O. K., Spectrophotometric determination of thiocyanate ions in stratal waters. *Mosc. Univ. Chem. Bull.* **2014,** *69* (1), 12-19.

[20]. Shahine, S.; Khamis, S., Indirect spectrophotometric determination of perchlorate using nitron as reagent. *Microchem. J.* **1975,** *20* (4), 409-414.

[21]. Pourreza, N.; Mousavi, H. Z., Extraction spectrophotometric determination of trace amounts of perchlorate based on ion-pair formation with thionine. *J. Anal. Chem.* **2005,** *60* (9), 816-818.

[22]. Destanoğlu, O.; Gümüş Yılmaz, G., Determination of cyanide, thiocyanate, cyanate, hexavalent chromium, and metal cyanide complexes in various mixtures by ion

chromatography with conductivity detection. *J Liq Chromatogr R T* **2016,** *39* (9), 465-474.

[23]. Hofmeister, F., Zur lehre von der wirkung der salze. *Archiv für experimentelle Pathologie und Pharmakologie* **1888,** *24* (4), 247-260.

[24]. Pesce, L.; Kopp, P., Iodide transport: implications for health and disease. *Int. J. Pediatr. Endocrinol.* **2014,** *2014* (1), 8-8.

[25]. Vesey, C. J.; Saloojee, Y.; Cole, P. V.; Russell, M. A., Blood carboxyhaemoglobin, plasma thiocyanate, and cigarette consumption: implications for epidemiological studies in smokers. *BMJ* **1982,** *284* (6328), 1516-1518.

[26]. van Haeringen, N. J.; Ensink, F. T. E.; Glasius, E., The peroxidase-thiocyanate-hydrogenperoxide system in tear fluid and saliva of different species. *Exp. Eye Res.* **1979,** *28* (3), 343-347.

[27]. Minarowski, Ł.; Sands, D.; Minarowska, A.; Karwowska, A.; Sulewska, A.; Gacko, M.; Chyczewska, E., Thiocyanate concentration in saliva of cystic fibrosis patients. *Folia Histochem. Cytobiol.* **2008,** *46* (2), 245-246-245-246.

[28]. Leung, A. M.; Braverman, L. E.; He, X.; Schuller, K. E.; Roussilhes, A.; Jahreis, K. A.; Pearce, E. N., Environmental perchlorate and thiocyanate exposures and infant serum thyroid function. *Thyroid* **2012,** *22* (9), 938-943.

[29]. Kirk, A. B.; Dyke, J. V.; Martin, C. F.; Dasgupta, P. K., Temporal patterns in perchlorate, thiocyanate, and iodide excretion in human milk. *Environ. Health Perspect.* **2007,** *115* (2), 182-186.

[30]. Chandler, J. D.; Day, B. J., Thiocyanate: a potentially useful therapeutic agent with host defense and antioxidant properties. *Biochem. Pharmacol.* **2012,** *84* (11), 1381-1387.

[31]. Honig, D. H.; Hockridge, M. E.; Gould, R. M.; Rackis, J. J., Determination of cyanide in soybeans and soybean products. *J. Agric. Food Chem.* **1983,** *31* (2), 272-275.

[32]. Buratti, M.; Xaiz, D.; Caravelliand, G.; Colombi, A., Validation of urinary thiocyanate as a biomarker of tobacco smoking. *Biomarkers* **1997,** *2* (2), 81-85.

[33]. Kenova, T. A.; Kormienko, V. L.; Drozdov, S. V., On Electrochemical oxidation of thiocyanates in solutions for cyanidation of gold-containing ores and concentrates. *Russ. J. Appl. Chem.* **2010,** *83* (9), 1589-1592.

[34]. EPA The final third contamination candidate list (CCL3). https://www.epa.gov/ccl/contaminant-candidate-list-3-ccl-3#ccl3-list (accessed 10/08/2009).

[35]. Ammazzini, S.; Onor, M.; Pagliano, E.; Mester, Z.; Campanella, B.; Pitzalis, E.; Bramanti, E.; D'Ulivo, A., Determination of thiocyanate in saliva by headspace gas chromatography-mass spectrometry, following a single-step aqueous derivatization with triethyloxonium tetrafluoroborate. *J. Chromatogr. A* **2015,** *1400*, 124-130.

[36]. Bakker, E.; Bühlmann, P.; Pretsch, E., Carrier-based ion-selective electrodes and bulk optodes. 1. general characteristics. *Chem. Rev.* **1997,** *97* (8), 3083-3132.

[37]. Lindner, E.; Pendley, B. D., A tutorial on the application of ion-selective electrode potentiometry: An analytical method with unique qualities, unexplored opportunities and potential pitfalls; Tutorial. *Anal. Chim. Acta* **2013,** *762*, 1-13.

[38]. Buck, R. P.; Lindner, E., Recomendations for nomenclature of ion-selective electodes. *Pure Appl. Chem.* **1994,** *66*, 2527-2536.

[39]. Mistlberger, G.; Crespo, G. A.; Bakker, E., Ionophore-based optical sensors. *Annu. Rev. Anal. Chem.* **2014,** *7* (1), 483-512.

[40]. Erenas, M. M.; de Orbe-Payá, I.; Capitan-Vallvey, L. F., Surface modified thread-based microfluidic analytical device for selective potassium analysis. *Anal. Chem.* **2016,** *88* (10), 5331-5337.

[41]. Cantrell, K.; Erenas, M. M.; de Orbe-Payá, I.; Capitán-Vallvey, L. F., Use of the hue parameter of the hue, saturation, value color space as a quantitative analytical parameter for bitonal optical sensors. *Anal. Chem.* **2010,** *82* (2), 531-542.

[42]. Suzuki, K.; Hirayama, E.; Sugiyama, T.; Yasuda, K.; Okabe, H.; Citterio, D., Ionophore-based lithium ion film optode realizing multiple color variations utilizing digital color analysis. *Anal. Chem.* **2002,** *74* (22), 5766-5773.

[43]. Phichi, M.; Imyim, A.; Tuntulani, T.; Aeungmaitrepirom, W., Paper-based cation-selective optode sensor containing benzothiazole calix[4]arene for dual colorimetric Ag+ and Hg2+ detection. *Anal. Chim. Acta* **2020,** *1104*, 147-155.

[44]. Choi, K.; Hamilton, A. D., Selective anion binding by a macrocycle with convergent hydrogen bonding functionality. *J. Am. Chem. Soc.* **2001,** *123* (10), 2456-2457.

[45]. Kubo, Y.; Tsukahara, M.; Ishihara, S.; Tokita, S., A simple anion chemosensor based on a naphthalene–thiouronium dyad. *ChemComm* **2000,** (8), 653-654.

[46]. Badr, I. H. A.; Meyerhoff, M. E.; Hassan, S. S. M., Potentiometric anion selectivity of polymer membranes doped with palladium organophosphine complex. *Anal. Chem.* **1995,** *67* (15), 2613-2618.

[47]. Bakker, E.; Malinowska, E.; Schiller, R. D.; Meyerhoff, M. E., Anion-selective membrane electrodes based on metalloporphyrins: The influence of lipophilic anionic and cationic sites on potentiometric selectivity. *Talanta* **1994,** *41* (6), 881-890.

[48]. Yang, S.; Meyerhoff, M. E., Study of cobalt(III) corrole as the neutral ionophore for nitrite and nitrate detection via polymeric membrane electrodes. *Electroanalysis* **2013,** *25* (12), 2579-2585.

[49]. Beer, P. D.; Hesek, D.; Nam, K. C.; Drew, M. G. B., Anion recognition properties of new upper-rim cobaltocenium calix[4]arene receptors. *Organometallics* **1999,** *18* (19), 3933-3943.

[50]. Lee, H. K.; Oh, H.; Nam, K. C.; Jeon, S., Urea-functionalized calix[4]arenes as carriers for carbonate-selective electrodes. *Sens. Actuators B Chem.* **2005,** *106* (1), 207-211.

[51]. Kivlehan, F.; Mace, W. J.; Moynihan, H. A.; Arrigan, D. W. M., Potentiometric evaluation of calix[4]arene anion receptors in membrane electrodes: Phosphate detection. *Anal. Chim. Acta* **2007,** *585* (1), 154-160.

[52]. Babu, J. N.; Bhalla, V.; Kumar, M.; Mahajan, R. K.; Puri, R. K., A chloride selective sensor based on a calix[4]arene possessing a urea moiety. *Tetrahedron Lett.* **2008,** *49* (17), 2772-2775.

[53]. Roy, D. R.; Shah, E. V.; Mondal Roy, S., Optical activity of Co-porphyrin in the light of IR and Raman spectroscopy: A critical DFT investigation. *Spectrochim. Acta A Mol. Biomol. Spectrosc.* **2018,** *190*, 121-128.

[54]. Górski, L.; Meyerhoff, M. E.; Malinowska, E., Polymeric membrane electrodes with enhanced fluoride selectivity using Zr(IV)-porphyrins functioning as neutral carriers. *Talanta* **2004,** *63* (1), 101-107.

[55]. Mitchell-Koch, J. T.; Pietrzak, M.; Malinowska, E.; Meyerhoff, M. E., Aluminum(III) porphyrins as ionophores for fluoride selective polymeric membrane

electrodes. *Electroanalysis* **2006,** *18* (6), 551-557.

[56]. Steinle, E. D.; Schaller, U.; Meyerhoff, M. E., Response characteristics of anion-selective polymer membrane electrodes based on gallium(III), indium(III) and thallium(III) porphyrins. *Anal. Sci.* **1998,** *14* (1), 79-84.

[57]. Badr, I. H. A.; Meyerhoff, M. E., Fluoride-selective optical sensor based on aluminum(III)−octaethylporphyrin in thin polymeric film: further characterization and practical application. *Anal. Chem.* **2005,** *77* (20), 6719-6728.

[58]. Kang, Y.; Kampf, J. W.; Meyerhoff, M. E., Optical fluoride sensor based on monomer–dimer equilibrium of scandium(III)-octaethylporphyrin in a plasticized polymeric film. *Anal. Chim. Acta* **2007,** *598* (2), 295-303.

[59]. Kang, Y.; Meyerhoff, M. E., Rapid response optical ion/gas sensors using dimer–monomer metalloporphyrin equilibrium in ultrathin polymeric films coated on waveguides. *Anal. Chim. Acta* **2006,** *565* (1), 1-9.

[60]. Zhang, W.; Rozniecka, E.; Malinowska, E.; Parzuchowski, P.; Meyerhoff, M. E., Optical chloride sensor based on dimer−monomer equilibrium of indium(III) octaethylporphyrin in polymeric film. *Anal. Chem.* **2002,** *74* (17), 4548-4557.

[61]. Brasuel, M. G.; Miller, T. J.; Kopelman, R.; Philbert, M. A., Liquid polymer nano-PEBBLEs for Cl− analysis and biological applications. *Analyst* **2003,** *128* (10), 1262-1267.

[62]. Pimenta, A. M.; Araújo, A. N.; Montenegro, M. C. B. S. M.; Pasquini, C.; Rohwedder, J. J. R.; Raimundo, I. M., Chloride-selective membrane electrodes and optodes based on an indium(III) porphyrin for the determination of chloride in a sequential injection analysis system. *J. Pharm. Biomed. Anal.* **2004,** *36* (1), 49-55.

[63]. Li, X.; Harrison, D. J., Measurement of concentration profiles inside a nitrite ion-selective electrode membrane. *Anal. Chem.* **1991,** *63* (19), 2168-2174.

[64]. Cosnier, S.; Gondran, C.; Wessel, R.; Montforts, F.-P.; Wedel, M., A poly(pyrrole-cobalt(II)deuteroporphyrin) electrode for the potentiometric determination of nitrite. *Sensors* **2003,** *3* (7).

[65]. Vlascici, D.; Fagadar-Cosma, E.; Bizerea-Spiridon, O., A new composition for Co(II)-porphyrin-based membranes used in thiocyanate-selective electrodes. *Sensors* **2006,** *6* (8).

[66]. Brown, D. V.; Chaniotakis, N. A.; Lee, I. H.; Ma, S. C.; Park, S. B.; Meyerhoff, M. E.; Nick, R. J.; Groves, J. T., Mn(III)—porphyrin-based thiocyanate-selective membrane electrodes: Characterization and application in flow injection determination of thiocyanate in saliva. *Electroanalysis* **1989,** *1* (6), 477-484.

[67]. Malinowska, E.; Niedziółka, J.; Rożniecka, E.; Meyerhoff, M. E., Salicylate-selective membrane electrodes based on Sn(IV)- and Mo(V)-porphyrins: differences in response mechanism and analytical performance. *J. Electroanal. Chem.* **2001,** *514* (1), 109-117.

[68]. Shahrokhian, S.; Hamzehloei, A.; Bagherzadeh, M., Chromium(III) Porphyrin as a Selective Ionophore in a Salicylate-Selective Membrane Electrode. *Anal. Chem.* **2002,** *74* (14), 3312-3320.

[69]. Brereton, R. G., *Chemometrics: data analysis for the laboratory and chemical plant*. John Wiley & Sons, Ltd: 2003; p 1-13.

[70]. Ryad, A.; Lakhdar, K.; Majda, K.-S.; Samia, A.; Mark, A.; Corinne, A.-D.; Eric, G., Optimization of the culture medium composition to improve the production of hyoscyamine in elicited Datura stramonium L. hairy roots using the Response Surface Methodology (RSM). *Int J Mol Sci* **2010,** *11* (11), 4726-4740.

[71]. Abdel-Haleem, F. M.; Rizk, M. S., Highly selective thiocyanate optochemical sensor based on manganese(III)-salophen ionophore. *Mater. Sci. Eng. C* **2017,** *75*, 682-687.

[72]. Kunthadee, P.; Watchasit, S.; Kaowliew, A.; Suksai, C.; Wongsan, W.; Ngeontae, W.; Chailapakul, O.; Aeungmaitrepirom, W.; Tuntulani, T., Intriguing sensing properties of a di-tripodal amine calix[4]arene ionophore towards anions from Donnan failure in ion-selective membranes induced by Cu^{2+}. *New J. Chem.* **2013,** *37* (12), 4010-4017.

[73]. Bhandari, R. K.; Manandhar, E.; Oda, R. P.; Rockwood, G. A.; Logue, B. A., Simultaneous high-performance liquid chromatography-tandem mass spectrometry (HPLC-MS-MS) analysis of cyanide and thiocyanate from swine plasma. *Anal. Bioanal. Chem.* **2014,** *406* (3), 727-734.

[74]. García, M. S.; Ortuño, J. A.; Sánchez-Pedreño, C.; Albero, M. I.; Fernández, M. J., Flow-through bulk optode for spectrophotometric determination of thiocyanate

and its application to water and saliva analysis. *Sensors* **2006,** *6* (10), 1224-1233.

[75]. Singh, A. K.; Singh, U. P.; Mehtab, S.; Aggarwal, V., Thiocyanate selective sensor based on tripodal zinc complex for direct determination of thiocyanate in biological samples. *Sens. Actuators, B* **2007,** *125* (2), 453-461.

[76]. Lamb, J. D.; Simpson, D.; Jensen, B. D.; Gardner, J. S.; Peterson, Q. P., Determination of perchlorate in drinking water by ion chromatography using macrocycle-based concentration and separation methods. *J. Chromatogr. A* **2006,** *1118* (1), 100-105.

[77]. Seiler, M. A.; Jensen, D.; Neist, U.; Deister, U. K.; Schmitz, F., Validation data for the determination of perchlorate in water using ion chromatography with suppressed conductivity detection. *Environ. Sci. Eur.* **2016,** *28* (1), 18-18.

[78]. Wilson, D.; Abbas, M. N.; Radwan, A. L.; del Valle, M., Potentiometric electronic tongue to resolve mixtures of sulfide and perchlorate anions. *Sensors* **2011,** *11* (3), 3214-26.

[79]. García, S.; Albero, I.; Ortuño, J. A.; Sánchez-Pedreño, C.; Expósito, R., Flow-through bulk optode for the spectrophotometric determination of perchlorate. *Microchim. Acta* **2003,** *143* (1), 59-63.

[80]. Pena-Pereira, F.; Lavilla, I.; Bendicho, C., Paper-based analytical device for instrumental-free detection of thiocyanate in saliva as a biomarker of tobacco smoke exposure. *Talanta* **2016,** *147*, 390-396.

[81]. Shibata, H.; Henares, T. G.; Yamada, K.; Suzuki, K.; Citterio, D., Implementation of a plasticized PVC-based cation-selective optode system into a paper-based analytical device for colorimetric sodium detection. *Analyst* **2018,** *143* (3), 678-686.

[82]. Malinowska, E.; Niedziółka, J.; Meyerhoff, M. E., Potentiometric and spectroscopic characterization of anion selective electrodes based on metal(III) porphyrin ionophores in polyurethane membranes. *Anal. Chim. Acta* **2001,** *432* (1), 67-78.

[83]. Malinowska, E.; Gawart, L.; Parzuchowski, P.; Rokicki, G.; Brzózka, Z., Novel approach of immobilization of calix[4]arene type ionophore in 'self-plasticized' polymeric membrane. *Anal. Chim. Acta* **2000,** *421* (1), 93-101.

[84]. Qin, Y.; Peper, S.; Bakker, E., Plasticizer-free polymer membrane ion-selective electrodes containing a methacrylic copolymer matrix. *Electroanalysis* **2002,** *14* (19-20), 1375-1381.

[85]. Tsujimura, Y.; Sunagawa, T.; Yokoyama, M.; Kimura, K., Sodium ion-selective electrodes based on silicone-rubber membranes covalently incorporating neutral carriers. *Analyst* **1996,** *121* (11), 1705-1709.

APPENDIX

APPENDIX A

AF 02-12

The Research Ethics Review Committee for Research Involving Human Research Participants, Group I, Chulalongkorn University

Jamjuree 1 Building, 2nd Floor, Phyathai Rd., Patumwan district, Bangkok 10330, Thailand,
Tel: 0-2218-3202, 0-2218-3049 E-mail: eccu@chula.ac.th

COA No. 281/2019

Certificate of Approval

Study Title No. 236.1/62 : DETERMINATION OF PERCHLORATE AND THIOCYANATE IONS BY ION-SELECTIVE MEMBRANE AND BULK OPTODE TECHNIQUES USING EXPERIMENTAL DESIGN APPORACH

Principal Investigator : MISS SUPACHA WIROJSAENGTHONG

Place of Proposed Study/Institution : Faculty of Science, Chulalongkorn University

The Research Ethics Review Committee for Research Involving Human Research Participants, Health Sciences Group, Chulalongkorn University, Thailand, has approved constituted in accordance with Belmont Report 1979, Declaration of Helsinki 2013, Council for International Organizations of Medical Sciences (CIOM) 2016, Standards of Research Ethics Committee (SREC) 2013, and National Policy and guidelines for Human Research 2015.

Signature: Prida Tasanapradit Signature: Nuntaree Chaichanawongsaroj

(Associate Prof. Prida Tasanapradit, M.D.) Chairman

(Assistant Prof. Nuntaree Chaichanawongsaroj, Ph.D.) Secretary

Date of Approval : 16 December 2019 Approval Expire date : 15 December 2020

The approval documents including:

1) Research proposal
2) Participant Information Sheet and Consent Form
3) Researcher

Protocol No. 236.1/62
Date of Approval 16 DEC 2019
Approval Expire Date 15 DEC 2020

The approved investigator must comply with the following conditions:

1. *The research/project activities must end on the approval expired date of the Research Ethics Review Committee for Research Involving Human Research Participants, Health Sciences Group, Chulalongkorn University (RECCU). In case the research/project is unable to complete within that date, the project extension can be applied one month prior to the RECCU approval expired date.*
2. *Strictly conduct the research/project activities as written in the proposal.*
3. *Using only the documents that bearing the RECCU's seal of approval with the subjects/volunteers (including subject information sheet, consent form, invitation letter for project/research participation (if available).*
4. *Report to the RECCU for any serious adverse events within 5 working days*
5. *Report to the RECCU for any change of the research/project activities prior to conduct the activities.*
6. *Final report (AF 02-14) and abstract is required for a one year (or less) research/project and report within 30 days after the completion of the research/project. For thesis, abstract is required and report within 30 days after the completion of the research/project.*
7. *Annual progress report is needed for a two- year (or more) research/project and submit the progress report before the expire date of certificate. After the completion of the research/project processes as No. 6.*

VITA

NAME	Supacha Wirojsaengthong
DATE OF BIRTH	09 November 1991
PLACE OF BIRTH	Trang, Thailand
HOME ADDRESS	124 Songpeenong Soi, Sukhumvit Road, Tumbon Chengnaeng, Amphur Maeng, Rayong 21000